
[All ETDs from UAB](#)

[UAB Theses & Dissertations](#)

2017

Endogenous Interferon-**B** Regulates Survival And Development Of Transitional B Cells

Jennie Ann Hamilton
University of Alabama at Birmingham

Follow this and additional works at: <https://digitalcommons.library.uab.edu/etd-collection>

Recommended Citation

Hamilton, Jennie Ann, "Endogenous Interferon-B Regulates Survival And Development Of Transitional B Cells" (2017). *All ETDs from UAB*. 1852.
<https://digitalcommons.library.uab.edu/etd-collection/1852>

This content has been accepted for inclusion by an authorized administrator of the UAB Digital Commons, and is provided as a free open access item. All inquiries regarding this item or the UAB Digital Commons should be directed to the [UAB Libraries Office of Scholarly Communication](#).

ENDOGENOUS INTERFERON- β REGULATES SURVIVAL AND DEVELOPMENT
OF TRANSITIONAL B CELLS

by

JENNIE A. HAMILTON

DR. JOHN D. MOUNTZ, MENTOR & COMMITTEE CHAIR
DR. PETER D. BURROWS
DR. JOHN F. KEARNEY
DR. CHANDER RAMAN
DR. TROY RANDALL

A DISSERTATION

Submitted to the graduate faculty of The University of Alabama at Birmingham,
in partial fulfillment of the requirements for the degree of
Doctor of Philosophy

BIRMINGHAM, ALABAMA

2017

ENDOGENOUS INTERFERON- β REGULATES SURVIVAL AND DEVELOPMENT OF TRANSITIONAL B CELLS

JENNIE A. HAMILTON

MICROBIOLOGY

ABSTRACT

The survival responses of transitional B cells play a key role in shaping the development of mature, antibody producing B cells. Abnormal transitional T1 B cell survival responses are associated with the generation of polyreactive self-antigen-reactive mature B cells in systemic lupus erythematosus (SLE). Type I interferon (IFN) dysregulation is strongly associated with autoantibodies (autoAbs) and disease flares, particularly in African American (AA) patients. B cells produce a variety of immune-modulatory cytokines, but B cell production of high affinity IFN β in SLE has not been investigated. In the present study, analysis of PBMCs from SLE patients (n=34) and healthy controls (n=9) revealed a significant increase in IFN β expression within transitional, naïve and memory B cell compartments of SLE patients. Endogenous T1 B cell IFN β acted in an autocrine mechanism to promote B cell activation and survival and was highly correlated with clinical disease including renal disease and anti-dsDNA, anti-Sm and anti-SSA autoAbs. Transitional B cell IFN β expression was also significantly correlated with the percent of 9G4⁺ autoreactive B cells and CD19^{lo}CD38^{hi}CD27⁺ plasma cell formation. African American SLE patients, a population disproportionately affected by SLE had significantly increased expression of IFN β . Mechanistic studies in mice including analyses of *Ifnb*^{-/-} and *Ifnb*^{+/+} B cells derived from reconstituted chimeric mice revealed that development of germinal center, autoreactive, and IgG class switched anti-DNA, anti-La and anti-Histone autoAb producing B cells were dependent upon B cell

endogenous IFN- β . Single-cell examination of *Ifnb*^{-/-} vs. *Ifnb*^{+/+} T1 B cells further revealed distinct gene expression signatures associated with endogenous IFN β , including significantly lower expression of CD86, TLR7, and PKR, and type I IFN genes in T1 B cells derived from *Ifnb*^{-/-} mice. Single cell analysis of autoimmune BXD2 T1 B cells that overexpressed IFN β revealed that IFN β is expressed in early T1 B cell development with subsequent upregulation of TLR7 and IFN α genes. Indeed IFN β was specifically required for optimal B cell activation and survival in response to TLR7 stimulation and TLR7 + B cell receptor (BCR) co-stimulation. Together, these studies suggest that endogenous IFN β -expressing T1 B cells are initially autonomous and that their expression of IFN β plays a key role in regulating their development and responsiveness to external factors, including externally-derived type I IFNs and TLR7.

DEDICATION

This dissertation is dedicated to my mother Deborah Newman and my stepfather Paul Newman. I cannot imagine the last five years without their constant love, support, and sacrifice.

ACKNOWLEDGMENTS

I would like to thank my mentor Dr. John D. Mountz for his strong guidance and support in my research training. I appreciate the many career development and learning opportunities he has provided me in his laboratory. I would also like to thank Dr. Hui-Chen Hsu for the support and research expertise she has contributed to my project over the years. I have enjoyed working with Dr. Mountz and Dr. Hsu and am thankful I had the opportunity to work with such excellent and devoted researchers. I also want to express my appreciation to all members of the Mountz laboratory who have provided assistance with experiments as well as a friendly, respectful, and professional environment in which to study.

Thank you to my Dissertation Committee members, Dr. Peter Burrows, Dr. John Kearney, Dr. Chander Raman, and Dr. Troy Randall. Their scientific and career advice and suggestions were always valuable and constructive.

I also want to thank Dr. Stephen Wright, my master's thesis mentor from Middle Tennessee State University who encouraged me to apply to UAB, without whom I may never have begun this challenging and rewarding PhD research journey.

TABLE OF CONTENTS

	<i>Page</i>
ABSTRACT.....	ii
DEDICATION.....	iv
ACKNOWLEDGMENTS	v
LIST OF TABLES.....	viii
LIST OF FIGURES	ix
1. INTRODUCTION	1
Significance.....	1
Systemic Lupus Erythematosus	2
BXD2 Mouse Model.....	4
B Cell Self-Tolerance	6
<i>Central Tolerance</i>	6
<i>Peripheral Tolerance</i>	7
Transitional B cells	8
<i>Developmental Stages and Location</i>	8
<i>Survival and Maturation T1 and T2 B cells</i>	12
<i>Human Transitional B cells</i>	18
<i>Transitional B cell Cytokine Production</i>	20
Type I Interferon: Basic Established Concepts.....	21
<i>Classes and Isoforms of the Type I Interferon Family</i>	21

<i>Signal Transduction for Type I IFN</i>	22
<i>Type I IFN in SLE</i>	24
<i>pDCs</i>	25
<i>Apoptotic Cell Clearance Defects</i>	27
Type I Interferon: Developing Concepts for Human Autoimmune Disease	30
<i>Cell-Specific Analysis of IFN Signaling</i>	30
<i>Constitutive Type I IFN in Homeostasis and Disease</i>	32
<i>Unique Properties of IFNβ</i>	35
Nucleic Acid Sensing.....	37
Questions.....	41
2. A PROMINENT ROLE OF INTERFERON-B PRODUCED BY TRANSITIONAL B CELLS IN LUPUS.....	42
3. GENERAL APPROACH FOR TETRAMER BASED IDENTIFICATION OF AUTOANTIGEN REACTIVE B CELLS: CHARACTERIZATION OF LA AND SNRNP REACTIVE B CELLS IN AUTOIMMUNE BXD2 MICE.....	99
4. DISCUSSION.....	150
pDCs vs. B Cells.....	150
B Cells and IFN Production.....	153
Significance of B Cell Type I IFN Heterogeneity	155
IFN β in Mouse Autoimmunity	159
IFN β in Human SLE.....	162
Conclusion	165
5. GENERAL LIST OF REFERENCES	167
6. APPENDIX A.....	193
7. APPENDIX B.....	195

<i>Table</i>	LIST OF TABLES	<i>Page</i>
	INTRODUCTION	
Table 1. Summary of pDC findings in SLE tissue.....		29
Table 2. The expression of endosomal TLRs across different cells		39
A PROMINENT ROLE OF INTERFERON- β PRODUCED BY TRANSITIONAL B CELLS IN LUPUS		
Supplementary Table 1. Clinical data for SLE patients recruited for this study		76
Supplementary Table 2. List of primers used for gene expression analysis		77
GENERAL APPROACH FOR TETRAMER BASED IDENTIFICATION OF AUTOANTIGEN REACTIVE B CELLS: CHARACTERIZATION OF LA AND SNRNP REACTIVE B CELLS IN AUTOIMMUNE BXD2 MICE		
Table 1. List of autoantigen epitopes used for reactivity comparisons between B6 and BXD2 mice.....		139
Table 2. Summary of epitopes used for ELISA, ELISPOT, and tetramer analyses		140

LIST OF FIGURES

Figure *Page*

INTRODUCTION

1. Transitional B cells in B6 mice.....	10
2. BAFFR and IFNAR1 expression on B cell subset.....	14
3. FACS analysis of spleen B cell development in the indicated mouse strain	15
4. FACS analysis of Ki67 expression in spleen B cells from B6 and BXD2 mice	17
5. Negative selection and fate of self-reactive immature B cells likely occurs at the T1 stage	18
6. Ternary complex formation	24

A PROMINENT ROLE OF INTERFERON- β PRODUCED BY TRANSITIONAL B CELLS IN LUPUS

1. Increased expression of intracellular IFN β in B cells from a subset of SLE patients.....	78
2. Increased IFN β in T1 B cells of BXD2 mice.....	79
3. Analysis of the effects of IFN β and type I IFN on La13-27 tetramer-reactive B cells	80
4. Analysis of Ifnb, Ifna and Tlr7 expression in single T1 B cells in BXD2 mice.....	81
5. IFN β promotes TLR7-induced transitional B cell activation and survival in BXD2 mice and SLE patients	82
6. IFN β blockade prevents rapid repopulation of spleen B cells after anti-CD20 depletion.....	83
S1. Validation of IFN β expression in B cells from PBMCs of SLE patients	84
S2. Quality controls to validate sorted cell identity	85

S3. Expression of intracellular IFN β in T1/T2 B cells from PBMCs of SLE patients with differential clinical characteristics	86
S4. Expression of IFN β gene in T1 B cells and pDCs from BXD2 mice.....	87
S5. Quantitation of nuclear IRF7 and three-dimensional imaging of T1 B cells	88
S6. La13-27 reactive cells expressed high levels of Cd19 but low levels of Cd317	89
S7. Specific inhibition of IFN β by anti-IFN β antibody, or both IFN α and IFN β by IFNAR1 blockade	90
S8. Verification of the purity of T1 B cells used for single cell gene expression analysis.....	91
S9. Principal component analysis (PCA) of single T1 B cells based on the expression of the indicated genes.....	92
S10. Segregation of CD93 and CD23 in subsets of T1 B cells.....	93
S11. PCA of single T1 B cells based on the expression of the indicated genes	94
S12. Endogenous IFN β production by transitional B cells is required for their development and directly stimulates production of IFN α	95
S13. B cell early activation response to TLR7 and BCR/TLR7 co-stimulation in Ifnb $^{-/-}$ and Ifnb $^{+/+}$ B cells	96
S14. Kinetics of B cell repopulation after anti-CD20 treatment and effects of IFNAR blockade with an anti-IFNAR blocking antibody.....	97
S15. Anti-IFN β and anti-IFNAR inhibited B cell repopulation post anti-CD20 B-cell depletion in BXD2 mice.....	98

GENERAL APPROACH FOR TETRAMER BASED IDENTIFICATION
OF AUTOANTIGEN REACTIVE B CELLS: CHARACTERIZATION
OF LA AND SNRNP REACTIVE B CELLS IN AUTOIMMUNE BXD2
MICE

1. Autoantibody binding to peptide epitopes in BXD2 mice	141
2. Autoreactive IgG and IgM signal intensities to peptide epitopes in BXD2 or control B6 mice at the indicated ages	142
3. Verification of synthesized peptides	143

4. Tetramer enrichment and gating strategy	144
5. Increased La ₁₃₋₂₇ and snRNP ₃₅₇₋₃₇₃ tetramer ⁺ MZ-P and T3 B cells in BXD2 mice	145
6. Increased percentage of activated tetramer ⁺ MZ-P and CD80 ⁺ PD-L2 ⁺ memory B cells in BXD2 mouse spleens.....	146
S1. Global autoantibody binding profile to peptide epitopes in BXD2 compared to B6 mice	147
S2. Tetramer enrichment and gating strategy	148
S3. Transitional B cell subsets in total splenocytes from B6 and BXD2 mice.....	149

DISCUSSION

1. Type I IFN expression in BXD2 mice	152
2. Functional verification of sorted DC populations.....	153
3. Variability in IFN and IRF genes in T1 B cells from BXD2 mice	155
4. Model for interaction of T1 B cell IFN communication network.....	157
5. Correlation plots showing co-expression of type I IFN genes.....	159
6. B cell endogenous IFN- β is required for autoAb formation.....	161
7. T1 B cell endogenous IFN β is associated with expansions in the plasma cell and IgD-CD27- double negative populations in SLE.....	164

CHAPTER 1

INTRODUCTION

Significance

Systemic lupus erythematosus (SLE) is a disease characterized by profound B cell tolerance loss to nucleic acid autoantigens. The disease mimics a sustained antiviral response including type I interferon (IFN) production which promotes feedback loops which progressively promote autoantibodies and immune complex formation.

Surprisingly, although B cells are known to actively regulate immune responses through cytokine production, the production of type I IFNs by B cells has not been investigated in lupus. Additionally, the contributions of specific type I IFN subtypes, including high affinity IFN β have not been determined in SLE. However, studies have shown that lupus patients exhibit heterogeneous type I IFN signatures, and some patients exhibit a type I IFN signature only in certain cell subsets but not others [1]. This suggests type I IFN production or dysregulation may originate in specific cell types and anatomical locations. A better understanding of the cellular source and target of type I IFN in lupus will be key to more specific targeting of the type I IFN pathway and precision medicine.

In mice and humans, newly emigrant B cells entering the spleen (T1 transitional B cells) are the formative link between the bone marrow immature B cells and the mature B cell repertoire. Abnormalities in transitional B cell development and cytokine production have been observed at the T1 B cell stage in humans with SLE. We observed similar transitional B cell abnormalities in BXD2 lupus prone mice, which develop type I IFN

dependent anti-ribonucleoprotein (RNP) autoantibodies (autoAb). These studies have identified increased expression of type I IFNs in spleen T1 B cells from BXD2 mice and increased endogenous IFN β in both transitional and mature circulating B cell subsets from SLE patients. Together, the present findings support a specific role for B cell produced high-affinity IFN β in autoreactive B cell development. Results from these studies will lead to better understanding of the mechanisms that drive development of autoreactive B cells in human disease.

Systemic Lupus Erythematosus

Systemic Lupus Erythematosus (SLE) is an autoimmune disease characterized by inappropriate immune response to self-antigens [2]. SLE is a relatively common disease with a prevalence ranging from 20 to 150 cases per 100,000 people [2]. SLE predominantly affects women and typically has manifestations in multiple organs [2]. In addition to the strong gender bias toward females (9:1 female to male ratio), SLE is also more commonly observed in people of African, Hispanic, or Asian ancestry, as compared with those of other racial or ethnic groups [2]. Common symptoms include rash, photosensitivity, arthritis, and fatigue [3]. In severe cases immune-complex-mediated damage to the kidney glomeruli (lupus nephritis or glomerulonephritis) can be a life-threatening manifestation of SLE. Lupus nephritis can occur in up to 60% of cases and is associated with worse disease outcomes [4]. Central nervous system involvement can also occur in some cases, leading to cognitive dysfunction, stroke or seizures [3].

Many of the disease manifestations in SLE have been attributed to the production of self-reactive autoantibodies (autoAbs) reactive with nucleic acids, nucleic acid–

binding proteins and ribonucleic acid binding proteins or (RBP) [5]. The serological presence of these anti-nuclear and anti-RBP autoAbs are diagnostic for SLE and can cause tissue damage and inflammation when they deposit in tissues in the form of immune-complexes [3]. Importantly, these autoantibodies are present years before diagnosis and the onset of clinical disease and accumulate in the years leading up to diagnosis [6].

There are known genetic influences that contribute to SLE [2]. Genetic susceptibility loci include genes that affect differentiation and survival of B cells, including genes that affect activation, proliferation, apoptosis, cytokine and chemokine secretion and responsiveness as well as genes that are involved in presentation and clearance of apoptotic material [7, 8]. The strongest genetic association lies in the single nucleotide polymorphisms in human leukocyte antigens (HLA) HLA-DR2 (DRB1*1501) and HLA-DR3 (DRB1*0301) major histocompatibility complex (MHC) class II. Other associated SNPs occur in non-HLA genes including IRF5, STAT4, PTPN22, C1q genes, TNFSF4, TREX1, the IRAK1-MECP2 region, IL10, and the Fc γ R genes and others [2, 9]. However, there is also a strong influence of environmental factors, as identical twin studies show that the concordance rates are 24% and 2% for monozygous and dizygous twins, respectively [10].

The early stages of the pathogenesis of SLE remain particularly poorly understood. However, the critical role for autoAbs in disease pathogenesis critically implicates B cell dysregulation in SLE development. In SLE, autoAbs were shown to develop years prior to disease manifestation. This phenomenon provides important clues about the immunological events leading to the disease manifestations, suggesting gradual

loss of B cell tolerance and the existence of different stages of disease progression prior to diagnosis [3]. There is now ample evidence that B cells play major initiating and/or amplifying pathogenic roles in a wide variety of autoimmune diseases through both antibody-dependent and antibody-independent mechanisms [11, 12]. It is not known whether the accumulation of certain intrinsic genetic susceptibility loci cause a primary defect in the B cells or whether primary defects in other cell types induce B cell abnormalities [7]. Nevertheless, it is increasingly realized that B cells facilitate the normal immune response as well as autoimmune disease not only by autoAb generation, but also through their antigen presentation function (presenting autoantigens to T cells) and by secreting immunoregulatory cytokines [13].

BXD2 Mouse Model

The BXD2 mouse is a recombinant inbred strain derived by breeding the intercross progeny between DBA/2J and C57BL/6J (B6) mice for more than 20 generations [14]. Spontaneous autoimmunity in BXD2 mice was first described in 2005 [14]. The autoimmunity in BXD2 mice is characterized by apoptotic cell clearance defects [15, 16], germinal center formation [17, 18], glomerulonephritogenic autoantibodies and arthritis [14]. Both the MHC gene (H2b) and Ig genes of BXD2 mice are derived from the B6 strain. Therefore, B6 mice have been used as healthy control in the study of BXD2 mice. Unlike other common mouse models of lupus (BXSb/Yaa, MLR-Faslpr mice), there is no identified single gene mutation in the BXD2 mouse model [14]. However, the Quantitative trait loci (QTL) influencing the titers of anti-DNA and RF autoantibodies in the mice are close to the previously mapped autoimmune

susceptibility loci that have been identified in NZM2410, NZB × NZW, B6, MRL and MRL-lpr background [14]. This multi-genetic autoimmune disease of the BXD2 mouse is similar to that of most human autoimmune diseases, which renders it as an attractive mouse model to elucidate mechanisms of immune tolerance loss.

Previous studies have been carried out to determine the mechanism of B cell tolerance loss in BXD2 mice. Overexpression of AID in B cells has been associated with the production of pathogenic autoantibodies [19], while suppression of AID inhibits the GC formation and autoantibody development [20]. Several previous studies were conducted to study the mechanisms leading to this pathogenic germinal center (GC) formation in the spleens of BXD2 mice. Elevated levels of serum IL-17 and an increased number of Th17 cells have been shown to promote the autoreactive GC formation [18], and type I IFN is also involved in the GC development in BXD2 mice through the regulation of B cell chemotaxis from the marginal zone (MZ) to the GC. Specifically, BXD2 mice exhibit an expansion of a population of CD93^{neg}CD1d^{hi} CD21^{hi}IgM^{hi}CD23^{hi} B cells, commonly known as marginal zone precursor (MZ-P) B cells [21]. IFN α was demonstrated to act directly on the type I IFN receptor (IFNAR) on marginal zone precursor B cells to upregulate CD69 and CD86. CD69 downregulates S1P1 thereby antagonizing the marginal zone-oriented migration of the MZ-P B cells in the spleen of BXD2 mice [21, 22], and CD86 enables the B cells to provide potent co-stimulation of T cells [23]. The MZ-P B cells were also found to be potent antigen-transporting B cells that can migrate directly to the vicinity of the GC light zone. Therefore, the type I IFN signaling on B cells in the spleens of BXD2 mice is a crucial mechanism of disease in this mouse model. However, whether the MZ-P dysregulation

in BXD2 mice is the origin of B cell dysregulation or rather preceded by earlier B cell defects is a remaining question.

B Cell Self-Tolerance

Central Tolerance

The mechanisms controlling B cell tolerance have been a major focus of immunologists in past decades. B cells develop in the bone marrow, where cells that have committed to the B cell fate go through a series of developmental stages, namely pro-B, pre-B, immature B, and then transitional T1 stage [24]. During the bone marrow developmental stages, the variable (V), diversity (D), and joining (J) gene segments of the immunoglobulin (Ig) genes are rearranged to generate the primary Ig or BCR repertoire, which provides the host with a diverse array of BCR specificities. However, this process of Ig gene recombination could result in BCRs that bind to self-antigens. It is at the immature B-cell stage that the surface BCR is tested for the first time for reactivity against autoantigens. Central B-cell tolerance refers to the process where immature B cells that react with a self-antigen in the bone marrow environment are negatively selected. This involves sequential stages of BCR heavy and light chain gene rearrangement in the bone marrow and probing with endogenous antigen for reactivity [25]. Appropriate operation of these central checkpoint mechanisms are fundamental to the generation of a naïve B cell repertoire that is self-Ag tolerant [26]. Studies using transgenic mice revealed the development of self-reactive B cells were restricted through three mechanisms: receptor editing, clonal deletion or inactivation (a state of unresponsiveness or anergy) [13, 27, 28]. Analysis of the bone marrow early immature

B-cell repertoire indicates that 50%–75% of these cells express a self-antigen reactive BCR while similar studies on transitional and naïve mature B cells in spleen and blood, show a much lower frequency (20%–40%) of cells expressing autoreactive antibodies [26, 29, 30].

Peripheral Tolerance

Following the bone marrow immature B cell stage is the transitional T1 B cell stage. It is at this T1 stage that the B cells emigrate from the bone marrow to the spleen for further development and maturation [24, 31]. Transitional B cells are the crucial link between bone marrow immature and peripheral mature B cells [32]. Transitional B cells undergo development in a series of discrete steps or stages marked by distinct phenotypic and functional differences [31, 32]. Data point to the late transitional T2 B-cell stage as a crucial juncture at which developing B cells gain access to splenic follicles, become responsive to T-cell help and lose sensitivity to negative selection, characterizing the immature B-cell response to B-cell antigen receptor (BCR) signaling in vitro and in vivo [32]. The transitional B cell stage in the spleen has been characterized as a major target of negative selection and thus a major site of tolerance induction against peripheral antigens (as opposed to the central tolerance induction which occurs in the BM) [33].

Induction of anergy or a state of unresponsiveness is a major mechanism of transitional B cell tolerance in the periphery. The most widely studied transgenic model of B-cell anergy uses hen-egg lysozyme (HEL) as a neo-self antigen. To construct this model (designated MD4 × ML5), MD4 mice were engineered to express transgenes encoding HEL-specific immunoglobulin μ and δ heavy chains and light chains. These

mice were bred with a second transgenic strain that expresses soluble HEL, referred to as ML5 [13, 27, 28]. In this model and Ars-specific mice [34], the self-tolerance is maintained by down-regulation of surface IgM [35] and a failure of B cells to colonize the splenic marginal zone [36]. These features are accompanied by inactivation of BCR signaling [37, 38]. Importantly, studies in which antibodies were cloned and expressed from single cells and then tested for autoreactivity with HEp-2 cell lysate ELISA and indirect immunofluorescence assays on fixed HEp-2 cells revealed that autoreactive antibodies fail to be removed at the transition between new emigrant and mature naive B cells in patients with SLE highlighting the transitional B cell stage as a critical early point of abnormal B cell development in SLE [39]. Patients with SLE, regardless of disease status (remission or not), were observed to have increased numbers of circulating mature naive B cells that express self-reactive and polyreactive antibodies. It has been speculated that these cells serve as precursors for cells that produce pathogenic lupus antibodies [40]. This same phenomenon of early B cell checkpoint defects was also observed in type I diabetes [41] and Wiskott Aldrich Syndrome [42].

Transitional B cells

Developmental Stages and Location

In adults, B cell generation from hematopoietic stem cells is initiated in the BM. However, the final maturation and selection of B cells takes place not in the BM, but primarily in the spleen. Thus, the final development of immature B cells in the spleen marks the formative link between bone marrow (BM) immature and peripheral mature B cells. This developmental stage between BM immature B cells and mature B cell subsets

was initially termed the “transitional” B cell stage by Carsetti and colleagues who further proposed that transitional B cells in the adult spleen may be subdivided into two distinct subsets (T1 and T2) [31]. In mice, T1 and T2 B cells are identifiable by analysis of expression of the AA4.1 antigen on the CD93 surface protein. CD93 is an approximately 130-140 kDa C-type lectin-like type I transmembrane protein, and some evidence suggests CD93 is a C1q receptor. CD93 was originally identified as an antigen expressed on early stages of B cell development in bone marrow, and is maintained through the T1 and T2 developmental stages in the spleen.

The original description of T2 B cells was as precursors to mature B cells [43]. The late transitional T2 subset was postulated to contain precursors for both follicular and MZ B cells [43]. Later, adoptive transfer experiments led other researchers to postulate that T2 B cells were enriched specifically in precursors for MZ B cell development or MZ B cell precursors (MZPs) [44]. However, the studies are generally consistent in concluding that transitional B cells in the adult spleen are heterogeneous and can be divided into at least three subsets based on AA4.1 surface expression and differential expression of the low affinity IgE receptor FcεRII or CD23 and surface IgM. These populations are T1 (AA4.1^{hi}IgM^{hi}CD23^{neg}IgD^{lo}), T2 (AA4.1⁺IgM^{hi}CD23⁺IgD⁺), and T3 (AA4.1^{+/lo}IgM^{low}CD23⁺ IgD⁺) suggesting that peripheral B cell maturation occurs in a step-wise process where expression of CD23 and IgD are gradually acquired [45] (Figure 1). The T1 subset of immature B cells transits from the BM, through the bloodstream, to the splenic periarteriolar lymphatic sheath or PALS [43]. In contrast, the T2 subset is primarily located in the splenic follicle, adjacent to mature B cells [43]. Examination of 4 week old B6 mouse spleen reveals the presence of AA4.1^{hi}IgM^{hi}IgD^{lo} B cells in and

around mature and developing splenic follicles (Figure 1). Examination of these subsets revealed striking phenotypic and functional differences, collectively pointing to the late transitional B-cell stage as a crucial juncture at which developing B cells gain access to splenic follicles, become responsive to T-cell help and lose sensitivity to negative selection [32, 43]. Each developmental step is tightly regulated by signals received through the BCR, as well as sensing of paracrine and autocrine cytokines, availability of nutrients, and cell-cell interactions [46].

Mouse splenic transitional B cells have been described more thoroughly than human, as studies in humans are normally limited to peripheral blood analysis. However, studies from multiple groups have characterized transitional B cell populations in human peripheral blood. These studies differ in gating strategies used to identify the populations, but are generally in agreement that the transitional B cell development

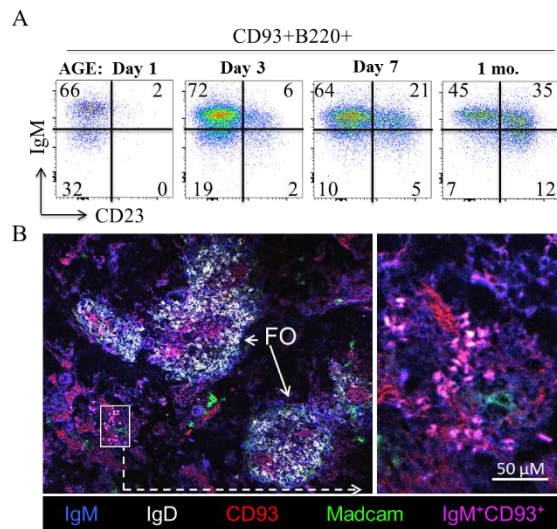


Figure 1. Transitional B cells in B6 mice. FACS (A) and confocal (B) analysis of developing transitional B cells in the spleens of B6 mice.

occurs in stages as the B cells acquire immune competence to respond to survival and proliferation signaling. In the bone marrow, CD10^{hi}, CD44^{lo}, CD24^{hi}, and CD38^{hi}

expression has been shown to be characteristic of all immature bone marrow B cells [47]. CD10 positivity has been adopted as a transitional B cell marker in the circulation, based in part on the observations that the first B cells repopulating the periphery 7 weeks after bone marrow transplantation are all CD10⁺ [47]. The lack of somatic Ig hypermutation and lack or diminished expression of activation markers, such as CD27, CD69, CD11b, CD80, CD86, and CD95, further supports that these cells are likely immature or naïve, are unlikely to have responded to antigen recently, and are not memory B cells [47]. An important study of B cell repopulation in humans on Rituximab B cell depletion therapy demonstrated the presence of several transitional B cell populations displaying phenotypic and functional differences [48]. This study also showed that transitional B cells in humans can be subdivided into multiple populations based on CD24 and CD38 expression, increased expression of CD10 and CD5 surface marker expression and lack of ABCB1 transporter expression. These studies further identified an additional late transitional B cell population intermediate between T2 and mature naïve stages that is a normal B cell developmental intermediate [48]. In human spleen, transitional B cells show a similar pattern with distinct subsets based on CD24, CD38 and CD10 expression, and gradual acquisition of mature markers (CD23, CD21) as they progress across the developmental continuum [48]. This suggests that the spleen may be the site of activation and differentiation of early transitional B cells [48], as has been shown for mice [31].

Survival and Maturation T1 and T2 B Cells

Of the 2×10^7 IgM⁺ B cells that are generated from the BM daily, 10% enter the spleen and only 1–3% enter the mature B cell pool [49, 50]. B cell fate to the MZ or FO pool has recently been proposed to occur at the T1 B cell stage [51]. Development of T2 and mature B cells from T1 precursors requires signals derived from the B cell receptor and that the induction of survival genes and maturation [31]. Mice with genetically deleted components of the BCR signaling cascade, including Btk deficient mice [52], CD45-deficient mice [53], PI3K deficient mice [54], BLNK/SLP-65-deficient mice [55], and mice with deletion of the cytoplasmic tail of Ig- α [31] display developmental arrest at the T1 or T2 stage.

B-cell activating factor receptor (BAFFR) signaling is a critical regulator of B cell function [56]. BAFF-deficient mice revealed an almost complete loss of follicular and marginal zone B lymphocytes [57]. BAFFR signaling is critical for survival of T2 B cells, but the requirement of BAFFR in T1 B cell survival is not fully defined. Spleen T1 B cells express low levels of BAFF-R [58], are not expanded in BAFF transgenic mice [59] nor in mice administered exogenous BAFF [58], and are largely unaffected in *baff*^{-/-} mice [57, 60]. In addition to CD23 and IgD upregulation, maturation of T1 B cells to the T2 stage is marked by the upregulation of BAFF-R expression, and the onset of responsiveness to BAFF-mediated survival signals [58]. Consistent with this, in BXD2 mice T1 B cells express low levels of BAFFR relative to other B cell subsets, while BAFFR is upregulated at the T2 B cell stage. IFNAR1 expression in contrast is expressed on all B cells and significantly higher on transitional and marginal zone precursor B cells relative to mature B cell subsets (Figure 2).

In a 2009 study, BCR signaling in T1 vs. follicular mature splenic B cells was comprehensively compared [61]. T1 B cells, in contrast to follicular mature B cells, failed to express key NF- κ B target genes in response to BCR engagement and exhibited a defect in the assembly of an active transcriptional complex at the promoter of the survival and proliferative genes A1 and c-Myc [61]. Intriguingly, however, the same study found that more proximal events in the BCR pathway, including classical protein kinase C and I κ B kinase activation, NF- κ B nuclear translocation, and even NF- κ B DNA binding were intact in T1 B cells. These researchers concluded that T1 B cells are programmed for signal and stage-specific "nuclear non-responsiveness" upon BCR stimulation alone [61]. However, an important point is that upon stimulation with CpG, a ligand for the endosomal pattern recognition receptor TLR9, T1 B cells exhibited normal expression of the key survival and proliferation genes A1 and c-Myc [61]. These results strongly suggest that T1 B cells receiving Ag-stimulation through the surface IgM receptor in the absence of other co-stimulatory signals results in death or negative selection of these B cells. In vivo, this would presumably result in the elimination of self-Ag reactive clones in the spleen [33]. Thus the T1 B cell stage represents an opportunity for negative selection or tolerance induction against peripheral antigens as opposed to central tolerance which depends on BM antigens and stromal signals in the BM [33].

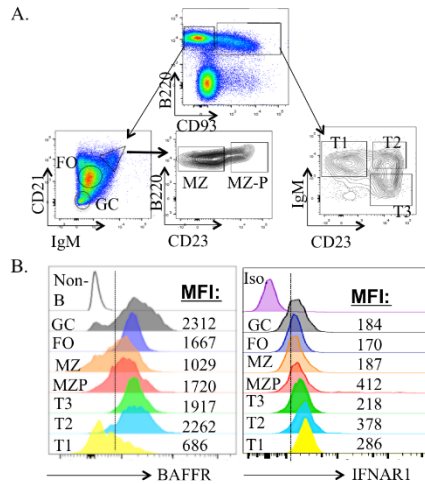


Figure 2. BAFFR and IFNAR1 expression on B cell subsets (A) B cell gating strategy and (B) FACS analysis of BAFFR and IFNAR1 expression on the indicated B cell subset in BXD2 mice.

Development of T1 B cells into T2 and T3 B cells requires some endogenous Ag stimulation or “BCR tickling”. Examination of BXD2 vs. BXD2 MD4 Tg mice where all B cells express a HEL-specific B cell receptor revealed that B cell development is blocked at the T1 stage in BXD2 MD4 Tg mice lacking endogenous Ag stimulation (Figure 3). Normally, T1 B cells are characteristically highly sensitive to negative selection [33, 62]. Rapid death of T1 B cells occurs in culture when the cells are unstimulated or stimulated through the BCR. This lack of survival and proliferation responses following strong BCR stimulation is a defining feature of T1 B cells, while T2 B cells exhibit a characteristic heightened activation and proliferation in response to BCR stimulation [62]. This was established clearly by Wasif Khan’s laboratory, which conducted studies to compare the induction of these BCR signaling pathways in discrete stages of B cell maturation, including the T1, T2 and mature B cell population.

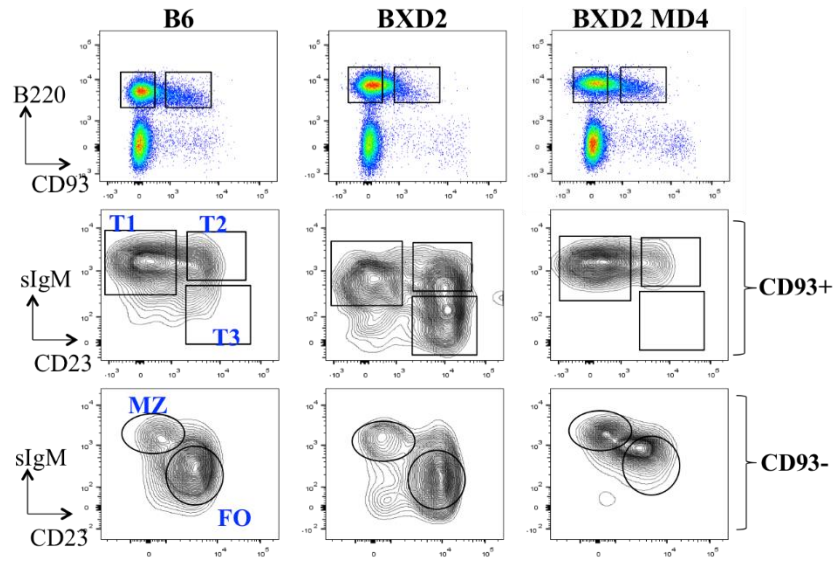


Figure 3. FACS analysis of spleen B cell development in the indicated mouse strain.

T1 B cells were shown to die in response to BCR signals, whereas T2 cells were stimulated to express activation markers and the pro-survival gene *Bcl-xL*, and to proliferate [62]. Importantly, BrdU labeling experiments from other laboratories have shown that T1, T2 and T3 B cell subsets lacked significant levels of proliferation *in vivo*, indicating that maturation of peripheral transitional B cells may not be accompanied by entry of developing cells into the cell cycle [45]. However, examination of BXD2 mice spleen transitional B cells revealed increased $Ki67^+$ T1 and T2 B cells vs. age matched B6 mice (Figure 4). Nevertheless, essential components of BCR signal transduction, including MAPK ERK1/2, p38, and Akt were preferentially activated in T2 B cells in response to BCR engagement *in vitro*, whereas T1 B cells did not induce significant phosphorylation of these [62]. Diacylglycerol (DAG), a lipid second messenger involved in proximal BCR signaling and another intermediate, inositol 1,4,5-triphosphate, were

also shown to be produced preferentially in T2 compared with T1 B cells upon BCR cross-linking [63]. It was proposed that the combined action of DAG and calcium signaling is necessary for survival and differentiation of T2 into mature B lymphocytes and that calcium signaling in the absence of DAG-mediated signals may lead to T1 B cell death [63].

These observations are consistent with Carsetti and colleagues' early 1995 proposal that the T1 B cell stage is the principle stage of peripheral negative selection. They showed that this negative selection occurs in the splenic B cell compartment in a defined window of differentiation between the immature and the mature stage (i.e. the transitional B cell stage) [33]. They further speculated that micro-environmental cues in the early phases of development most likely modulate the continuum of effects following IgM cross-linking [33]. Crosslinking of membrane IgM normally results in the rapid phosphorylation on tyrosine residues of different substrates including phospholipase C- γ . Activated phospholipase C- γ initiates a signaling pathway leading to Ca^{2+} influxes and to protein kinase C activation [64]. The fact that T1 and T2 B cells exhibit different sensitivities and responses to BCR crosslinking suggests that these responses are developmentally regulated [62]. Together, the studies suggest that differentiation of T1 B cells to the T2 stage may depend upon the physiological milieu of the spleen [62] (Figure 5).

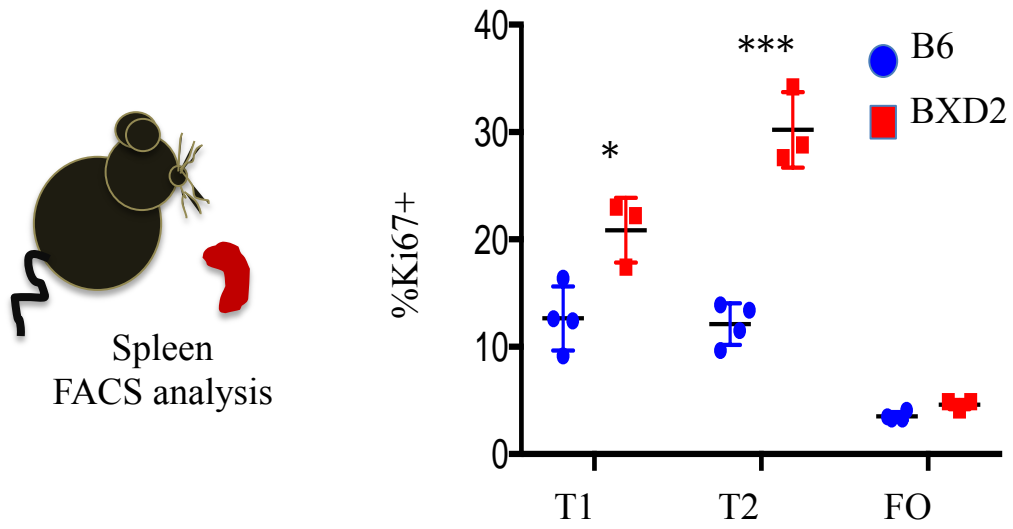


Figure 4. FACS analysis of Ki67 expression in spleen B cells from B6 and BXD2 mice

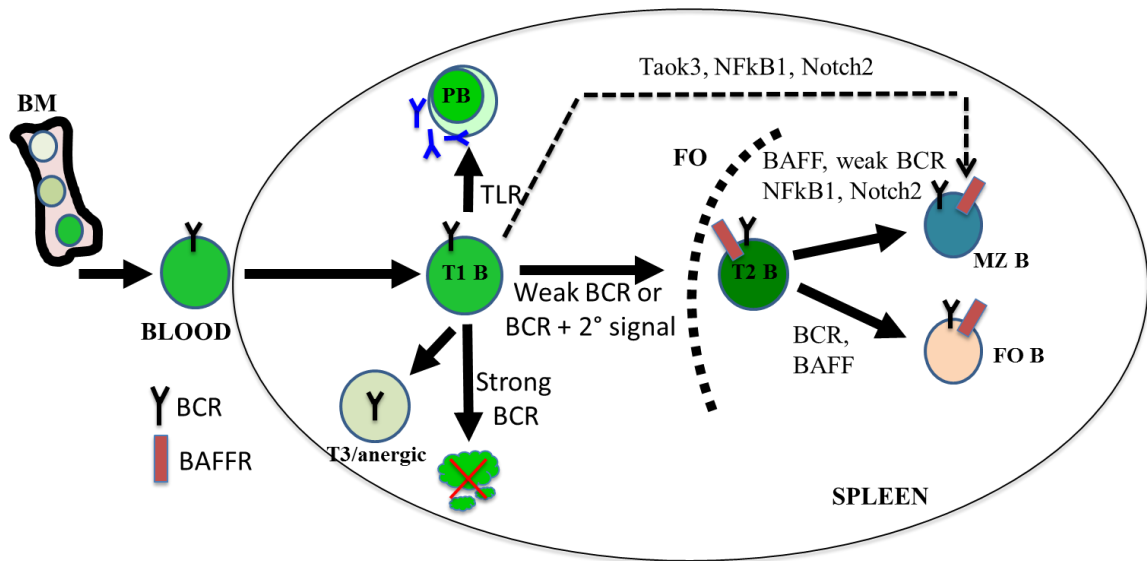


Figure 5. Negative selection and fate of self-reactive immature B cells likely occurs at the T1 stage [51]. Negative selection can occur by multiple mechanisms, including deletion or anergy [56]. Positive selection to the T2 stage is accompanied by upregulation of the BAFFR [58] and increased dependence BAFFR-mediated survival.

Human Transitional B Cells

There have been varying reports describing whether transitional B cells are increased or decreased in SLE patients. Lee *et al.* reported an expanded population of CD5⁺ B cells in SLE patients with some features of transitional B cells and some features of naïve B cells [65]. Chang *et al.* in 2008 described an increased population of activated (CD80/CD86⁺) naïve B cells in SLE patients [66]. They also describe increased activation in transitional B cells, though the percentage increase in T1 and T2 B cells was either not significant or modestly significant [66]. There have been few studies characterizing human spleen transitional B cells, but one study examined different lymphoid tissues for transitional B cells by combining surface markers (CD38, CD24,

CD27, IgD) with dye extrusion. They found that T1, T2, and T3 B cells were dominant in cord blood. Splenic B cells displayed a shift towards poor R123 extrusion with enrichment for T2 and late transitional B cells relative to mature naïve, suggesting that this is the site of their development at least under physiological circumstances. They also resolved nine populations of B cells in human spleen including T1, T2, T3, and MZP subsets using FACS analysis. Importantly, they found that one distinction in the human spleen compared to peripheral blood and cord blood was the up-regulation of activation markers on a fraction of all B cell subsets, although most pronounced on the T1 and T2 cells, further suggesting that the spleen is the site of activation and differentiation of early transitional B cells [48].

Peripheral counter-selection of self-reactive and polyreactive peripheral B cells occurs at the transitional B cell stage in the spleen. In a seminal study, 222 Abs were cloned and expressed from single transitional vs mature naïve B cells derived from the peripheral blood of three untreated adolescent SLE patients [39]. These Abs were tested for reactivity to nuclear antigens. The investigators found that, in the Abs derived from transitional B cells, the same level of HEp-2 reactive Abs was detected in the SLE patients and healthy control subjects. However, Abs from mature naïve B cells from all three SLE patients differed from healthy controls in that they retained high levels of HEp-2 ANA ELISA-reactive Abs (41.5–50.0% compared with 20.4% in controls). The authors also found significantly increased polyreactive autoAbs expressed in the mature naïve B cell subsets of the SLE patients [39]. This study concluded that this peripheral pre-naïve B cell selection checkpoint was defective in SLE [39]. Another study using a similar approach with rheumatoid arthritis (RA) patients concluded that RA patients also

fail to remove autoreactive B cells in the periphery between the new emigrant and mature naïve B cell stages, revealing a defective second checkpoint in B cell tolerance. This suggests that failure to induce B cell tolerance at the transitional B cell stage may be a common feature of multiple autoimmune diseases.

Transitional B Cell Cytokine Production

Transitional B cells in mice and humans have been proposed to be regulatory B cells or “B_{reg}” cells [67, 68]. Transitional B cells appear to have a heightened ability to secrete both regulatory and inflammatory cytokines including IL10 [69] and type I IFNs [70]. Ward *et al.* recently identified B cell endogenous IFN α production in a subset of SLE patients expressing high levels of the transcription factor A-T rich interacting domain 3a (ARID3a) in their B cells. In healthy controls, ARID3a was not expressed in early naïve B cells; yet in SLE naïve and transitional B cells, the ARID3a protein was abundantly expressed and strongly correlated with IFN α expression [70]. Interestingly, transitional B cells in this study exhibited the highest secretion of IFN α (mean 40% IFN α ⁺) compared to naïve and MZ memory sub-populations (<5 and 20% IFN α ⁺, respectively) [70].

Transitional have also shown to produce more IL-10 and express higher levels of IL-10 receptor after CD40 engagement compared to other B-cell subsets [69]. Furthermore, under this stimulatory condition, the transitional B cell produced IL10 induced downregulation of CD86 which led to reduced T-cell proliferation [69]. An important clinically relevant role for cytokine production by human transitional B-cells has been described in transplant patients. Cheruruki *et al.* reported that that T1 cells in humans expressed a significantly higher IL10 vs. T2 and mature B cells. The ratio of IL-

10 to TNF- α was higher in T1 B cells compared to T2 B cells or other B subsets. Furthermore, the ratio of T1/T2 B cells was strongly and independently associated with allograft dysfunction in patients who had undergone renal transplant [71]. A recent study in human SLE patients suggested that positive crosstalk between CpG-stimulated pDCs and CD24^{hi}CD38^{hi} transitional B cells can promote or suppress the development of IL10⁺ B_{reg} cells depending on the concentration of type I IFNs, suggesting that transitional B cells and multiple other cell types are involved in the dysregulated type I IFN network [72].

Type I Interferon: Basic Established Concepts

Classes and Isoforms of the Type I Interferon Family

The type I interferon family consists of at least 13 IFN α genes in humans (14 in mice) and a single IFN β gene, and several poorly defined single gene products (IFN δ , IFN ϵ , IFN κ , IFN τ , IFN ω , and IFN ζ) [73, 74]. IFN- α , IFN- β , IFN- ϵ , IFN- κ , IFN- ω are expressed in humans, whereas IFN- δ and IFN- τ are expressed in porcine and ovine or bovine embryonic development, respectively [74]. In the human genome, all the type I IFN genes are located on chromosome 9, with fifteen genes clustered in a single 364-kb region (21.0–21.4 Mb) [75]. The mouse type I IFN gene cluster has been localized to a cluster of similar size on the centromere-proximal region of *Mus musculus* chromosome 4 [76].

All type I interferons (13 different IFN α s, 1 IFN β and 1 IFN ω) signal via binding to the same receptor chains, IFNAR1 and IFNAR2 [77]. However, their downstream effects on target cells are not redundant, and appear to be highly plastic

and tunable depending on the target cell [78, 79] and other molecular factors [80]. Although type I IFNs share a similar range of potential activities, they vary substantially in their binding affinities to the common receptor chains (IFNAR1 and IFNAR2) [81], their potency to respond to different viruses, anti-proliferative activity, and ability to activate cells of the immune system [80]. The pleiotropic character of the type I IFNs is partly due to their large range of specific binding affinities for IFNAR1 and IFNAR2. Most IFN α subtypes bind the IFNAR1 receptor at μ M affinity, and the IFNAR2 receptor at nM affinity [81]. The weakest binder to IFNAR2 is IFN α 1 and the tightest is IFN β (200 nM versus 0.2 nM affinity). All IFN α s bind IFNAR1 with similar low affinities of 1–5 μ M, while IFN β binds significantly more tightly, at 50 nM affinity.

Signal Transduction for Type I IFN

All type I IFNs signal through interaction with the two type I IFN receptor chains, IFNAR1 and IFNAR2 [77]. These human proteins were cloned in the 1990s [82] along with their murine homologues [83]. These studies supported the view that the murine IFN system is similar to the human system in ligand complexity, specificity of receptors, and signaling components and thus represented a good system to model human effects [84]. The most accepted molecular mechanism for is that for all type I IFNs, the initial interaction is binding to the high affinity IFNAR2. This recruits the lower affinity IFNAR1 into a dynamic equilibrium which forms a trimeric structure with conformational changes enabling signaling [80, 85]. Intracellularly, the formation of this ternary complex also brings together the intracellular domains of these receptors and their

associated signaling adaptors, which initiate signal transduction [74] (Figure 6). The recruitment of IFNAR1 and formation of the ternary signaling complex is a major point of regulation for type I IFN signaling [85]. The negative feedback regulator ubiquitin-specific protease 18 (USP18) potentially interferes with the recruitment of IFNAR1 into the ternary complex. Thus, the responsiveness to lower affinity type I IFNs like IFN α 2 is potentially down-regulated after the first wave of gene induction, while IFN β , due to its 100 fold increased affinity is still able to effectively recruit IFNAR1 [85]. Stable ternary complexes are recycled to the endosome [86]. The differential binding affinities have also been linked to differential receptor endocytosis which is thought to be another key regulator in the differential signaling outcomes of the various IFN subtypes [80, 86]. Together the receptor dimerization, receptor endocytosis and intracellular IFNAR-associated proteins regulate the duration and strength of signaling activity, which is responsible for tunable cellular responses including cytotoxicity and immune-modulatory activities [80].

The best characterized signal transduction proteins that pre-associate with the type I IFN receptor chains are Tyk2 (with IFNAR1) and JAK1 (with IFNAR2) [87, 88]. Upon ligand binding, these kinases phosphorylate latent cytoplasmic transcription factors signal transducer and activator of transcription 1 (STAT1) and STAT2 [89]. Tyrosine-phosphorylated STAT1 and STAT2 dimerize and translocate to the nucleus, where they assemble with IFN-regulatory factor 9 (IRF9) to form a trimer complex called IFN-stimulated gene factor 3 (ISGF3). ISGF3 binds to IFN-stimulated response elements (ISREs; consensus sequence TTTCNNTTTC) in the DNA, thereby directly activating the transcription of a variety of type I IFN stimulated genes (ISGs) [90]. This pathway is

active in most cell types and functions to elicit a robust antiviral response [90]. Although the Jak/Tyk/STAT1/STAT2 pathway is the best characterized canonical pathway, there are other STAT proteins that can be induced by type I IFN. STAT5 and STAT6 can be induced by type I IFN in certain cell types [91]. Additionally, other kinases besides Jak and Tyk can be induced by various IFN subtypes depending on the target cell. The PI3K and p38 kinase pathways have also emerged as important mediators of IFN-induced signal transduction in T and B lymphocytes [92-94].

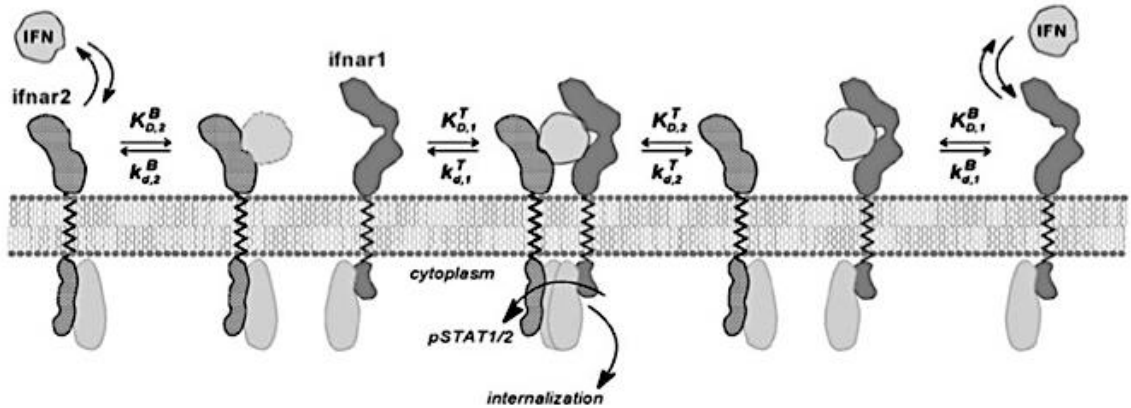


Figure 6. Ternary complex formation. Image from *Kalie et al. J Biol Chem. 2008.*

Type I IFN in SLE

The dysregulation of type I IFN is one of the strongest correlations with SLE. In addition to its well-documented role in antiviral host responses, dysregulated production of and responses to type I IFN are significant events in disease development and progression [2]. The first indications of a causative role for type I IFN in human autoimmune diseases was the observation of an increased

occurrence of autoantibodies and autoimmune diseases during type I IFN treatment [95]. There are reports of increased IFN α in the sera of lupus patients compared to healthy controls [96]; however, the circulating levels are generally so low that it is difficult to measure serum IFN directly with sensitivity and reproducibility. For this reason, measurements of serum IFN often involve the measurement of type I IFN stimulated gene expression in peripheral blood mononuclear cells (PBMCs) [97]referred to as a “type I IFN signature.” This type I IFN signature is highly associated with autoantibodies to RNA binding proteins (RBP) [98] and has been associated with renal flares and SLEDAI [99]. Correlation of the type IFN gene signature with disease flares has been reported in some cohorts [100], and a lack of correlation found in others [101]. Although the clinical significance of these IFN clusters is not yet completely clear, it is of interest that recent transcriptional repertoire analyses have identified distinct type I IFN signatures, some of which appear to be driven by IFN- α , and a separate cluster more signature of IFN- β induction [102].

pDCs

The identification of pDCs in mice in 2001 stimulated intensive research into the role of pDCs in infection and autoimmunity [103]. Plasmacytoid dendritic cells are a small population of cells specialized for producing large amounts of type IFN- α following acute stimulation with virus nucleic acids. These specialized cells are activated in rheumatic diseases, and are thought to be major producers of IFN- α which acts as an immune adjuvant and contributes to the autoimmune process [104, 105]. Plasmacytoid

dendritic cells detect viral nucleic acids through TLR7 and TLR9, which are located in specialized endosomes [106]. These receptors trigger a MyD88-dependent signaling pathway that leads to production of IFN- α/β . Most of the data linking pDCs to SLE pathogenesis in humans are correlative. The phenotype and frequency of pDCs in the circulation have been inconsistent, though they are relatively low in circulation relative to other cell types. Several studies have reported that pDCs and DCs accumulate in the kidney [107, 108] and cutaneous tissue lesions [109] of SLE patients (tissue pDC findings in humans summarized in Table 1). However, the data that these cells produce large amounts of IFN at these sites is lacking, and few studies include measurement of type I IFN genes or protein in isolated pDCs. In a recent comprehensive study of B cell and pDC dysregulation in SLE patients, the authors reported a modest (<2 fold) increase in IFN α 1 expression within freshly isolated pDCs in SLE patients vs. healthy control pDCs [72]. Another recent study specifically investigated cellular sources of IFN α protein and reported consistent results that circulating pDC IFN- α was not higher in SLE patients compared to healthy controls, though pDCs from patients harboring dominant mutations in *IFIH1* and *TMEM173* (STING) did exhibit higher IFN- α production [110].

Consistent with this, studies in mice have shown that autoAb generation combined with abnormalities in pDCs can occur in the absence of increased IFN- α pDC production, suggesting that there must be additional complexity in the generation and regulation of IFN- α beyond this mechanism [111]. Nevertheless, pDCs are widely thought to be the primary drivers of autoreactive B cell generation in human lupus based in part on the dependency of B cells on type I IFN for TLR7 and TLR9 mediated activation and subsequent differentiation into Ab producing cells [112, 113]. However,

unlike autoreactive B cells, pDCs lack a specific antigen receptor capable of delivering TLR ligands to endosomal compartments, and are thus unlikely to be the primary sensors of nuclear antigens. Instead, pDCs appear to be stimulated “downstream” of B cell activation and autoantibody production and immune complex formation [114-116]. Consistent with this, available data regarding pDC accumulation in SLE tissues suggests pDC infiltration into kidney tissue is associated with later stages or more severe disease. Fiore *et al.* found that pDCs (BDCA-1, BDCA-3, or BDCA-4+ cells) were increased in the class III-IV kidneys, but not in class I, II, or V kidneys [107]. Tucci *et al.* had a higher sample number, and showed similar findings that BDCA-2⁺ cells were associated with more severe nephritis [108]. The authors did not study type I IFN production but focus on the cytokine IL18, which exhibited strong staining in severe LN kidneys. The authors propose that IL18 production by resident kidney cells recruits pDCs, which in turn skew the Th1-Th2 balance resulting in increased IL12, IFN γ and reduced IL4 in the sera. In contrast, experiments involving manipulation of pDCs in mouse models of SLE suggested an important role for pDCs during the onset of disease in BXSB lupus-prone mice [117].

Apoptotic Cell Clearance Defects

Although dysregulation of the type I IFN system in SLE has been known for decades, it is still unclear exactly what is the cause of the dysregulation. Certainly, as SLE mimics a sustained antiviral response, it has been hypothesized that a viral infection may trigger onset of SLE [3], though no causative virus has been identified. Apoptotic cell clearance defects have been shown to be associated with the development of lupus in

mice and humans [118], and apoptotic debris immune complexes can stimulate type I IFN production in various cell types [3, 119]. An important question is what comes first, type I IFN dysregulation or AC clearance defects? Our laboratory has previously shown that type I IFN signaling is elevated and required for disease in BXD2 mice [21-23]. In BXD2 mice, type I IFN-induced follicular shuttling of membrane lymphotoxin- β (LT- β) expressing MZ B cells disengaged interactions between these MZ B cells and LT- β receptor-expressing marginal zone macrophages (MZMs), leading to defects in MZM actin polymerization and mechano-sensing mechanisms. The resulting defective F-actin polymerization led to an inability to clear apoptotic cells (ACs), and, eventually, MZM dissipation which was identified in the spleens of BXD2 mice and lupus patients [15]. This study provided a mechanism where type I IFN signaling initiated AC clearance defects, while the resulting stimulation by uncleared AC leads to a “vicious cycle” of more type I IFN production [15].

In these aforementioned studies and others from our laboratory [15, 16, 23] MZ and MZ-P B cells were the target of type I IFN signaling. However, an important question is whether type I IFN dysregulation of MZ B cells might be preceded by earlier defects in B cell development or IFN dysregulation. Recently, MZ B cell commitment has been proposed to occur at the T1 B cell stage [51]. Other studies have highlighted the action of type I IFN at the transitional B cell stage [70, 120]. Chang *et al.* reported that, in SLE patients, altered BCR signaling, decreased apoptosis, and increased proliferation was most marked in the transitional B cell subset and that these phenotypes could be recapitulated by pre-incubation with type I IFN [120]. This suggests that type I IFN dysregulation of B cells may be imprinted at the earliest B cell developmental stage in the

spleen, an event which could potentially affect the B cell repertoire as type I IFN can promote B cell survival [121] and alter the stringency of B cell selection [122], thus altering the MZ and FO B cell pool.

	Patient #	Tissue	Main Finding	Measurement of cellular IFN	DC markers	# citations
Blomberg et al., Lupus, 2001	11	Skin	IFN α ⁺ cells present in biopsy	ISH, IHC	None	>100
Farkas et al. Am. J. Pathol., 2001	10 (DLE)	Skin	MxA ⁺ CD123 ^{high} CD45RA ⁺ cells in biopsy	IFN response gene (MxA ⁺)	CD123 ^{high} CD45RA ⁺	>600
Rönnblom and Alm, Human Immunology, 2002	1	Lymph node	IFN α ⁺ cells present in biopsy	IHC	None	19
Fiore et al.* Mol. Immunol., 2008	15 (LN)	Kidney	BDCA-1/3/4 ⁺ cells increased in late stage LN	None	BDCA-1/3/4 ⁺	96
Tucci et al.** Arth. & Rheum., 2008	35	Kidney	IL18 and BDCA-2 ⁺ cells increased in severe LN	None	BDCA-2 ⁺	>100

Table 1: Summary of pDC findings in SLE tissue.

*In Fiore et al, the authors studied lupus nephritis kidney biopsies using immunofluorescence. The biopsies were segregated based on classical diagnostic histological severity (Weening et al., 2004). The authors found that pDCs (BDCA-1, BDCA-3, or BDCA-4⁺ cells) were increased in the class III-IV kidneys, but not in class I, II, or V. This suggests that pDC infiltrate into lupus kidneys is associated with later stages of disease, but wanes in the most advanced lupus nephritis cases.

**Tucci et al. had a higher sample number, and showed consistent findings that BDCA-2⁺ cells were associated with more severe nephritis. The authors did not study type I IFN production but focus on the cytokine IL18, which exhibited strong staining in severe LN kidneys. The authors propose that IL18 production by resident kidney cells recruits pDCs, which in turn skew the Th1-Th2 balance resulting in increased IL12, IFN γ and reduced IL4 in the sera. (*DLE, discoid lupus erythematosus; LN, lupus nephritis; ISH, in situ hybridization; IHC, immunohistochemistry*)

Type I Interferon: Developing Concepts for Human Autoimmune Disease

Cell-Specific Analysis of IFN Signaling

Ligation of IFNAR has classically been associated with three major outcomes: antiviral and antimicrobial response, anti-proliferative response, and activation of innate and adaptive immune cells [90]. The antiviral state induced by type I IFN is very robust and characterized by the induction of IFN-inducible genes within a couple hours even after stimulation with picomolar quantities of IFNs [80, 123]. However, the anti-proliferative and immunomodulatory functions induced by type I IFNs is cell-type specific and requires higher interferon concentrations or high-affinity IFN β [80]. These disparate cellular responses to IFNAR ligation depend not only on the IFN subtype, but also on the target cell type and developmental stage, as well as the duration (acute vs. chronic) of stimulation. For example, data suggest that virus induced type I IFNs can have either a positive or a negative influence on dendritic cell (DC) development and activation [124], likely dependent on the DC developmental state and virus specific contexts which may lead to the selective induction of STAT1 or STAT2 [124, 125]. Similarly, acute type I IFN signaling can promote the development and differentiation of antigen presenting cells through enhancing granulocyte-macrophage colony-stimulating factor (GM-CSF)-mediated differentiation of monocyte precursors into mature DCs [126]. However, chronic type I IFN was shown to inhibit DC function and induction of immune-regulatory IL10 [127].

In B cells, type I IFN induces expression of activation proteins including the C-Type lectin surface protein CD69 [21, 128] and co-stimulatory surface protein CD86 [23]. It also promotes B cell receptor (BCR) induced survival responses [121] and T cell

independent B cell responses [113]. Three recent studies reported an opposite and timing-specific effect of Type I IFN on virus-specific B cells using a model of LCMV infection [129-131]. These studies found that type I IFN promoted “B cell decimation” of virus-specific B cells, which was due in part to rapid formation of plasmablast formation [129] and indirect effects via activation of cytotoxic T cells [129, 130]. Interferon- α can also activate dormant hematopoietic stem cells in vivo [132].

The effects of type I IFN on T cells is also wide-ranging and dependent on the context. Type I IFN signaling on T cells prevented their rapid elimination in vivo by upregulating molecules that inhibited cytotoxic natural killer (NK) cells [133]. More generally, type I IFNs function as “signal 3” cytokines, supporting T cell differentiation, proliferation and survival [134]. Conversely, type I IFN can also induce anti-proliferative and pro-apoptotic programs in T cells. The divergent outcomes are generally thought to be determined based on the relative timing of co-signals, such as T cell receptor (TCR) signaling and molecularly, differential STAT homo and hetero-dimer activation.

In SLE specifically, it is becoming increasingly recognized that different cell types contribute uniquely to the IFN signature [91, 135]. Importantly, there is also heterogeneity among different lupus patients and different ancestral background in terms of the IFN-stimulated gene (ISG) expression. Measurement of ISG in sorted peripheral blood CD4 T-cells, CD8 T-cells, monocytes, and B cells collected from African-American (AA) and European-American (EA) SLE patients revealed that ISGs were not upregulated synchronously in all cell types from a given patient. Moreover, the ancestral background of the patients significantly affected the concordance of ISG expression across various subtypes [1]. Another recent study identified distinctive cell type specific

contributions to the blood IFN signature [136]. Interestingly, SLE B cells exhibited approximately 30% more differentially expressed transcripts than their CD4⁺ T lymphocyte counterparts [136]. However, an important potential confounding variable raised by the authors is the altered subset composition in SLE relative to healthy controls [136, 137]. Thus, the transcriptional profiles identified in whole CD19⁺ B cells may be influenced by the distributions of different B cell subtypes. These previous studies, however, did not include measurement of IFN genes themselves. This is due in part to an underlying concept that pDCs are the reservoir from which excessive amounts of type I IFN are generated. Thus, IFN signature measurements of human PBMCs do not include analysis of the expression of IFN genes themselves [99-101, 138, 139]. However, it is becoming evident that different cell populations can contribute to type I IFN production and also respond differently to the IFN exposure. There is currently a lack of knowledge about the relative contribution of different cell types to IFN α and IFN β production and how this may modulate the immune response.

Constitutive Type I IFN in Homeostasis and Disease

In the late 1950s and 1960s after IFN was discovered, type I IFN it was considered to be a specific virally induced substance without any effect on normal cellular metabolism [140]. However, it is accepted today that low levels of spontaneously produced (i.e. absent any apparent specific inducer) type I IFN secretion can have important regulatory effects on normal cellular functions [140]. Constitutive production of type I IFN in uninfected cells is a well-established phenomenon both in vitro and in vivo [91, 141-146]. What is the normal function of such ‘spontaneous’

interferon production, and is this relevant to human disease? Considering the half-life of type I IFN is only a few hours, the proximity of cells to an IFN source may be essential for a timely immune-response [147]. Consistent with this, low-level constitutive or endogenous IFN production is essential for setting expression levels of important signal intermediates such as IRFs [142] and STATs [91] thus determining whether or not downstream signaling mechanisms will operate effectively upon challenge. The constitutive weak IFN- α/β signal is capable of exerting effects on virtually all cells, effectively priming immune cells to enhance their specialized response to other stimuli [145]. What is the mechanism for the constitutive type I IFN production? Secondly, how does the spontaneous type I IFN from diverse cell types contribute to the pathogenesis of type I IFN mediated diseases such as SLE and the various other interferonopathies [148]?

Normally, activation of type I IFN transcription occurs when regulatory elements in the IFN- α/β promoter regions bind members of the IRF family of transcription factors [149]. The IRF family contains nine members, of which IRF-3 and IRF-7 are crucial for expression of IFN- α/β , though induction of the short-lived IRF7 appears to be the critical factor for maximal induction [150]. Both IRF-3 and IRF-7 reside in the cytoplasm of uninfected cells, and undergo nuclear translocation upon viral infection [150, 151]. These factors have non-redundant roles, as demonstrated by the fact that IRF7 is short lived, while IRF3 is more stable and is constitutively expressed. Consistent with this, early type I IFN induction of IFN- α 4 and IFN- β can occur in the absence of IRF7, although IRF7 is required for positive feedback [145, 151].

What drives the spontaneous type I IFN production in the absence of any virus infection? The low-level production occurs in the absence of IRF3 and IRF7 [151], so

what is the mechanism of the spontaneous IFN? The IFN- β enhancer and promoter is one of the most well-studied and well-characterized gene-regulatory elements [152]. The IFN β promoter contains four positive regulatory domains (PRD I-IV), which are occupied by overlapping transcription factor complexes [143]. IRF3 and IRF7 bind PRDI and III; the AP-1 heterodimer of ATF-2 and c-Jun binds PRDIV; and the NF- κ B p50-RelA heterodimer binds PRDII [143]. IRF3 and IRF7 are critical for virus induced IFN and positive feedback [151], but less is known regarding the mechanism of constitutive IFN β . It has been proposed that constitutive IFN β is characterized by a switch from dependency on IRF3 and IRF7 to c-Jun and NF- κ B components. In contrast to pathogen-induced IFN β production, deletion of IRF3 does not prevent constitutive IFN β expression in MEFs [142]. In addition, deletion of IRF9, which resulted in undetectable amounts of IRF7 had no impact on constitutive IFN β [142]. In contrast, deletion c-Jun, which normally occupies PRDIV on the IFN β promoter in uninfected cells, decreased constitutive IFN β expression by half [153]. The importance of NF- κ B subunit RelA to constitutive IFN β has not been directly measured, but is likely important as well, as RelA binds to PRDII in unstimulated cells and loss of RelA causes gene expression defects in unstimulated cells resembling loss of IFN [143, 154]. Additionally, it has been suggested that repressive p50 homodimers which bind the PRD1 and PRDIII regions may be incompletely repressive, enabling basal levels of IFN β production [155]. Regarding the stimulus of the constitutive type I IFN production, basal production may be maintained by commensal microbiota, though this has not been thoroughly investigated in germ-free mice.

Unique Properties of IFN β

There is a perception in the lupus research field that IFN- α is the main driver of SLE pathogenesis. This idea is partially due to the relative abundance of the type I IFN subtypes, where some IFN- α subtypes are more readily detectable in circulation vs. IFN- β [156-158]. Consistent with this, the induction of IFN-response genes PRKR, IFIT1, IFI44, MX1 by SLE plasma was inhibited >90% by anti-IFN α antibody, but not by anti-IFN β or anti-IFN γ antibodies [159] leading to the conclusion that IFN α , rather than IFN β or IFN γ , is present in many SLE plasma samples [159]. A positive correlation between serum IFN α and various disease parameters has also been established [160]. However, these studies have been limited by an inability to detect more rare IFN species including IFN- β . The relative lack of detectable IFN- β in serum is likely due to its fold higher affinity for the IFNAR1 and IFNAR2 [80, 161].

In addition to higher affinity to the IFN receptor chains, another unique property of IFN- β is its unique properties of early induction and ability to stimulate other type I IFN gene expression. It has been reported that in the absence of priming amounts of IFN β , mouse embryo fibroblasts do not produce other type I IFNs [162], highlighting IFN β as an early response master regulator of other type I IFN activities. Priming with IFN β is also required for optimal responses to other cytokines. Priming IFN β -deficient MEFs with low dose IFN β restored IFN γ -mediated antiviral responses and increased resistance to influenza virus by promoting activation of DCs [143, 163, 164]. Selective effects of IFN- β compared to IFN- α have been reported in different cell types [91] including osteoclasts [165],

dendritic cells [166], monocytes and B cells [79]. A study of multiple sclerosis patient samples showed that monocytes, B cells, and T cells showed substantial differences in signaling and cellular effects in cells stimulated in vitro [79]. Interestingly, stimulation of different cell types with IFN β resulted in completely different cell fates. In monocytes and granulocytes stimulated with IFN β , there was a strong induction of cell-surface TNF-related apoptosis-inducing ligand (TRAIL). In contrast in B and T cells, TRAIL was not induced; however, IFN β induced activation of p38 and/or NF- κ B in these cell populations [79].

As mentioned above, constitutive IFN β has a unique property to set the expression levels of the various STAT proteins. In IFN β ^{-/-} cells, the expression of STAT1 and STAT2 is diminished enabling receptor binding access for other STAT proteins. In this way, low levels of IFN β is critical to regulate responses to diverse stimuli of the JAK-STAT pathway by shifting the ratio of active STATs [143, 145]. Interestingly in IFNAR2 knockout mice, IFN β can bind to and signal through the low-affinity IFNAR1, but does not activate the conventional JAK/STAT signaling pathway [167]. This is significant, as different combinations of STAT protein availability and action can produce different downstream effects. Signaling through STAT1 is known to be pro-inflammatory, anti-proliferative and pro-apoptotic, as opposed to signaling through STAT3, STAT4 and STAT5, which induces gene transcription that promotes cell survival, proliferation and differentiation [168, 169]. Thus, the intracellular competition between STAT1, and STAT3, STAT4 and STAT5 determines the transcriptional and functional consequences of type I IFN signaling [135].

The differential responses induced by IFN β vs the IFN α subtypes are likely

to be important in mediating specific IFN-dependent effects on various tissues or cells [91]. IFN β is the tightest binder to IFNAR1 and IFNAR2 is IFN β (10 and 100-1000 fold greater than most of the other type I IFNs, respectively) [81]. The relative affinities of the IFN subtypes are conferred by differences in amino acid residues, and this is thought to be the molecular basis for the differential signaling activities of IFN β [80].

Primary work by Lamken et al [161] reported that IFN β exhibited higher affinity for both receptor chains, IFNAR1 and IFNAR2 [80]. This is an important and biological meaningful point, as allows for “a more efficient ternary complex formation at low receptor surface concentrations and longer stability of individual ternary complexes compared to IFN α 2 [and other IFN α s] [161].” Regulation of IFNAR1 and IFNAR2 expression levels is a major mechanism controlling the potency of cell responsiveness to IFN β [170]. Several studies have demonstrated that IFN β induces endocytosis and degradation of IFNAR1 to regulate the cell signaling [80, 90, 171]. Down-regulation of IFNAR1 appears to occur rapidly in a tunable fashion, while IFNAR2 expression displays a slower basal turnover [172]. Additionally both IFNAR2 and IFNAR1 can interact with IFN β , and thus both complexes (IFN β /IFNAR1 and IFN β /IFNAR2) are able to transmit signals to induce genes [167] a relevant fact that could explain differences in the response to IFN β treatment [170].

Nucleic Acid Sensing

The presence of autoAbs targeting self-nucleic acid or nucleic acid-binding proteins implicates dysregulation of nucleic acid sensing pathways in SLE [173]. Viral

and bacterial DNA and RNA potently stimulate innate immunity through toll-like receptors (TLR) and non-TLR signaling cascades. Self-nucleic acid and nuclear DNA/RNA binding proteins are normally restricted to the nucleus or the mitochondria, away from the DNA/RNA sensors. In SLE, activation of these sensors occurs leading to activation of the innate and adaptive immune system [3, 173]. Additionally, genetic variations in many of the components of the TLR signaling pathway have been associated with SLE, such as TLR-7, IRF5, IRF7, IRF8, IRAK1, and TNFAIP [173-175].

All TLR family members, including TLRs-7, -8, -9 are type I membrane proteins composed of a ligand-binding ectodomain, a transmembrane domain, and a conserved cytoplasmic toll/interleukin-1 receptor (TIR) domain [173, 176]. Ligand-induced dimerization and conformational rearrangement of the TIR domains leads to intracellular activation of two main adaptors are utilized by TLRs, namely Myeloid Differentiation Factor-88 (MyD88) (TLR-7, -8, and -9) and TIR domain-containing adaptor inducing IFN- β (TRIF) (TLR-3) [173]. Different immune cell types are known to express a cell-specific set of TLRs [176]. Human B cells and pDCs are the only cells known to express both TLR7 and TLR9 [177] (Table 2).

There are also TLR independent nucleic acid sensors that are important in antiviral immunity and implicated in autoimmune disease. RIG-I (retinoic acid – inducible gene I) and MDA5 (melanoma differentiation – associated gene 5) are RNA helicases with caspase recruitment domains (CARDs) and signal through the mitochondrial antiviral signaling protein (MAVS) and IRF3–IRF7 to induce type I IFNs following RNA recognition [173, 178]. Currently, cGAS is the most widely accepted dsDNA sensor which activates innate immune responses through production of the

second messenger cGAMP, which activates the adaptor stimulator of interferon genes or STING [179].

	Human				Mouse			
	TLR3	TLR7	TLR8	TLR9	TLR3	TLR7	TLR8*	TLR9
pDCs		+		+		+		+
B cells		+		+		+		+
Monocytes	+		+		+	+		+
XCR1- DCs			+			+		+
XCR1+ DCs	+				+			
Neutrophils			+			+		

Table 2. The expression of endosomal TLRs across different cells. Adapted from [176].

A major consequence of innate nucleic acid sensing through nucleic acid sensing pathways is the secretion of type I IFNs [176]. However, both endosomal and cytosolic nucleic acid sensors are themselves ISGs: that is, their expression is inducible by innate immune activation and IFN receptor signaling [176]. Studies of SLE-associated genetic factors has confirmed that there are multiple genes that contribute to the high IFN levels observed in SLE [180-183]. A study that compared patients with high vs. low IFN and autoAb levels identified genetic regions associated with the IFN and autoAb specificities [181]. There also appear to be different genetic bases for different ancestral backgrounds, though high IFN is clearly seen in both African American and European American populations [98]. In 2013, Ko et al reported that both AA and EA patients with positive anti-RBP antibodies showed over-expression of similar IFN-related canonical pathways. Interestingly, anti-RBP negative EA subjects demonstrated similar IFN-related pathway activation, whereas no IFN-related pathways were detected in RBP negative AA

patients [98]. Thus type I IFN is a common pathway to SLE susceptibility, and molecules operating upstream of type I IFN production may also modulate disease [98, 183].

TLR7 is particularly important in the pathogenesis of SLE [184]. Overexpression of TLR7 causes severe lupus in multiple mouse models of SLE [185]. Male BXSB mice bearing the Y-linked autoimmune accelerating locus (Yaa), where a translocation from the X to Y chromosome leads to the duplication of several genes. Duplication of *Tlr7* in these mice was shown to be essential for development of autoAbs to RNA-containing complexes [184, 186]. Several studies have reported the induction of TLR7 transcription in immune cells including B cells following stimulation with microbes and viruses [187, 188], IFN α [187], nucleic acids and nucleic acid mimics such as Poly(I:C) and CpG [189]. Upregulated TLR7 and TLR9 mRNA expression have been reported in PBMCs from SLE patients, and levels correlate with the expression of IFN α [190, 191]. This increase in TLR7 may be part of a positive feedback mechanism to increase IFN α during normal infection with bacteria or virus [192]. A 2013 study by Chauhan et al. showed that TLR7 was preferentially increased in SLE patients with antibodies against RNA-associated antigens, while TLR9 induction correlated with anti-dsDNA antibody titers [193]. Overall, data suggest higher levels of TLR7 may lead to an acquired responsiveness in cells which are normally unresponsive to TLR7 ligands. This is supported by the observation that pDCs are responsible for the majority IFN α produced by healthy PBMCs, but account only for 57% of IFN α produced by PBMCs from SLE patients [194, 195].

There is accumulating evidence that the source of TLR7 ligands in autoimmunity may derive from uncleared apoptotic cells [196-198]. Our laboratory has previously

identified apoptotic cell clearance defects in BXD2 mice involving defective follicular exclusion of apoptotic antigens due to dysregulation of marginal zone macrophages that normally clear dead cells in the spleen [15, 16].

Questions

Type I IFNs have a prominent role in many aspects of normal innate and adaptive immunity and autoimmunity. However, cell-type specific information about type I IFN expression and autocrine/paracrine signaling through the two receptor chains is sparse and mostly focused on non-lymphocyte and non-immune cell populations. A major function of B cells is cytokine production, but surprisingly, type I IFN production in SLE has not been thoroughly investigated due to an assumption that pDCs are the most significant source of type I IFN in lupus. What B cell populations express the highest levels of type I IFN? Can B cell intrinsic type I IFN modulate B cell function and TLR7 signaling competence in lupus and in BXD2 mice, and is there a specific role for high affinity IFN β in the type I IFN dysregulation? Finally, are there sub-populations of type I IFN producing cells in vivo that may represent distinct inflammatory effector subsets in lupus?

A PROMINENT ROLE OF INTERFERON- β PRODUCED BY TRANSITIONAL B
CELLS IN LUPUS

by

JENNIE A. HAMILTON, QI WU, PINGAR YANG, BAO LUO, SHANRUN LIU,
HUIXIAN HONG, JUN LI, MARK R. WALTER, IÑAKI SANZ, ELEANOR N. FISH,
W. WINN CHATHAM, HUI-CHEN HSU, AND JOHN D. MOUNTZ

Submitted to *Journal of Immunology*

Format adapted for dissertation

Abstract

Type I interferon (IFN) is commonly associated with plasmacytoid dendritic cells. Here we report that IFN β is significantly increased in transitional stage 1 (T1) B cells in African American systemic lupus erythematosus (SLE) patients and in patients with anti-Smith, anti-SSA and renal disease. In lupus prone BXD2 mice, B-cell production of IFN β was required for optimal activation and survival of autoreactive B cells. At the single cell transcriptional level, there were distinct T1 B-cell subpopulations distinguished by their expression pattern of *Ifnb*, *Ifna* and *Tlr7* in BXD2 mice. T1 B-cell production of IFN β was an important regulator of TLR7-induced B-cell activation and survival *in vitro*. Blockade of IFN β reduced autoantibodies and glomerulonephritis in BXD2 mice, and anti-IFN β therapy during transitional B-cell repopulation post B-cell depletion inhibited autoantibodies. Together, these results implicate endogenous production of IFN β by T1 B cells as a key mechanism for autoreactive B-cell development in SLE.

INTRODUCTION

The transitional B-cell stage represents the formative link between immature bone-marrow (BM) B cells and mature peripheral B cells¹⁻³. During this stage, new emigrant immature B cells develop into immune-competent B cells capable of entry into the mature naïve B cell pool⁴⁻⁷. In humans, counter-selection of self-reactive peripheral B cells occurs during this stage⁸. Failures in this selection checkpoint are associated with aberrant activation and development of polyreactive self-antigen-reactive mature B cells in systemic lupus erythematosus (SLE)⁸⁻¹². In mice, the maturation of B cells occurs in the spleen where transitional type 1 (T1) B cells (CD93^{hi}IgM⁺IgD^{lo}CD23^{lo/-}) develop into transitional type 2 (T2) B cells (CD93⁺IgM⁺IgD⁺CD23⁺)¹³. Ligand engagement of the B cell receptor (BCR) results in upregulation of survival signals, activation, and maturation of T2 B cells^{6,7} but results in induction of apoptosis in T1 B cells. The factors that regulate the abnormal survival responses of T1 B cells in SLE have not been delineated.

A possible role for type I interferons (IFNs) was suggested by the well-established ability of type I IFNs to stimulate B cells¹⁴⁻¹⁶, the identification of the type I IFN signature in SLE^{17,18} and the mounting evidence that strong Toll-like receptor (TLR) signaling induces plasmacytoid dendritic cells (pDCs) to produce type I IFNs that subsequently act on B cells¹⁹⁻²⁴. We found previously that SLE patients, BXD2 mice and B6.*Slc1.2.3* autoimmune mice have high numbers of spleen marginal zone (MZ) pDCs that are associated with follicular migration of MZ B cells²⁵. A deficiency of the IFNAR1 ameliorated autoantibody production in BXD2 mice.^{26,27} Transitional B cells appear to

be important targets of type I IFN, as hyper-responsiveness to type I IFN was found to be most prominent in the transitional B cell population of SLE patients.²⁸ Additionally, ARID3a⁺ transitional and naïve B cells from SLE patients were shown to express high levels of IFN α ²⁹. Most studies have focused on IFN α , with the exception of one study which did not report a specific role for IFN β in NZB-*Ifnb*^{-/-} mice³⁰. IFN β differs from IFN α in that it has higher affinity for the type I IFN receptors (IFNARs)³¹⁻³³, has been proposed to be an initial signal that enables stronger signaling by other cytokines³⁴, and is important for optimal TLR7 responses in B cells³⁵.

Here, we report that freshly isolated human and murine T1 B cells express high levels of IFN β . Overexpression of endogenous IFN β in T1 B cells was associated with anti-Sm, anti-SSA, African American race, and an increased percentage of autoreactive 9G4⁺ B cells in SLE patients. Genetic deletion of IFN β in BM reconstituted chimeric mice and similarly, IFN β neutralization experiments, indicate that endogenous production of IFN β plays a critical role to promote autoreactive T1 B-cell survival and maturation. Single-cell gene expression analyses together with analysis of *in vitro* responses suggest a model where T1 to T2 B cell development occurs among distinct sub-populations of *Ifna* and *Ifnb* producing cells involving the regulated expression of different type I IFN subtypes and *Tlr7*. The clinical relevance of these results is supported by the finding that targeting of IFN β during transitional B-cell repopulation in BXD2 mice promoted long-term remission after anti-CD20 B-cell depletion therapy.

RESULTS

Endogenous IFN β in T1/T2 transitional B cells in SLE

We analyzed endogenous IFN β in PBMCs of 34 well-characterized SLE subjects (**Table S1**) by FACS (**Fig. 1a, S1a**). There was significantly higher expression of IFN β in transitional T1/T2 (CD27⁻IgD⁺CD24^{hi}CD38^{hi}), naive (CD27⁻IgD⁺CD24^{lo/+}CD38^{lo/+}) and memory (CD27⁺IgD⁻) B cells from SLE patients compared to healthy controls (**Fig. 1a**). There was a significant positive correlation between the percentages of IFN β ⁺ T1/T2 B cells and the percentages of 9G4⁺ B cells³⁶ within the mature naïve sub-population (**Fig. 1b**). Compared to CD4 T cells, B cells (T1/T2 and naïve) and pDCs expressed significantly higher levels of intracellular IFN β (**Fig. 1c, S1b**). At the mRNA level, T1/T2 B cells expressed the highest levels of *Ifnb*, *Ifna1* and *Ifna7*, compared to pDCs and CD4 T cells (**Fig. 1d, S2**). Significantly increased IFN β expression in the T1/T2 B cell population was seen in patients seropositive for anti-Sm, anti-SSA, patients with active renal disease and in African Americans (AA) patients (**Fig. 1e, S3, Table S1**). There was no significant correlation of IFN β with other clinical parameters or treatment with hydroxychloroquine (HCQ) or hydrocortisone (**Table S1 and Fig. S3**).

Elevation of IFN β in T1 B cells of BXD2 mice

Increased expression of *Ifnb* was also observed in spleen T1 B cells from lupus prone BXD2 mice (**Fig. 2a**). All FACS sorted cells were >98% pure, and cell identities were confirmed by the expression of cell lineage signature genes (**Fig. S4a, b**). Interestingly, although pDCs induced 10-fold more *Ifnb* upon *in vivo* poly(I:C) stimulation (**Fig. S4c**), *Ifnb* in freshly isolated spleen T1 B cells was comparable to purified pDCs (**Fig. 2b**). The expression of IFNAR was comparable between B6 and BXD2 B cells (**Fig. S4d**).

Ifnb induction requires assembly of IFN β enhanceosome composed of IRF7, NF- κ B p65, and 13 other factors³⁷; however, IRF-7 is short-lived and its expression requires positive-feedback regulation of IFN β /IFN α induction³⁸. Confocal image analyses of BXD2 mouse spleens (**Fig. 2c, d**) revealed significantly increased nuclear IRF7 in IgM⁺ cells. High resolution confocal imaging analysis of FACS sorted T1 B cells from BXD2 compared to B6 mouse spleens confirmed higher expression and also co-localization of IRF7 with NF- κ B p65 in the nucleus (**Fig. 2e**). Quantitative analysis further revealed significantly higher expression and colocalization of IRF7 and p65 in the chromatin open region of the nucleus in T1 B cells from BXD2 mice, compared to B6 mice (**Fig. 2e, S5**). Nuclear localization of p65 and IRF7 in BXD2 T1 B cells was further visualized by 3-dimensional rendering of high-resolution images (**Fig. S5b, S5c and Video S1, S2**). In BXD2 mice treated with anti-IFN β neutralizing antibody (Ab), there was a reduction of serum autoAbs to DNA and histone (**Fig. 2f**) and significantly reduced glomerulonephritis (**Fig. 2g**).

IFN β promotes autoreactive T1 B cells

In BXD2 mouse spleen, La₁₃₋₂₇ autoantigen reactive B cells³⁹ expressed significantly higher levels of type I IFN genes, compared to La₁₃₋₂₇⁻ total B cells (**Fig. 3a**). To exclude pDC contamination, B cell identity was verified by the expression of high levels of *Cd19* and low levels of *Cd317* (**Fig. S6**). The importance of endogenous IFN β in promoting the development of La₁₃₋₂₇ reactive B cells was established in a triple chimeric CD45.2 B6-*Ifnb*^{-/-}, CD45.1 B6-*Ifnb*^{+/+} and CD45.2 GFP⁺ BXD2 (1:1:1) BM transfer experiment.

IgM⁺ T1, T2 and T3 transitional B cell subsets derived from CD45.2 B6-*Ifnb*^{-/-} BM exhibited the highest percent of Annexin V⁺ apoptotic cells (**Fig. 3b**). B cells from the BM of *Ifnb*^{-/-} origin exhibited a significantly lower percentage (**Fig. 3c**) and total number of La₁₃₋₂₇⁺ B cells (**Fig. 3d**) and a decreased total number of transitional B cells at all stages (**Fig. 3e**), compared to B cells derived from the BM of B6-*Ifnb*^{+/+} and more strikingly compared to BM of GFP⁺ BXD2 mice.

These results suggested that high levels of endogenous IFN β in BXD2 T1 B cells may promote abnormal selection of La₁₃₋₂₇⁺ B cells. To determine the specific requirement of IFN β , B6-*Rag1*^{-/-} mice were reconstituted with BM from BXD2 mice and were administered neutralizing Abs to IFN β or IFNAR during T1 B cell repopulation. The effects of *in vivo* anti-IFN β and anti-IFNAR in suppressing the repopulation of La₁₃₋₂₇⁺ B cells were comparable (**Fig. 3f**), and both treatments had the most profound effect on CD93⁺ transitional B cell development (**Fig. 3g**). Development of all transitional B cell subsets was significantly abrogated by administration of either anti-IFN β or anti-IFNAR (**Fig. 3h**). It was verified that anti-IFN β neutralized IFN β only, while anti-IFNAR neutralized both IFN α and IFN β (**Fig. S7**). These results indicate that specific blockade of IFN β is sufficient to abrogate development of autoreactive transitional B cells.

Endogenous type I IFN circuit in T1 B cells

To determine whether a distinct sub-population of *Ifnb*^{hi} T1 B cells could be identified and also gain insights into the dynamics of *Ifnb* expression in relation to other *Ifns* and *Tlr7* in T1 B cells of BXD2 mice, we carried out a quantitative single cell qRT-PCR.

FACS sorted T1 B cells were >98% pure (**Fig. S8a**) and cell identities were further confirmed by the expression of cell lineage signature genes (**Fig. S8b**). Hierarchical clustering and principal component (PC) analyses showed that, in all three mice analyzed, there was distinct segregation of *Ifnb*^{hi} versus *Ifna*^{hi} T1 B cells (**Fig. 4a, b, and S9**). Among all *Ifna* genes analyzed, *Ifna7* exhibited the most distinct segregation from the expression of *Ifnb* (**Fig. 4a**).

Interestingly, heatmap and PC analyses revealed a distinctly inverse expression pattern of *Cd93* and *Cd23* in single T1 B cells from all three BXD2 mice analyzed, suggesting their utility in identifying sub-populations of T1 B cells (**Fig. S10a**). Flow cytometry analysis confirmed down-regulation of CD93 coincided with upregulation of CD23 during transitional B cell maturation (**Fig. S10b**). *Cd93* and *Cd23* were thus used to define subpopulations ranging from early (*Cd93*^{hi}*Cd23*^{lo}) to late T1 (*Cd93*^{lo}*Cd23*^{hi}). Distinct expression patterns of *Ifnb*, *Ifna7* and *Tlr7* were identified in these subpopulations of T1 B cells (**Fig. 4c, d**)^{13,40}. In the *Cd93*^{hi}*Cd23*^{lo} (Cluster I) subset, *Ifnb* expression was significantly higher than *Ifna7* (**Fig. 4c, S11a**) or *Tlr7* (**Fig. 4d and Fig. S11b**). However, marked elevation of *Ifna7* and *Tlr7* expression was observed from the *CD93*^{hi}*CD23*^{lo} subset to the *CD93*^{Int}*CD23*^{lo} subset (Cluster II). Although *Tlr7* expression was down-modulated in Cluster III, *Ifnb* and *Ifna7* expression peaked in this subset. All 3 genes were expressed at the lowest level in the *Cd93*^{lo}*Cd23*^{hi} (Cluster IV) subset (**Fig. 4c, d**).

IFN β promotes TLR7 response

At the protein level, we confirmed that IFN β expression was highest in late stage (IgM^{hi}CD23^{low}) T1 B cells in B6 and BXD2 mice (**Fig. 5a**) but was downregulated at the T2 stage. The requirement for endogenous *Ifnb* in T1 B cells to promote *Ifna7* and *Tlr7* expression in T1 B cells was ascertained at the single cell level using T1 B cells isolated from mixed *Ifnb*^{+/+} vs. *Ifnb*^{-/-} BM chimeric recipients. The expression of *Ifna7*, *Tlr7* and also *Ifna1* was significantly reduced in *Ifnb*^{-/-} T1 B cells (**Fig. S12a**). Consistent with this, there was a significantly diminished *Ifnb*^{-/-} IgM⁺ B cell repopulation, compared to *Ifnb*^{+/+} IgM⁺ B cells, in recipient mice (**Fig. S12b**).

The requirement of IFN β for CL264-mediated TLR7 stimulation of B cells was determined by CD69 induction after stimulation in the presence of neutralizing antibodies to IFN β or IFNAR1 (**Fig. 5b**). Specific blocking of IFN β inhibited >60% of T1 B cell activation following CL264 and CL264+anti-IgM stimulation (**Fig. 5b**). There was no significant additional inhibition of activation generated by IFNAR blockade in either stimulation (**Fig. 5b**). Neutralization of IFN β or IFNAR also significantly inhibited cell survival measured at 56 hrs (**Fig. 5c**). In B6 mice, endogenous IFN β was also required for optimal for TLR7 activation of T1 B cells, but not T2/T3 or follicular (FO) B cells obtained from double-chimeric mice (CD45.2 B6-*Ifnb1*^{-/-} and CD45.1 B6 WT) (**Fig. S13**).

In B cells derived from PBMCs of human SLE patients, CL264+anti-IgM/IgG-induced B cell activation (**Fig. 5d**) and survival (**Fig. 5e**) responses were suppressed by blockade of

anti-IFN β . Furthermore, blockade of IFNAR1 using an anti-IFNAR did not provide additional effects, suggesting that B-cell production of IFN β is an essential component of the type I IFN response in promoting the effects of TLR7.

IFN β blockade post BCDT promotes tolerance

The translational implication of type I IFN blockade in lupus was investigated using an anti-CD20 B-cell depletion therapy (BCDT) to eliminate the majority of B cells followed by administration of type I IFN blockade during transitional B cell repopulation (**Fig. S14**). The most active period of transitional B cell repopulation occurred between wk 1 to wk 3 with complete repopulation at wk 9 post-BCDT (**Fig. S14**). Neutralization of IFNAR signaling inhibited transitional B-cell maturation between wks 1 – 4 post anti-CD20 (**Fig. S14**).

We next determined if anti-IFN β or anti-IFNAR therapy suppressed transitional B cell repopulation resulting in a long-term suppression of autoantibody formation in BXD2 mice. At wk 2 post-BCDT, there were significantly reduced percentages and total numbers of T1, T2, and mature B cell subsets in the spleen (**Fig. 6a, b**). Treatment with anti-IFN β and anti-IFNAR significantly compromised the repopulation of B cells starting at the T1 stage (**Fig. 6a, b**). There were significantly lower IgM⁺ and IgD⁺ B cells in and surrounding the follicle in spleens from anti-IFN β and anti-IFNAR treated mice (**Fig. 6c, S15a**). There were also significantly decreased percentages of Ki67⁺ T1 and T2 B cells that were repopulating in anti-IFN β and anti-IFNAR treated mice compared to isotype treated mice (**Fig. 6d, S15b**). At 8 weeks post therapy, there was a significantly

decreased percentage and number of germinal center B cells (**Fig. 6e**) as well as autoantibodies to histone, DNA and La₁₃₋₂₇ (**Fig. 6f**) in anti-IFN β treated mice compared to isotype control treated mice.

DISCUSSION

The specific contribution of different type I IFNs, particularly IFN β , in lupus has been enigmatic⁴¹. Differential activity of IFN α and IFN β has been known for over a decade⁴², and more recently, modular transcriptional studies in SLE patients revealed distinct gene expression signatures not restricted to IFN α ⁴³. The present finding that T1 B cells in the spleen produce self-modulatory IFN β suggests that an early event in B-cell tolerance loss may involve nucleic acid-Ag stimulation of these B cells. Our comparison of B-cell development in mice reconstituted with B6-*Ifnb*^{-/-}, B6-*Ifnb*^{+/+}, and GFP⁺ BXD2 BM demonstrated that the expression of IFN β in new emigrant transitional B cells in the spleen provided a survival advantage for repopulating T1 B cells, including those that were La₁₃₋₂₇⁺. Previous studies have shown a similar defect in B-cell development⁴⁴ and type I IFN antiviral responses in IFN β deficient mice on the C57BL/6 genetic background⁴⁵. In SLE patients, our findings that B-cell endogenous IFN β correlated positively with percentages of 9G4 autoreactive mature naïve B cells and anti-Sm and anti-SSA autoAbs implicates B-cell IFN β as both a potential biomarker and effector of disease. Together these results suggest that T1 B cell autocrine and paracrine IFN β signaling through IFNAR is a B-cell intrinsic factor that can promote survival and maturation of T1 B cells.

In the present study, neutralization of IFN β reduced autoAbs and glomerulonephritis in BXD2 mice. To our knowledge, the only previous study that specifically studied IFN β in a multi-genetic lupus-prone NZB mouse strain suggested that IFN β was not required for anti-chromatin Abs or renal disease³⁰. In contrast, treatment of MRL-Fas^{lpr/lpr} mice with IFN β improved disease⁴⁶. These results suggest that the effects of IFN β in mouse models of autoimmunity depend on genetic background. Our finding that African American SLE patients were significantly enriched in B-cell expression of high levels of IFN β suggests that polymorphisms in the IFN β enhanceosome genes or other upstream genes may predispose these individuals to development of type I IFN dysregulation and autoimmune disease. Notably in the present study, B cell endogenous IFN β was significantly increased in SLE patients with renal disease. These results are consistent with recent findings by Cherukuri et al. which reported that the T1/T2 B cell ratio and associated cytokine production strongly correlated with renal allograft dysfunction⁴⁷.

Our data reveal for the first time that a prominent feature of T1 B-cell development in the spleen of BXD2 mice is the well-orchestrated expression of *Ifnb* and its downstream genes in T1 B cell subsets. B-cell fate commitment has recently been proposed to occur at the T1 stage⁴⁸. Previous studies have estimated that T1 B-cell fate and the acquisition of mature B-cell marker CD23 is determined relatively quickly within 48 hours^{1,49}. Our single T1 B cell gene expression analyses revealed that *Ifnb* is expressed in the earliest *Cd93*^{hi}*Cd23*^{lo} T1 B cell subset, while peak *Ifnb* expression occurred in T1 B cells that are beginning to acquire *Cd23* expression, suggesting that amplification of *Ifnb* occurs as T1 B cells progress to the mature T2 phenotype. At the protein level, FACS analysis

confirmed that peak expression of IFN β occurred in late T1 B cells that are beginning to acquire CD23 surface expression.

At a more basic level, the single cell gene expression analysis revealed that splenic T1 B cell development occurs among distinct *Ifna* and *Ifnb* producing cells in which the induction of IFN α and IFN β gene expression is temporally separated. This is consistent with the role of IFN β in promoting IFN α and IFN response gene expression^{34,50}. The present work demonstrates that during T1 B cell development, autocrine IFN β promotes the subsequent production of IFN α subtypes in the spleen. Consistent with this, there were significantly lower levels of *Ifna* genes expressed in T1 B cells derived from *Ifnb*^{-/-} BM in a BM chimeric transfer experiment. Interestingly, in the spleen of BXD2 mice, the early expression of *Ifnb* in the CD93^{hi} T1 B cell population preceded the upregulation of both *Tlr7* and *Ifna7*, consistent with a role for constitutive priming with IFN β to subsequently facilitate other cytokines and sensing pathways³⁴. TLR7 signaling plays a key role in production of RNA-associated autoantigens including La and anti-Sm/RNP⁵¹. In mice, forced expression of TLR7 has been demonstrated to promote expansion of the T1 B cell pool and their direct recruitment into IgG autoantibody-producing B cells⁵². The present model supports a novel concept that initial IFN β production by developing T1 B cells may serve as the central mediator to prime B cells for subsequent production and responses to IFN α and nucleic acid sensing responses. These results suggest that in a subgroup of SLE patients whose transitional B cells utilize IFN β signaling for survival and maturation, blockade of IFN β may dampen the type I IFN pathway without completely shutting it down making it a desirable therapeutic treatment in some patients.

BCDT with anti-CD20 is effective in managing some SLE complications in humans and in mouse models of SLE^{53,54}. However, in some patients, B cell repopulation after BCDT is associated with development of autoreactive B cells⁵⁴. Interestingly, although BCDT by rituximab (RTX) is effective in the treatment of rheumatoid arthritis (RA), which is clinically and serologically distinct from SLE, three independent studies showed consistent results that RA patients who responded poorly to RTX exhibited higher levels of type I IFN signature gene expression in PBMCs, and that serum levels of IFN α were inversely associated with a positive clinical response⁵⁵⁻⁵⁷. Interestingly, HCQ, which has been reported to impair IFN α production,⁵⁸ did not appear to affect B cell endogenous IFN β levels in the patients in our study. This is consistent with the reports that IFN β is constitutively expressed^{38,59}. Thus B cell intracellular IFN β expression may be helpful to explain the occurrence of flares in patients receiving HCQ or during repopulation after anti-CD20 therapy.

Our present work suggests a need for future human studies of type I IFNs that pioneer beyond the well-established and accepted view of pDC/IFN α . These results also provide a mechanistic basis for development of more effective therapies^{60,61} to dampen the type I IFN cascade by specifically targeting the high-affinity IFN β or the enhanceosome components that promote its induction.

METHODS

Clinical Samples. Peripheral blood mononuclear cells (PBMCs) from 34 SLE patients and 9 healthy controls were isolated from heparinized blood by density gradient centrifugation (Lymphoprep/SepMate, StemCell Technologies). SLE subjects were recruited from the UAB Rheumatology Clinic. Clinical data were described in detail in **Supplementary Table 1**. T1 B cells, cellular phenotypes and clinical data were collected in a double blinded manner until all data collection was completed. All SLE patients met the American College of Rheumatology 1997 revised criteria for SLE⁶². These studies were conducted in compliance with the Helsinki Declaration and approved by the institutional review board at UAB. All participants provided informed consent.

Mice. Wild type C57BL/6 (B6), B6-CD45.1, CD45.2 B6-*Rag1*^{-/-}, and BXD2 recombinant inbred mice were obtained from the Jackson Laboratory. B6-*Ifnb*^{-/-} mice⁴⁴ were provided by Dr. Eleanor Fish, University of Toronto, Canada. All mice were housed in the University of Alabama at Birmingham Mouse Facility under specific pathogen-free conditions in a room equipped with an air-filtering system. The cages, bedding, water, and food were sterilized. All mouse procedures were approved by the University of Alabama at Birmingham Institutional Animal Care and Use Committee.

BM transplantation. Recipient CD45.2 B6- *Rag1*^{-/-} mice were irradiated sub-lethally (450 rad) 6 hours prior to bone marrow transfer. The day of transfer, BM cells were harvested from CD45.1 B6, CD45.2-B6-*Ifnb*^{-/-}, and GFP⁺ transgenic BXD2 mice. BM cells (1.5×10^7 total) from the indicated donors were transferred or mixed at a 1:1 ratio of

CD45.1 B6 : CD45.2-B6-*Ifnb*^{-/-} or a 1:1:1 ratio of CD45.1 B6 : CD45.2- B6-*Ifnb*^{-/-} : GFP⁺ BXD2 and injected i.v. into recipient mice. Mice were kept on sulfatrim water for 21 days or until sacrificed at the indicated times after BM transfer.

***In vivo* treatment.** BXD2 BM transferred recipients were treated i.v. with 250 µg anti-IFNAR (clone MAR1-5A3, BioXCell) or 100 µg anti-IFNβ (clone MIB-5E9.1, BioLegend). For B cell depletion of BXD2 mice, 1-month-old BXD2 mice were injected i.v. with 200 µg neutralizing anti-CD20 mAb (clone 5D2, Genentech). Beginning 3 days post B cell depletion, mice were treated with anti-IFNAR (500 µg for the first injection, 250 µg for maintenance) or anti-IFNβ (300 µg for the first injection, and 250 thereafter). IFN neutralizing Abs were injected twice per week for the indicated times post B cell depletion. Nonspecific IgG isotypes (BioXCell) were injected as a negative control. For anti-IFNβ treatment to naïve BXD2 mice, groups of BXD2 mice were administered anti-IFNβ or isotype-control antibody (250 µg/2x per week for 6 weeks). For BXD2 mouse poly(I:C) injections, 2-3 month old BXD2 mice were injected intraperitoneally with 100 µg Poly(I:C) (Invivogen) and sacrificed after 4 hours.

***In vitro* stimulation and type I interferon neutralization.** B cells were purified by negative selection using EasySep™ Mouse B Cell Isolation Kit (Stemcell Technologies) and cultured in 96 well plates at 10⁶/mL in complete RPMI for 6 or 56 hours. In some experiments, B cells were stimulated with mouse IFNα or IFNβ (gift from Dr. Vithal Ghanta, CytImmune) 2 µg/mL CL264 (Invivogen) or CL264 + a polyclonal anti-mouse IgM (1 µg/mL, Jackson ImmunoResearch) or non-specific rat-IgG isotype control. For

specific neutralization of type I IFNs, cells were pre-incubated with 50 µg/mL anti-IFNAR (clone MAR1-5A3, BioXCell) or 500 IU/mL anti-IFNβ (Rabbit IgG, Protein A purified, PBL Assay Science). Human peripheral B cells were isolated for *in vitro* culture using Human EasySep™ Human B Cell Enrichment Kit. Purified B cells were cultured *in vitro* 10⁶ cells/mL in complete RPMI and stimulated with 2 µg/mL CL264 or 2 µg/mL F(ab')₂ Anti-Human IgM+IgG (eBioscience). For specific neutralization of type I interferons, 50 µg/mL anifrolumab (Creative BioLabs) or 1000 IU/mL polyclonal anti-IFNβ (PBL Assay Science) or non-specific isotype controls were added to the culture.

Real-time quantitative RT-PCR. RNA isolation, cDNA synthesis, and real-time PCR reactions were carried out as described previously^{27,63}. All primers are described in **Supplementary Table 2**.

Single cell qRT-PCR. Gene expression analysis of single T1 B cells obtained from 3 BXD2 mice (4-mo-old) was performed using the BioMark Real-Time quantitative PCR (qPCR) system (Fluidigm Co., South San Francisco, CA). Bulk T1 B cells from each mouse spleen were sorted using flow cytometry sorting. Following verification of the purity of sorted T1 B cells (**Fig. S8a**), cells were subjected to Fluidigm single cell capture. Single cell capture was manually examined under a light microscope. Wells with missing cells or multiple cells (>1) were removed from the analysis. qRT-PCR is performed in two steps after total RNA purification and conversion to single stranded cDNA using polyT priming: the targeted genes are pre-amplified in a single 14-cycle PCR reaction for each sample by combining 100 ng cDNA with the pooled primers and

EVA Green Pre-Amp Mastermix (Fluidigm BioMark™) following the manufacturer's protocol. Secondly qRT-PCR reactions were performed on a 96.96 array. The EvaGreen detection assay was applied for BioMark gene expression analysis using the standard Fluidigm protocols. Primer sets amplifying the mRNAs of the relevant genes are presented in **Supplementary Table 2**. The averaged C_T values were calculated from the system software [BioMark Real-Time PCR (polymerase chain reaction) Analysis, Fluidigm] ⁶⁴.

Single cell gene expression hierarchical clustering analysis. Gene expression values were calculated using the $2^{-\Delta C_T}$ value. Briefly, the C_T value of each gene in each cell obtained from the BioMark system was normalized with the C_T value of *Gapdh* (ΔC_T) of each cell, and this was further converted to $2^{-\Delta C_T}$ to show the expression value of each gene. The $2^{-\Delta C_T}$ values were transferred to the ClustVis online web tool for hierarchical clustering analysis ⁶⁵. ClustVis uses the heatmap feature available from the R package (version 0.7.7) for plotting the values as a heatmap. Expression levels of all genes were auto-scaled to provide all the genes equal weight in the classification algorithms. Missing data in the BioMark system were assigned a Ct of 999 by the instrument software and were removed. Since high C_T s in the BioMark 96 × 96 microfluidic card were expected to be false positives due to baseline drift or formation of aberrant products, and since a sample with a single template molecule is expected to generate a lower C_T , C_T values that were larger than a cutoff of 25 were also removed ⁶⁶. Cells not expressing the *Gapdh* housekeeping gene, or expressing it at extremely low values ($C_t > 35$), were

removed from the analysis, on the assumption that these cells were dead or damaged during the preparation process.

Hierarchical clustering and principal component analyses were performed on both cells and genes, with a correlation distance metric and complete linkage. Clustering analysis was carried out based on the results for the indicated genes in each assay. Statistical analysis of single cell gene expression in different clusters was calculated including 0.95% confidence interval by one-way ANOVA (Tukey-Kramer pairwise comparison) or unpaired 2-tailed *t*-test using the GraphPad Prism software (La Jolla, CA). Data used for the BXD2 T1 B cell clustering analysis can be obtained at

<http://biit.cs.ut.ee/clustvis/?s=YkgzIkieGaEjvOi> (for the *Ifna* vs *Ifnb* dataset),

<http://biit.cs.ut.ee/clustvis/?s=nEZOTPHFyskUeNk> (for the *Cd93* vs *Cd23* dataset),

<http://biit.cs.ut.ee/clustvis/?s=WsDQpwrnYRSdxLf> (for the *Cd93*, *Cd23*, *Ifnb*, and *Ifna7*

dataset), and <http://biit.cs.ut.ee/clustvis/?s=SvjLZSSqPnpGBzi> (for the *Cd93*, *Cd23*, *Ifnb*, and *Tlr7* dataset).

Flow cytometry. Cell suspensions were prepared from mouse spleens, and peripheral blood mononuclear cells were isolated by ACK lysis of RBCs. Cell suspensions were stained at 4°C in PBS containing 2% FBS and 0.5% EDTA after FcγRII/III blocking. Surface staining was performed with the following anti-mouse antibodies: BioLegend Pacific Blue–anti-B220 (RA3-6B2), BV510-anti-CD23 (B3B4), FITC-anti-CD21/35 (7E9), Pacific Blue-anti-CD45.1 (A20), AF647-anti-CD45.2 (104), PE-anti-CD4 (GK1.5), AF488-anti-Ki67 (11F6); BD Bioscience BV650-anti-CD93 (AA4.1), BV510-

anti-IgD (11-26c.2a); eBioscience PE-anti-CD95 (15A7), APC-anti-GL7 (GL-7), anti-CD69 (H1.2F3), PECy7-anti-IgM (eB121-15F9), APC-anti-CD317 (PDCA1, eBio129c); PBL Assay Science FITC-anti-IFN β (RMMB-1). La₁₃₋₂₇ tetramer staining was carried out as previously described³⁹.

Human PBMCs were isolated using SepMate (StemCell Technologies) and stained in FACS buffer. Human antibodies included BioLegend BV510-anti-CD24 (ML5), PE-anti-CD303 (clone 201A), BV510-anti-IgM (clone MHM-88), Pacific-Blue-anti-CD4 (clone RPA-T4), PE-Cy7-anti-CD10 (clone HI10a), BV650-anti-CD27 (O323), Pacific Blue-anti-CD19 (HIB19), PE-Cy7-anti-CD38 (HB-7); eBioscience APC-anti-CD69 (FN50); Southern Biotech PE-IgD (IADB6), and PBL Assay Science FITC-anti-IFN β (MMHB-3). Dead cells were excluded from analysis with APC-eFluor® 780 Organic Viability Dye (eBioscience).

For intracellular staining, cells were stained with ef780 viability dye, followed by fixation in 2% PFA. Cells were permeabilized in ice-cold 70% methanol, washed and stained for intracellular and surface Abs. Cells were washed twice with 3 mL FACS buffer and suspended in 2% paraformaldehyde/FACS solution for cell surface marker analysis. Cells (300,000–1 X 10⁶ /sample) were analyzed by flow cytometry. FACS data were acquired with an LSRII FACS analyzer (BD Biosciences) and analyzed with FlowJo software (Tree Star Ashland, OR). All flow cytometry analysis was carried out using a combination use of forward light scatter and side scatter height, area, and width parameters to exclude aggregated cells.

Histology. For paraffin sections, tissue were fixed in formalin, embedded in paraffin and stained with Hematoxylin & Eosin. Image acquisition was carried out using an Olympus BX41 microscope.

For frozen sections, tissue were embedded in OCT tissue media (Tissue-Tek) and frozen on dry ice. Frozen sections (7 μm thickness) were fixed to slides in ice-cold acetone for 15 minutes and air dried for 30 seconds. The sections were blocked with 10% horse serum for 30 minutes at room temperature and then stained for 30 minutes at room temperature in a humidified chamber with fluorescently labeled antibody cocktails. The following antibodies were applied according to the manufacturer's instructions: goat-anti-mouse IgG H+L (Invitrogen), goat-anti mouse IgM-AF555 (Invitrogen), anti-mouse IgD AF647 (11-26c.2a, BioLegend), anti-mouse CD45.1 BV421 (A20, BioLegend), and anti-mouse CD45.2 (104, BioLegend). Slides were washed, mounted with Fluoromount G (Southern Biotech), sealed, and confocal imaging was carried out using a Zeiss LSM 710 confocal microscope. Imaging quantitation was carried out using the ImageJ software⁶⁷.

LSM 880 super-high resolution imaging of IRF and NF-kB p65. Sorted T1 B cells (CD93⁺IgM⁺CD23⁻) were adhered onto microscope slides using centrifugation (800 RPM for 6 minutes). Cells were fixed and permeabilized with acetone, blocked with 2% BSA and Fc block (2.4G2), followed by staining with goat-ant-mouse IgM (Invitrogen), rabbit-anti-mouse IRF7 (Abcam), anti-mouse p65 (R&D), and DAPI nuclear stain (200 ng/mL). High resolution imaging of IRF7 and p65 transcription factors in IgM T1 B cells was

carried out using the Zeiss LSM 880 AIRY scan detector with fast modules. Super-high resolution imaging was enabled by the use of 32 single detectors, each with a 0.2 AIRY units with 16 simultaneous detectors capable of exciting 4 pixels at the same time. Lasers used for excitation consisted of an Argon laser (458 nm, 488 nm, 514 nm), a diode laser (405 nm), a solid state laser (461 nm), and helium-neon lasers (494 nm and 633 nm). The microscope objectives were 63× and 40× with a 1.4 numerical aperture. Image acquisition was acquired using the ZEN Black software and rendered for 3-dimensional imaging on the ZEN Blue software. Co-localization of IRF7 and p65 was carried out using the ImageJ software.

Autoantibody detection. Assays for serum autoantibodies were carried out as described previously⁶³. Briefly plates were coated with 5 µg/mL DNA from calf thymus (Sigma), histone from calf thymus (Sigma), affinity purified rat IgG (Sigma), or La₁₃₋₂₇ (Genescript)³⁹³⁹. ELISAs were developed with an HRP-labeled goat anti-mouse IgG (Southern Biotechnology Associates) and tetramethylbenzidine substrate (Sigma-Aldrich). OD_{450–650} was measured on an Emax Microplate reader.

Statistics. Results are shown as the mean ± standard deviation (s.d.) or mean ± standard error of the mean (s.e.m.) as described in figure legends. Pearson's normality test was used to determine normal distribution of each dataset. A 2-tailed, unpaired Student's t test was used when 2 normally distributed groups of dataset were compared for statistical differences. The Mann–Whitney non-parametric test was used when the 2 datasets for comparison were not normally distributed. An ANOVA test was used when more than 2

groups were compared for statistical differences. P values of less than 0.05 were considered significant. Analysis of correlation between variables was performed using linear regression in GraphPad Prism software (La Jolla, CA).

AUTHOR CONTRIBUTIONS

J.A.H. and J.D.M. initiated the study. J.A.H., J.D.M., and H-C.H. designed the experiments and interpreted the data. J.A.H. was involved in all experiments with assistance from Q.W., P.Y. B.L., and J.L on specific experiments. P.Y. performed bulk RNA analyses. S.L. performed single cell RNA reverse transcription and amplification and contributed to primer design. H.H. assisted with anti-CD20 confocal analysis. M.W. provided key suggestions and expertise. I.S. provided critical reagents (human 9G4 antibodies) and suggestions. E.N.F. provided IFNB^{-/-} BM and contributed to writing the paper. W.W.C. recruited SLE patients and assembled clinical data for the study. J.A.H., J.D.M., and H-C.H. primarily wrote the paper. J.D.M. supervised the research.

ACKNOWLEDGEMENTS

This work was supported by grants from the NIH grants (R01-AI-071110 to J.D.M, R01-AI-083705 to H.-C.H., 2T32AI007051-39 Immunology T32 Training Grant to support J.A.H., R37-AI049660 and U19 AI110483 Autoimmunity Center of Excellence to I.S., P30-AR-048311 P&F Project to J.L., P30-AR-048311, P30-AI-027767 for the UAB Comprehensive Flow Cytometry Core, P30-AR-048311 for the Analytic Imaging and Immunoreagent Core, and the joint Birmingham VA/UAB Single Cell Analysis Core), the Department of Veterans Affairs Merit Review grant 1I01BX000600 to J.D.M, the Lupus Foundation of America Finzi Summer Fellowship to J.A.H, the Lupus Research Institute Novel Research Award to M.W. and H.-C.H., and a Tier 1 Canada Research Chair grant to E.N.F.

REFERENCES

1. Chung, J.B., Silverman, M. & Monroe, J.G. Transitional B cells: step by step towards immune competence. *Trends in immunology* **24**, 343-349 (2003).
2. Monroe, J.G. & Dorshkind, K. Fate decisions regulating bone marrow and peripheral B lymphocyte development. *Adv Immunol* **95**, 1-50 (2007).
3. Vossenkamper, A. & Spencer, J. Transitional B cells: how well are the checkpoints for specificity understood? *Arch Immunol Ther Exp (Warsz)* **59**, 379-384 (2011).
4. Sims, G.P., *et al.* Identification and characterization of circulating human transitional B cells. *Blood* **105**, 4390-4398 (2005).
5. Lee, J., Kuchen, S., Fischer, R., Chang, S. & Lipsky, P.E. Identification and characterization of a human CD5+ pre-naïve B cell population. *Journal of immunology* **182**, 4116-4126 (2009).
6. Petro, J.B., *et al.* Transitional type 1 and 2 B lymphocyte subsets are differentially responsive to antigen receptor signaling. *The Journal of biological chemistry* **277**, 48009-48019 (2002).
7. Su, T.T. & Rawlings, D.J. Transitional B lymphocyte subsets operate as distinct checkpoints in murine splenic B cell development. *Journal of immunology* **168**, 2101-2110 (2002).
8. Yurasov, S., *et al.* Defective B cell tolerance checkpoints in systemic lupus erythematosus. *The Journal of experimental medicine* **201**, 703-711 (2005).

9. Chang, N.H., *et al.* Expanded population of activated antigen-engaged cells within the naive B cell compartment of patients with systemic lupus erythematosus. *Journal of immunology* **180**, 1276-1284 (2008).
10. Manjarrez-Orduno, N., *et al.* CSK regulatory polymorphism is associated with systemic lupus erythematosus and influences B-cell signaling and activation. *Nat Genet* **44**, 1227-1230 (2012).
11. Jacobi, A.M., Zhang, J., Mackay, M., Aranow, C. & Diamond, B. Phenotypic characterization of autoreactive B cells--checkpoints of B cell tolerance in patients with systemic lupus erythematosus. *PloS one* **4**, e5776 (2009).
12. Malkiel, S., *et al.* Checkpoints for Autoreactive B Cells in the Peripheral Blood of Lupus Patients Assessed by Flow Cytometry. *Arthritis & rheumatology* **68**, 2210-2220 (2016).
13. Kleiman, E., *et al.* Distinct Transcriptomic Features are Associated with Transitional and Mature B-Cell Populations in the Mouse Spleen. *Frontiers in immunology* **6**, 30 (2015).
14. Lopez de Padilla, C.M. & Niewold, T.B. The type I interferons: Basic concepts and clinical relevance in immune-mediated inflammatory diseases. *Gene* **576**, 14-21 (2016).
15. Ronnblom, L. & Pascual, V. The innate immune system in SLE: type I interferons and dendritic cells. *Lupus* **17**, 394-399 (2008).
16. Braun, D., Caramalho, I. & Demengeot, J. IFN-alpha/beta enhances BCR-dependent B cell responses. *International immunology* **14**, 411-419 (2002).

17. Baechler, E.C., *et al.* Interferon-inducible gene expression signature in peripheral blood cells of patients with severe lupus. *Proceedings of the National Academy of Sciences of the United States of America* **100**, 2610-2615 (2003).
18. Crow, M.K., Kirou, K.A. & Wohlgemuth, J. Microarray analysis of interferon-regulated genes in SLE. *Autoimmunity* **36**, 481-490 (2003).
19. Ding, C., Cai, Y., Marroquin, J., Ildstad, S.T. & Yan, J. Plasmacytoid dendritic cells regulate autoreactive B cell activation via soluble factors and in a cell-to-cell contact manner. *J Immunol* **183**, 7140-7149 (2009).
20. Gujer, C., *et al.* IFN-alpha produced by human plasmacytoid dendritic cells enhances T cell-dependent naive B cell differentiation. *J Leukoc Biol* **89**, 811-821 (2011).
21. Harris, J.E. & Marshak-Rothstein, A. Editorial: Interfering with B cell immunity. *J Leukoc Biol* **89**, 805-806 (2011).
22. Eloranta, M.L., Alm, G.V. & Ronnblom, L. Disease mechanisms in rheumatology--tools and pathways: plasmacytoid dendritic cells and their role in autoimmune rheumatic diseases. *Arthritis and rheumatism* **65**, 853-863 (2013).
23. Ronnblom, L. & Alm, G.V. The natural interferon-alpha producing cells in systemic lupus erythematosus. *Human immunology* **63**, 1181-1193 (2002).
24. Bekeredjian-Ding, I.B., *et al.* Plasmacytoid dendritic cells control TLR7 sensitivity of naive B cells via type I IFN. *Journal of immunology* **174**, 4043-4050 (2005).

25. Li, H., *et al.* Cutting Edge: defective follicular exclusion of apoptotic antigens due to marginal zone macrophage defects in autoimmune BXD2 mice. *J Immunol* **190**, 4465-4469 (2013).
26. Wang, J.H., *et al.* Marginal zone precursor B cells as cellular agents for type I IFN-promoted antigen transport in autoimmunity. *J Immunol* **184**, 442-451 (2010).
27. Li, H., *et al.* Interferon-induced mechanosensing defects impede apoptotic cell clearance in lupus. *The Journal of clinical investigation* **125**, 2877-2890 (2015).
28. Chang, N.H., *et al.* Interferon-alpha induces altered transitional B cell signaling and function in Systemic Lupus Erythematosus. *J Autoimmun* **58**, 100-110 (2015).
29. Ward, J.M., *et al.* Human effector B lymphocytes express ARID3a and secrete interferon alpha. *Journal of autoimmunity* (2016).
30. Baccala, R., *et al.* Anti-IFN-alpha/beta receptor antibody treatment ameliorates disease in lupus-predisposed mice. *Journal of immunology* **189**, 5976-5984 (2012).
31. Schreiber, G. & Piehler, J. The molecular basis for functional plasticity in type I interferon signaling. *Trends Immunol* **36**, 139-149 (2015).
32. Wilmes, S., *et al.* Receptor dimerization dynamics as a regulatory valve for plasticity of type I interferon signaling. *The Journal of cell biology* **209**, 579-593 (2015).
33. Lamken, P., Lata, S., Gavutis, M. & Piehler, J. Ligand-induced assembling of the type I interferon receptor on supported lipid bilayers. *Journal of molecular biology* **341**, 303-318 (2004).

34. Taniguchi, T. & Takaoka, A. A weak signal for strong responses: interferon-alpha/beta revisited. *Nature reviews. Molecular cell biology* **2**, 378-386 (2001).
35. Green, N.M., *et al.* Murine B cell response to TLR7 ligands depends on an IFN-beta feedback loop. *Journal of immunology* **183**, 1569-1576 (2009).
36. Richardson, C., *et al.* Molecular basis of 9G4 B cell autoreactivity in human systemic lupus erythematosus. *Journal of immunology* **191**, 4926-4939 (2013).
37. Panne, D., Maniatis, T. & Harrison, S.C. An atomic model of the interferon-beta enhanceosome. *Cell* **129**, 1111-1123 (2007).
38. Hata, N., *et al.* Constitutive IFN-alpha/beta signal for efficient IFN-alpha/beta gene induction by virus. *Biochemical and biophysical research communications* **285**, 518-525 (2001).
39. Hamilton, J.A., *et al.* General Approach for Tetramer-Based Identification of Autoantigen-Reactive B Cells: Characterization of La- and snRNP-Reactive B Cells in Autoimmune BXD2 Mice. *Journal of immunology* **194**, 5022-5034 (2015).
40. Merrell, K.T., *et al.* Identification of anergic B cells within a wild-type repertoire. *Immunity* **25**, 953-962 (2006).
41. Crow, M.K. Autoimmunity: Interferon alpha or beta: which is the culprit in autoimmune disease? *Nature reviews. Rheumatology* **12**, 439-440 (2016).
42. Der, S.D., Zhou, A., Williams, B.R. & Silverman, R.H. Identification of genes differentially regulated by interferon alpha, beta, or gamma using oligonucleotide arrays. *Proceedings of the National Academy of Sciences of the United States of America* **95**, 15623-15628 (1998).

43. Chiche, L., *et al.* Modular transcriptional repertoire analyses of adults with systemic lupus erythematosus reveal distinct type I and type II interferon signatures. *Arthritis & rheumatology* **66**, 1583-1595 (2014).
44. Deonarain, R., *et al.* Critical roles for IFN-beta in lymphoid development, myelopoiesis, and tumor development: links to tumor necrosis factor alpha. *Proceedings of the National Academy of Sciences of the United States of America* **100**, 13453-13458 (2003).
45. Deonarain, R., *et al.* Impaired antiviral response and alpha/beta interferon induction in mice lacking beta interferon. *Journal of virology* **74**, 3404-3409 (2000).
46. Alba, A., *et al.* IFN beta accelerates autoimmune type 1 diabetes in nonobese diabetic mice and breaks the tolerance to beta cells in nondiabetes-prone mice. *Journal of immunology* **173**, 6667-6675 (2004).
47. Cherukuri, A., *et al.* Reduced human transitional B cell T1/T2 ratio is associated with subsequent deterioration in renal allograft function. *Kidney international* **91**, 183-195 (2017).
48. Hammad, H., *et al.* Transitional B cells commit to marginal zone B cell fate by Taok3-mediated surface expression of ADAM10. *Nature immunology* **18**, 313-320 (2017).
49. Loder, F., *et al.* B cell development in the spleen takes place in discrete steps and is determined by the quality of B cell receptor-derived signals. *The Journal of experimental medicine* **190**, 75-89 (1999).

50. Zaritsky, L.A., Bedsaul, J.R. & Zoon, K.C. Virus Multiplicity of Infection Affects Type I Interferon Subtype Induction Profiles and Interferon-Stimulated Genes. *Journal of virology* **89**, 11534-11548 (2015).
51. Lau, C.M., *et al.* RNA-associated autoantigens activate B cells by combined B cell antigen receptor/Toll-like receptor 7 engagement. *The Journal of experimental medicine* **202**, 1171-1177 (2005).
52. Giltiay, N.V., *et al.* Overexpression of TLR7 promotes cell-intrinsic expansion and autoantibody production by transitional T1 B cells. *The Journal of experimental medicine* **210**, 2773-2789 (2013).
53. Wang, W., *et al.* Long-term B cell depletion in murine lupus eliminates autoantibody-secreting cells and is associated with alterations in the kidney plasma cell niche. *Journal of immunology* **192**, 3011-3020 (2014).
54. Palanichamy, A., *et al.* Novel human transitional B cell populations revealed by B cell depletion therapy. *Journal of immunology* **182**, 5982-5993 (2009).
55. Raterman, H.G., *et al.* The interferon type I signature towards prediction of non-response to rituximab in rheumatoid arthritis patients. *Arthritis research & therapy* **14**, R95 (2012).
56. Sellam, J., *et al.* Use of whole-blood transcriptomic profiling to highlight several pathophysiologic pathways associated with response to rituximab in patients with rheumatoid arthritis: data from a randomized, controlled, open-label trial. *Arthritis Rheumatol* **66**, 2015-2025 (2014).

57. Thurlings, R.M., *et al.* Relationship between the type I interferon signature and the response to rituximab in rheumatoid arthritis patients. *Arthritis and rheumatism* **62**, 3607-3614 (2010).
58. Sacre, K., Criswell, L.A. & McCune, J.M. Hydroxychloroquine is associated with impaired interferon-alpha and tumor necrosis factor-alpha production by plasmacytoid dendritic cells in systemic lupus erythematosus. *Arthritis research & therapy* **14**, R155 (2012).
59. Gough, D.J., Messina, N.L., Clarke, C.J., Johnstone, R.W. & Levy, D.E. Constitutive type I interferon modulates homeostatic balance through tonic signaling. *Immunity* **36**, 166-174 (2012).
60. Kalunian, K.C., *et al.* A Phase II study of the efficacy and safety of rontalizumab (rhuMAb interferon-alpha) in patients with systemic lupus erythematosus (ROSE). *Annals of the rheumatic diseases* **75**, 196-202 (2016).
61. Furie, R., *et al.* Anifrolumab, an Anti-Interferon-alpha Receptor Monoclonal Antibody, in Moderate-to-Severe Systemic Lupus Erythematosus. *Arthritis Rheumatol* **69**, 376-386 (2017).
62. Hochberg, M.C. Updating the American College of Rheumatology revised criteria for the classification of systemic lupus erythematosus. *Arthritis and rheumatism* **40**, 1725 (1997).
63. Hsu, H.C., *et al.* Interleukin 17-producing T helper cells and interleukin 17 orchestrate autoreactive germinal center development in autoimmune BXD2 mice. *Nature immunology* **9**, 166-175 (2008).

64. Igci, M., *et al.* Gene expression profiles of autophagy-related genes in multiple sclerosis. *Gene* **588**, 38-46 (2016).
65. Metsalu, T. & Vilo, J. ClustVis: a web tool for visualizing clustering of multivariate data using Principal Component Analysis and heatmap. *Nucleic acids research* **43**, W566-570 (2015).
66. Conrad, S., *et al.* Expression of Genes Related to Germ Cell Lineage and Pluripotency in Single Cells and Colonies of Human Adult Germ Stem Cells. *Stem cells international* **2016**, 8582526 (2016).
67. Schneider, C.A., Rasband, W.S. & Eliceiri, K.W. NIH Image to ImageJ: 25 years of image analysis. *Nature methods* **9**, 671-675 (2012).

Supplementary Table 1 – Clinical data for SLE patients recruited for this study†

Subject	% INFβ in T1	% 9G4+	SLEDAI	α-dsDNA*	C3/C4	α-Sm**	α-SSA	Renal*	AM	IS	CS	Race	Sex	Age
59	98.9	ND	20	+	low	+	+	+	HCQ	-	+	AA	F	28.3
68	94.4	ND	6	+	low	+	+	+	HCQ	MMF	+	AA	F	35.6
69	92.9	ND	2	neg (+)	low	neg	neg	neg	HCQ	-	-	AA	F	34.6
60	91.2	ND	2	neg	normal	+	neg	neg	-	-	-	AA	F	30.5
27	88.1	16.6	4	neg (+)	normal	+	+	+	HCQ	MMF	-	AA	F	59.1
04	83.2	16.9	24	+	normal	+	ND†	+	-	RTX, MMF	+	AA	F	67.3
71	83.0	ND	0	neg	normal	neg	+	neg (+)	-	-	-	AA	F	61.2
54	76.7	ND	12	neg (+)	low	+	neg	+	HCQ	-	+	AA	F	26.7
66	67.1	ND	0	neg (+)	normal	+	neg	neg	HCQ	B, MTX	-	AA	F	59.9
33	62.6	6.82	0	neg	normal	+	+	neg (+)	HCQ	MMF	-	AA	F	39
56	60.4	ND	4	+	low	+	neg	+	HCQ	B, MMF	-	C	F	60.4
65	52.8	ND	2	neg (+)	low	+	ND	neg (+)	HCQ	-	+	AA	F	46.7
05	51.8	12.6	3	+	normal	+	+	neg (+)	HCQ	-	+	AA	F	26.5
47	46.9	ND	20	+	low	ND	ND	ND	HCQ	MMF, MTX	+	AA	F	24
61	46.7	4.13	6	neg	normal	neg	ND	neg	QC	MTX, RTX	-	AA	F	44.3
14	46.4	ND	8	+	low	+	neg	neg	HCQ	-	-	AA	F	31.3
45	43.7	ND	6	+	low	neg	ND	neg	HCQ	-	+	AA	F	23.5
19	42.9	5.26	0	neg	normal	neg	neg	neg	HCQ	-	+	AA	F	54.7
63	42.0	10.0	4	neg (+)	low	neg	+	+	HCQ	B, CTX	+	AA	F	31.7
70	41.3	6.85	4	neg	normal	neg	neg	neg	HCQ	-	-	AA	F	64.6
13	38.5	4.13	8	neg	normal	neg	neg	neg	HCQ	-	+	C	F	58.8
57	36.8	2.24	5	+	low	+	neg	neg (+)	HCQ	MMF	+	AA	M	50.8
20	33.6	3.03	0	neg	normal	neg	+	neg	HCQ	MMF	-	C	F	59
52	29.2	ND	8	+	low	ND	neg	+	HCQ	MMF	-	C(h)	F	49
29	17.8	2.18	8	neg	normal	+	ND	neg	HCQ	MTX	+	AA	F	38.8
67	17.1	6.33	6	neg (+)	low	ND	+	neg	HCQ	MTX	-	C	F	62.6
64	14.5	4.9	0	neg	normal	neg	ND	ND	HCQ	-	-	C	F	37.7
44	10.9	3.99	0	neg	normal	ND	neg	neg	HCQ	B	+	C	F	32.2
15	9.4	3.96	6	neg	normal	neg	neg	neg	-	LF	-	C	F	29.8
26	7.97	2.8	4	neg (+)	normal	ND	neg	neg	HCQ	-	-	AA	F	41.1
55	7.11	6.82	2	neg (+)	low	neg	neg	neg	HCQ	-	-	AA	F	21.2
34	5.46	5.33	4	neg	low	+	neg	neg (+)	HCQ	MMF	-	AA	F	24.4
35	3.89	2.58	4	neg (+)	low	neg	neg	neg	-	RTX	-	C(h)	F	22.9
38	0.93	5.66	6	neg	normal	neg	neg	neg	HCQ	-	-	AA	F	41.5

† Unless specified, clinical data were collected at the time of PBMC collection.

* Anti-dsDNA and renal diseases were checked multiple times - table entry noted "neg" if not present at time sample was obtained, adjacent (+) if previously present.

** Anti-Smith (α-Sm) and anti-Sjogren's syndrome antigen (SSA) antibodies are checked once. If the patient was ever positive, a "+" was noted.

† ND – not determined. ND data points were removed for statistical analysis.

Abbreviations used in the table: (+) previously present or active but not at the time sample drawn; neg, not ever present; AM, anti-malaria drug, HCQ, hydroxychloroquine; QC, quinacrine; IS, immunosuppressant; MMF, mycophenolate mofetil; B, belimumab; CTX, cyclophosphamide; RTX, rituximab; MTX, methotrexate; LF, leflunomide; CS, corticosteroid; AA, African American; C, Caucasian; C (h), Hispanic Caucasian; F, Female; M, Male.

Supplementary Table 2 - List of primers used for gene expression analysis

Primers used for amplification of human genes			
Name		Sequence	Size
<i>Cd20</i>	F	TGCACCCATCTGTGTGACTG	99
	R	TTCCTGGAGTTTTTCTCCGTTG	
<i>Cd303</i>	F	ACCTGCGTCATGGAAGGAAAG	109
	R	TCCAAGATTGCATCCCAGTAGA	
<i>Gapdh</i>	F	GCACTCACTGGAATGACCTC	113
	R	TTCTTCGCACTGACACACTG	
<i>Ifnb1</i>	F	GTCTCCTCCAAATTGCTCTC	114
	R	ACAGGAGCTTCTGACACTGA	
<i>Ifna1</i>	F	CTTCAACCTCTTTACCACAAAAGATTC	84
	R	TGCTGGTAGAGTTCGGTGCA	
<i>Ifna7</i>	F	GCCCGTCCTTTTCTTTACTG	171
	R	TTCATGTCTGTCTTCAAGC	
Primers used for amplification of mouse genes			
Name		Sequence	Size
<i>Cd19</i>	F	AGTGATTGTCAATGTCTCAGACC	115
	R	CTCCCCACTATCCTCCACGTT	
<i>Cd23</i>	F	CCAGGAGGATCTAAGGAACGC	72
	R	TCGTCTTGGAGTCTGTTCAAG	
<i>Cd3</i>	F	ATGCGGTGGAACACTTTCTGG	126
	R	GCACGTCAACTCTACACTGGT	
<i>Cd317</i>	F	TGAAGTCACGAAGCTGAACC	150
	R	TGACACTTTGAGCACCAGTAG	
<i>Cd93</i>	F	ATCTCAACTGGTTTGTTCCTGC	186
	R	ACTCTTCACGGTGGCAAGATT	
<i>Gapdh</i>	F	AGGTCGGTGTGAACGGATTTG	136
	R	TGTAGACCATGTAGTTGAGGTCA	
<i>Ifna1</i>	F	AGTGAGCTGACCCAGCAGAT	100
	R	GGTGGAGGTCATTGCAGAAT	
<i>Ifna11</i>	F	CCCAGCAGATCTTGAACCTC	90
	R	GGTGGAGGTCATTGCAGAAT	
<i>Ifna4</i>	F	TCTGCAATGACCTCCATCAG	100
	R	TATGTCCTCACAGCCAGCAG	
<i>Ifna7</i>	F	AGGACTTTAGATTCCCCCAGGA	76
	R	TCATGCAGAACACAGAGGGCT	
<i>Ifnb1</i>	F	CTCCACCACAGCCCTCTC	157
	R	CATCTTCTCCGTCATCTCCATAG	
<i>Tlr7</i>	F	ATTCCTTGCCTCCTGAGGTT	134
	R	GCTGAGGTCCAAAATTTCCA	

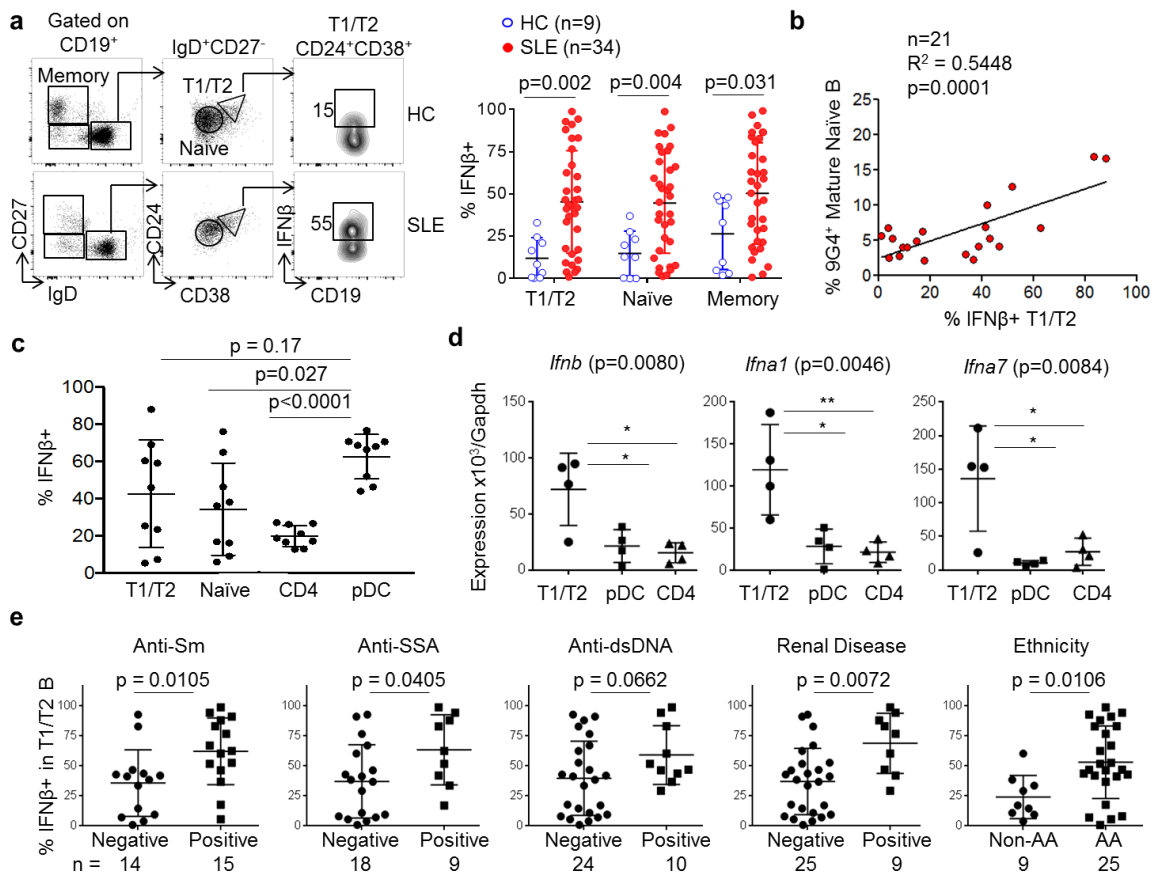


Figure 1. Increased expression of intracellular IFN β in B cells from a subset of SLE patients. (a) Left: Representative flow cytometry plots of intracellular IFN β in circulating B subsets of cells isolated from SLE and healthy control (HC) subjects. Right: Percentage of IFN β ⁺ B cells in T1/T2, naïve, or CD27⁺IgD⁻ memory subpopulation in SLE compared to HC subjects. (b) Correlation between the percent of mature naïve 9G4⁺ B cells vs. percent of intracellular IFN β ⁺ T1/T2 B cells in PBMCs. (c) Quantification of the percentages of IFN β ⁺ cells in the indicated cell populations (n = 9 SLE patients). (d) qRT-PCR analysis of the expression of *Ifnb*, *Ifna1* and *Ifna7* in sorted cells from SLE patients (n = 4). (e) The percentages of IFN β ⁺ T1/T2 B cells in SLE patients segregated by the indicated clinical characteristics (anti-Sm, anti-SSA, anti-DNA, renal disease) and in non-African Americans (non-AA) versus African Americans (AA). All clinical characteristics were data collected at the time of PBMC sample collection. For panels a, c, d, and e, the mean and standard deviation (s.d.) are indicated by the bar and whisker, respectively. Statistical differences were determined by Mann–Whitney U test (a, e), linear regression analysis (b), and one-way ANOVA Tukey’s multiple comparison test (c, d).

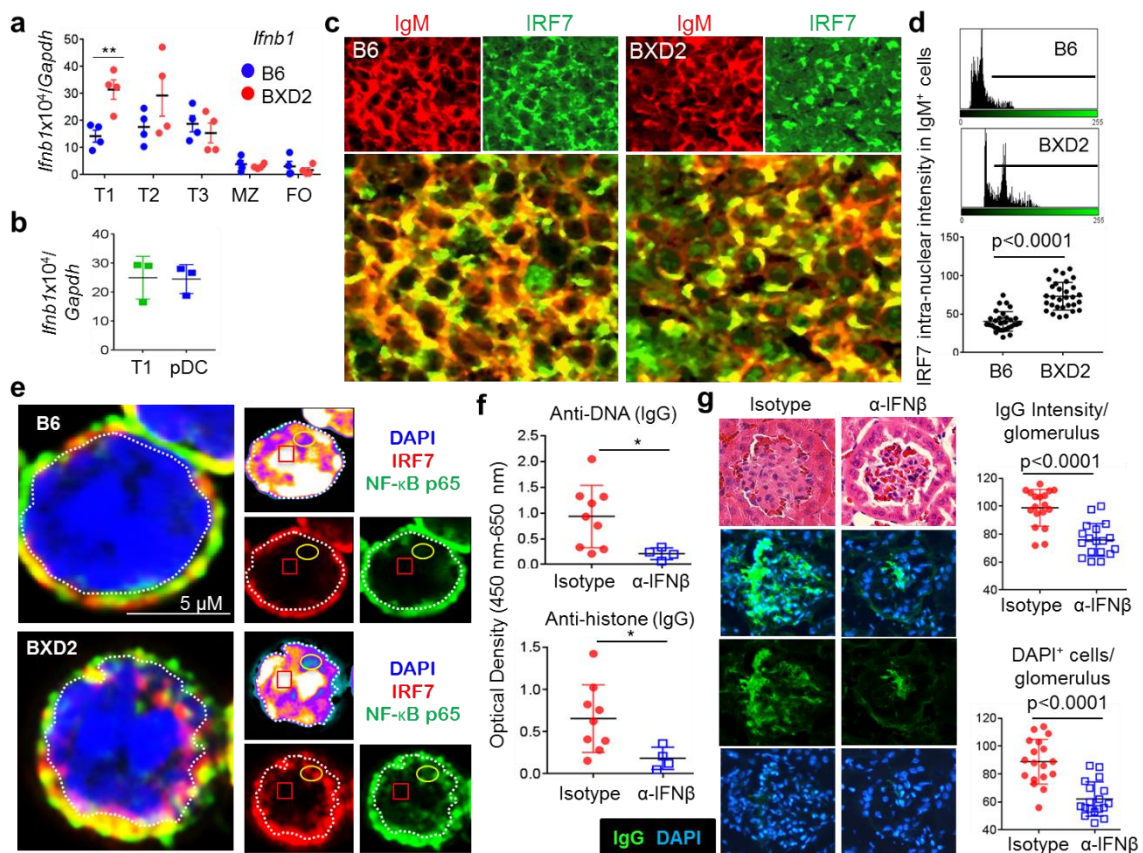


Figure 2. Increased IFN β in T1 B cells of BXD2 mice. (a) qRT-PCR analysis of *Ifnb1* expression in flow cytometry sorted T1, T2, T3, marginal zone (MZ) and follicular (FO) B cells in B6 and BXD2 mice ($n = 4$). (b) qRT-PCR analysis of *Ifnb1* expression in flow cytometry sorted T1 B cells and pDCs isolated from spleens of naïve BXD2 mice ($n = 3$). (c) Confocal imaging analysis of IRF7 and IgM expression in a representative spleen histologic section from B6 and BXD2 mice. Single color image from each is shown on the top (objective lens = 40 \times). (d) ImageJ quantitation of IRF7 intra-nuclear mean fluorescent intensity (MFI) in individual IgM $^{+}$ cells in spleen histologic sections from B6 and BXD2 mice. The results shown are derived from 10 different cells from 3 mice each. (e) High resolution confocal imaging showing the expression of IRF7 and NF- κ B p65 in a representative T1 B cell from each mouse strain (objective lens = 63 \times). Based on the border of DAPI staining, the dotted line marks the nuclear and cytoplasmic junction. (f, g) Groups of 4 week old BXD2 mice were treated with anti-IFN β (250 μ g/2x per week for 6 weeks) or isotype-control antibody and were analyzed two months following the treatment. (f) Serum titers of IgG anti-DNA and anti-histone. (g) Left: H&E staining and fluorescent IgG imaging from a representative glomerulus in each group. Right: ImageJ quantitation of IgG intensity in each glomerulus and DAPI $^{+}$ cell count in each glomerulus ($n = 18$ from 4 different kidney sections each). Data are mean \pm s.d. (* $P < 0.05$, ** $P < 0.01$, *** $P < 0.005$; by two-tailed unpaired Student's t-test).

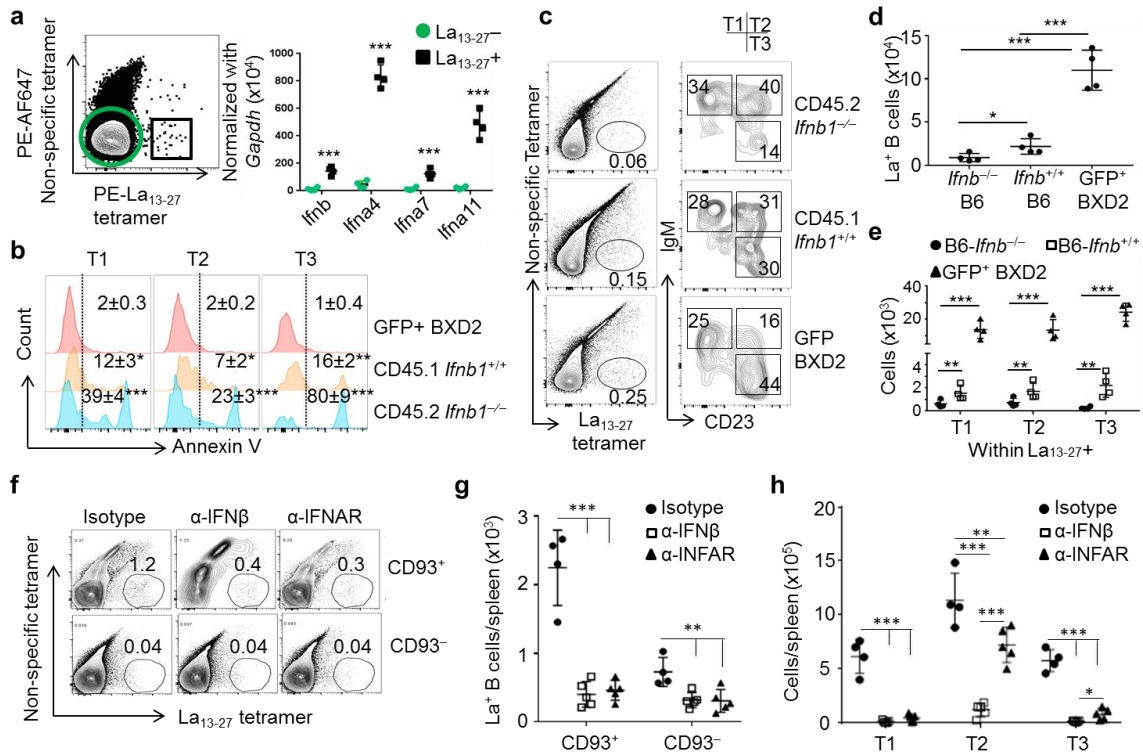


Figure 3. Analysis of the effects of IFN β and type I IFN on La₁₃₋₂₇ tetramer-reactive B cells. (a) qRT-PCR analysis on the expression of *Ifnb*, *Ifna4*, *Ifna7* and *Ifna11* in La₁₃₋₂₇ tetramer reactive versus non-La₁₃₋₂₇-reactive B cells in spleens of BXD2 mice. (b-e) BM-chimeric mice (B6-*Rag1*^{-/-}) were generated by reconstitution with equal numbers of BM cells from CD45.1 B6-*Ifnb1*^{+/+} mice, CD45.2 B6-*Ifnb1*^{-/-} mice and GFP⁺ BXD2 mice. Recipient mice were sacrificed at day 15 post-reconstitution. (b) FACS analysis of Annexin V⁺ apoptotic cells in different transitional B cell subpopulations in triple-chimeric mice (**P* < 0.05, ***P* < 0.01, ****P* < 0.005, compared to BXD2 mice). (c) Flow cytometry analysis showing the percent of La₁₃₋₂₇⁺ B cells (left) and percent of transitional B cells in the CD93⁺ La₁₃₋₂₇⁺ subpopulation (right) in triple-chimeric recipient mice. (d) Quantitation of absolute numbers of La₁₃₋₂₇⁺ B cells. (e) Quantitation of absolute numbers of La₁₃₋₂₇⁺ B cells in the indicated transitional B cell subpopulation. (f-h) BM derived from BXD2 mice were transferred into B6-*Rag1*^{-/-} mice. Recipients were treated *in vivo* with isotype-control antibody, anti-IFN β (α -IFN β) or anti-IFNAR (α -IFNAR) at day 18, 21, and 25 after BM reconstitution. Recipient mice were sacrificed at day 26. FACS analysis of La₁₃₋₂₇⁺ B cells under different treatment conditions. The percent of CD93⁺ (top) or CD93⁻ (bottom) (f), absolute number (g) of La₁₃₋₂₇⁺ B cells, and absolute number of B cells in each indicated transitional B cell subpopulation (h) in the spleens of recipient mice. Throughout, data are mean \pm s.d. (n = 2 mice per group for 2 independent experiments). **P* < 0.05, ***P* < 0.01, ****P* < 0.005; by two-tailed unpaired Student's t-test (a) and by one-way ANOVA with Tukey's post hoc test (b, d, e, g, h).

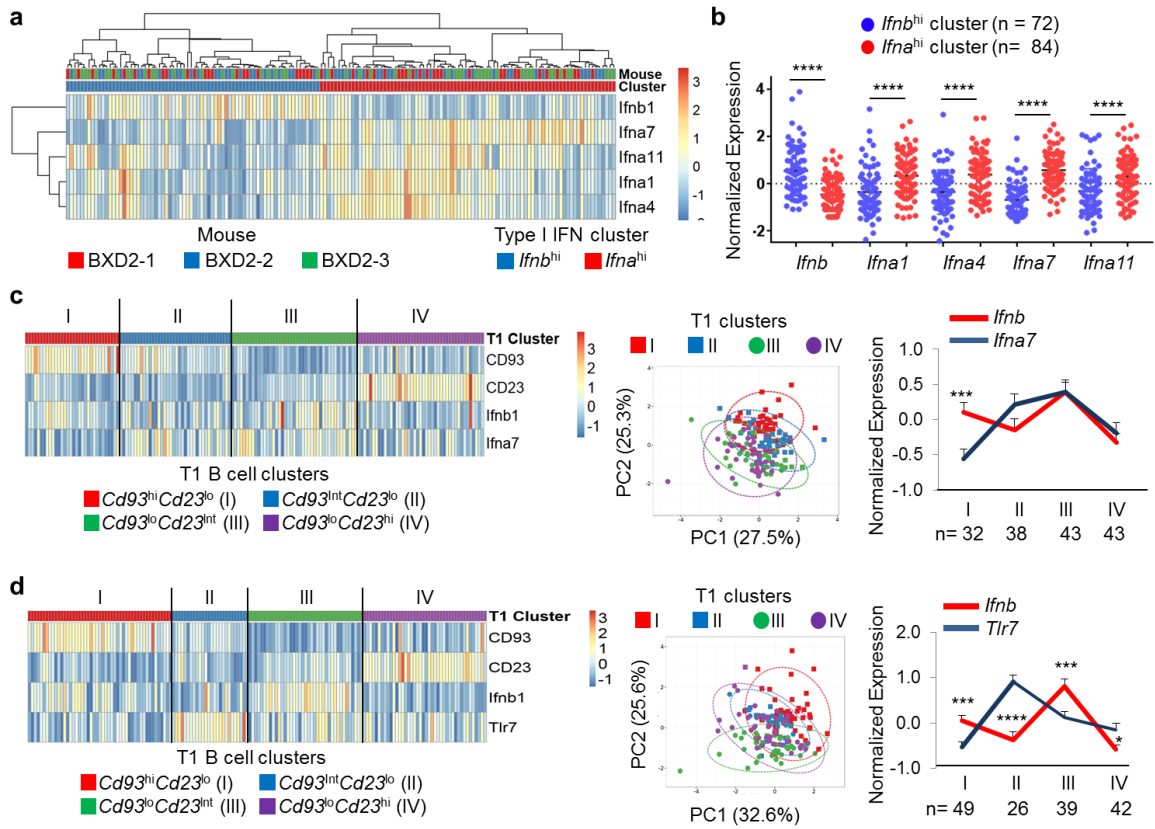


Figure 4. Analysis of *Ifnb*, *Ifna* and *Tlr7* expression in single T1 B cells in BXD2 mice. T1 B cells isolated from the spleen of 3 BXD2 mouse were prepared for single cell gene expression analysis. **(a)** Heatmap of hierarchical type I IFN gene expression clustering in individual T1 B cells ($n = 156$ data points). The top row above the heatmap is color-coded to denote mouse origin. The second row above the heatmap is color-coded to denote the *Ifnb*^{hi} cluster (blue) or *Ifna*^{hi} cluster (red). **(b)** Dot plots showing the normalized expression type I IFN genes in *Ifnb*^{hi} versus *Ifna*^{hi} cluster. The mean and s.d. are indicated by the bar and whisker, respectively. The significance between the indicated genes in each cluster is indicated (**** $P < 0.0001$, unpaired t-test). The original data can be retrieved at <http://biit.cs.ut.ee/clustvis/?s=YkgzIkieGaEjvOi>. **(c, d)** Left: Heatmap showing the normalized expression of *Ifnb* and *Ifna7* **(c)** or *Ifnb* and *Tlr7* **(d)** in the four major clusters of T1 B cells based on the expression levels of *Cd93* versus *Cd23*. Middle: principle component analysis of cells segregated in the four T1 B cell clusters based on PC2 versus PC1. Prediction ellipses are such that with probability 0.95, a new observation from the same group will fall inside the ellipse. Right: Mean expression of *Ifnb* vs *Ifna7* **(c)** or the expression *Ifnb* vs *Tlr7* **(d)** in the indicated cluster of T1 B cells. Data are mean and s.e.m. The significance of the expression difference between *Ifnb* and *Ifna7* **(c)** or between *Ifnb* and *Tlr7* **(d)** in the indicated cluster is shown. The original data can be retrieved at <http://biit.cs.ut.ee/clustvis/?s=WsDQpwrnYRSdxLf> **(c)** and <http://biit.cs.ut.ee/clustvis/?s=SvjLZSSqPnpGBzi> **(d)** (* $P < 0.05$, *** $P < 0.005$, **** $P < 0.0001$, paired t-test).

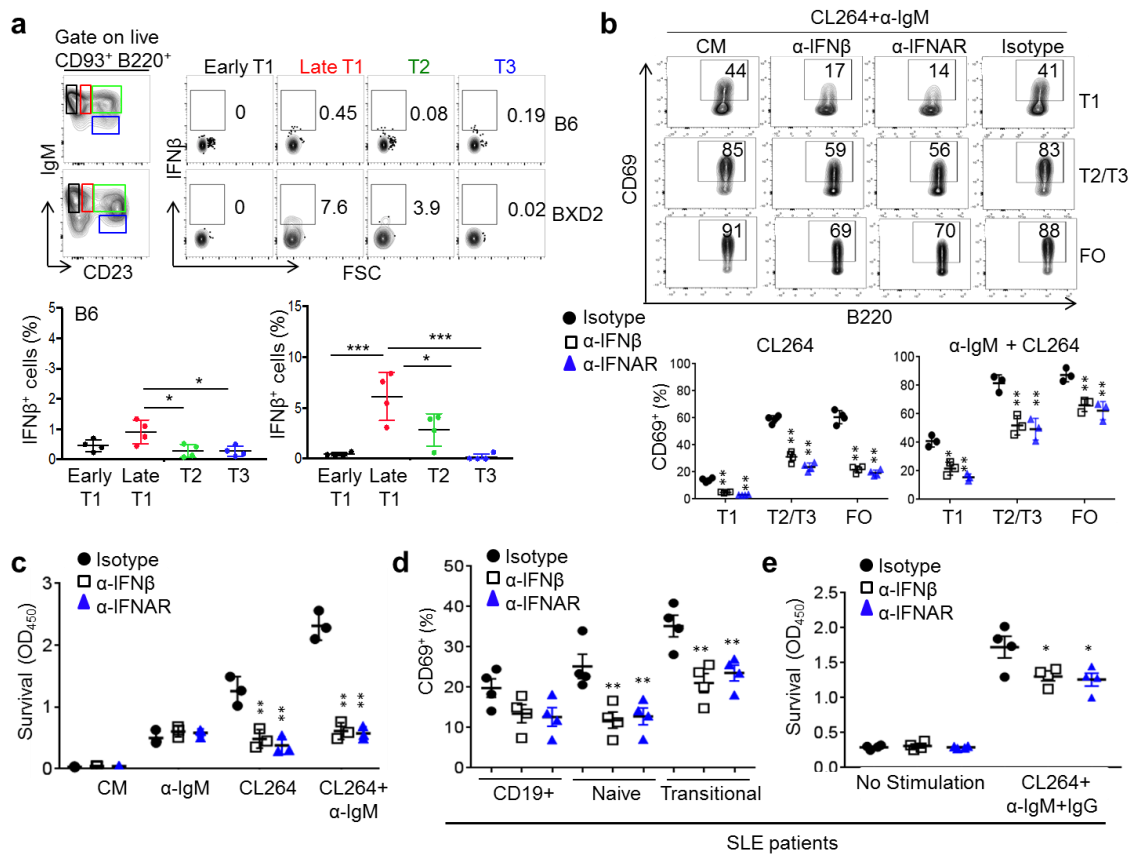


Figure 5. IFN β promotes TLR7-induced transitional B cell activation and survival in BXD2 mice and SLE patients. (a) (Top) Representative FACS plots of IFN β expression in the indicated B cell subset isolated from B6 or BXD2 mice and (Bottom) quantification of IFN β ⁺ cells in the indicated B-cell population (mean \pm s.d., $n = 4$, one way ANOVA Tukey's multiple comparison test; * $P < 0.05$, ** $P < 0.01$, *** $P < 0.001$ between the indicated comparisons). (b, c) B cells purified from BXD2 mice were stimulated *in vitro* with TLR7 agonist CL264 or CL264 plus anti-IgM (α -IgM) in the presence of control media (CM) or neutralizing antibodies to IFN β (α -IFN β), IFNAR (α -IFNAR), or isotype-control antibody. Representative FACS plots (Top) and quantification (Bottom) show the percent CD69⁺ in T1, T2/T3 and FO B cells 4 hours after the indicated stimulation (b). Analysis of survival determined by Dojindo at 56 hours after stimulation by the indicated reagents (c). (d-e) B cells purified from SLE patients were pre-treated with CM, α -IFN β (human), α -IFNAR (human), or isotype-antibody control before stimulation *in vitro* CL264 + anti-human IgM+IgG. (d) Percentage of CD69 in total CD19⁺ B cells, naïve and transitional T1/T2 B cells 4 hours after the stimulation. (e) Analysis of survival determined by Dojindo at 56 hours after stimulation ($n = 4$). The results represent mean \pm s.d. (b, c) or mean \pm s.e.m. (d, e), compared to results obtained from isotype treated group; one-way ANOVA test with Tukey's post-hoc test) (* $P < 0.05$, ** $P < 0.01$).

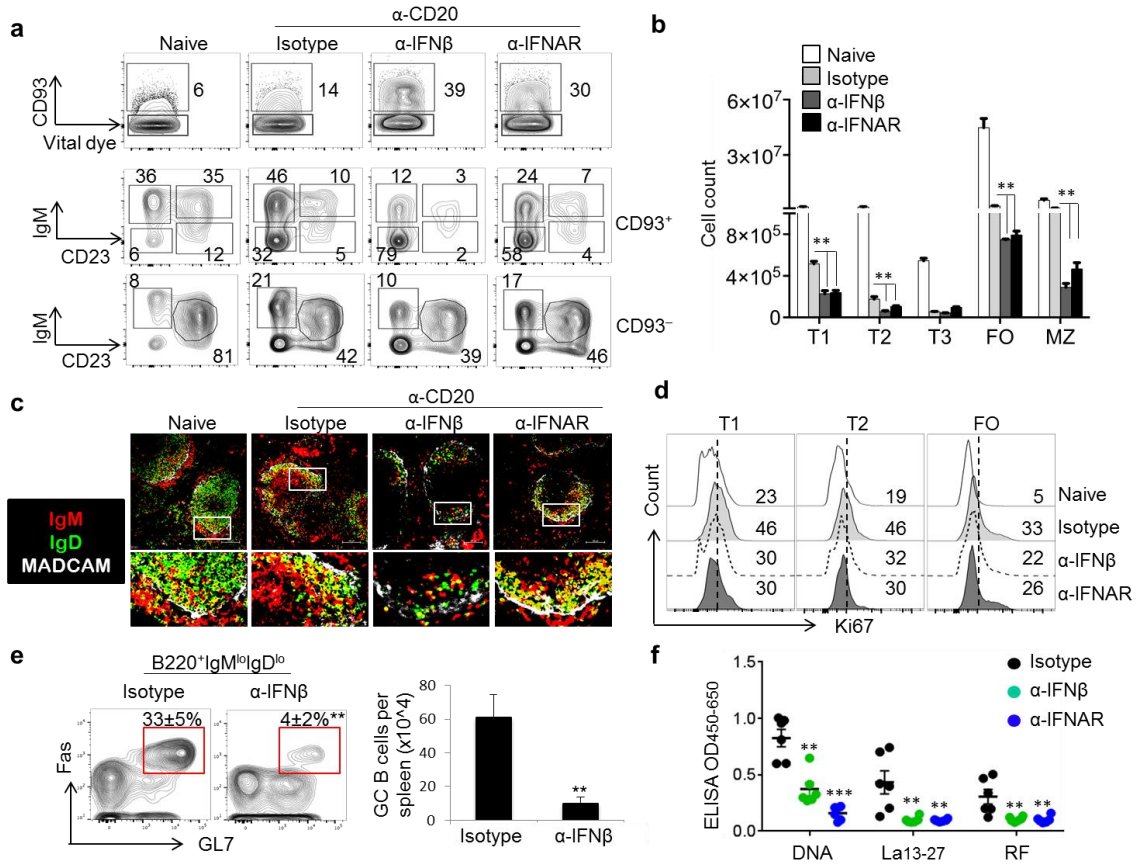
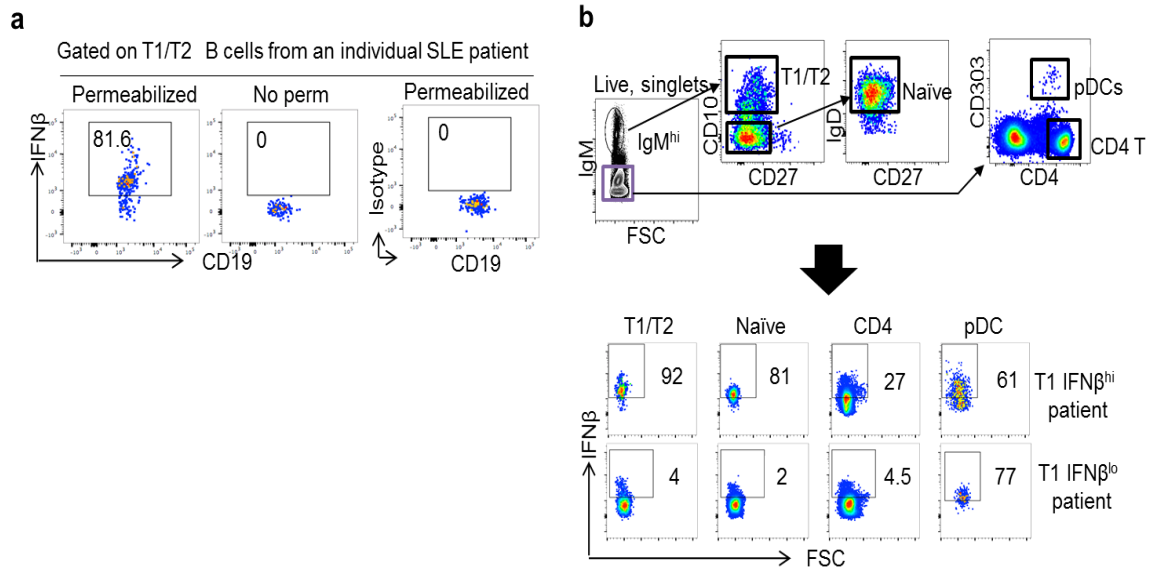
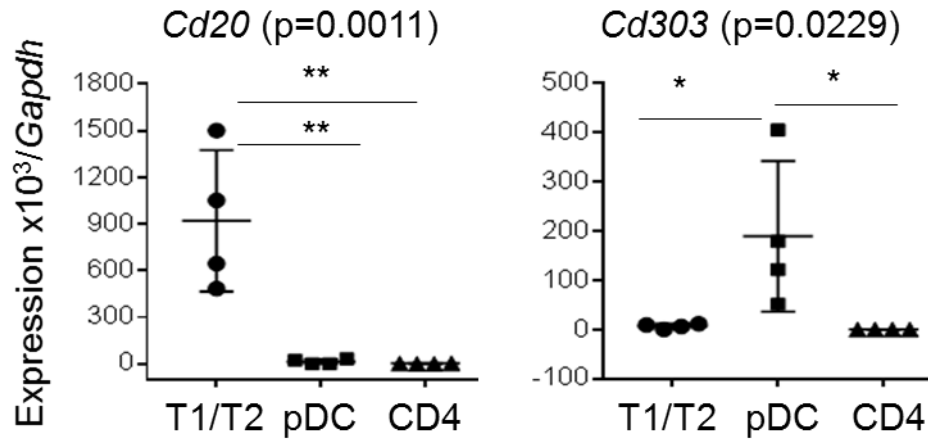


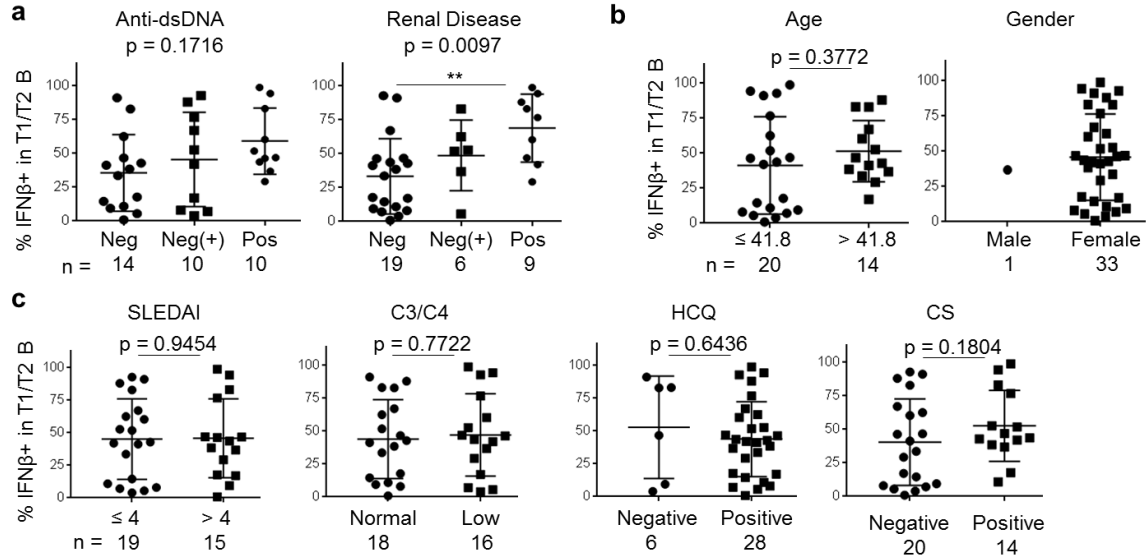
Figure 6. IFN β blockade prevents rapid repopulation of spleen B cells after anti-CD20 depletion. Groups of BXD2 mice (4-wk-old) were untreated (naïve) or treated with anti-CD20 followed by treatment with isotype-control antibody anti-IFN β (α -IFN β) or anti-IFNAR (α -IFNAR) and sacrificed at 2 weeks for analysis of spleen lymphocyte subpopulation. **(a)** FACS analysis of percent of CD93⁺ transitional B cells (top panels), and different subpopulations of transitional (middle panels) or non-transitional B cells (bottom panels). **(b)** FACS analysis of total B cell numbers contained in the indicated subpopulations in the spleen. **(c)** Confocal image analysis of IgM⁺ and IgD⁺ B cells in and surrounding the follicle in spleens from each treatment group. **(d)** Flow cytometry analysis of cell cycle indicated by Ki67 staining of repopulating T1, T2, and FO B cells after BCDT. **(e)** FACS analysis of the percentage of post-switched (IgM^{lo}IgD^{lo}) GL-7⁺Fas⁺ GC B cells at week 9 post anti-CD20 treatment followed by isotype control or anti-IFN β treatment. Percent of switched GC B cells (Left) and absolute count of post-switched GC B cells per spleen (Right). **(f)** ELISA analysis of sera levels of IgG anti-DNA, anti-La₁₃₋₂₇ or RF autoantibodies at week 9 in mice treated with anti-CD20 followed by isotype control, anti-IFN β , or α -IFNAR. Throughout, the results represent mean \pm s.e.m. (* $P < 0.05$, ** $P < 0.01$, *** $P < 0.005$ between the indicated groups or comparing to results obtained from isotype treated group, $n = 2$ for 3 independent experiments, one-way ANOVA test with Tukey's post-hoc test).



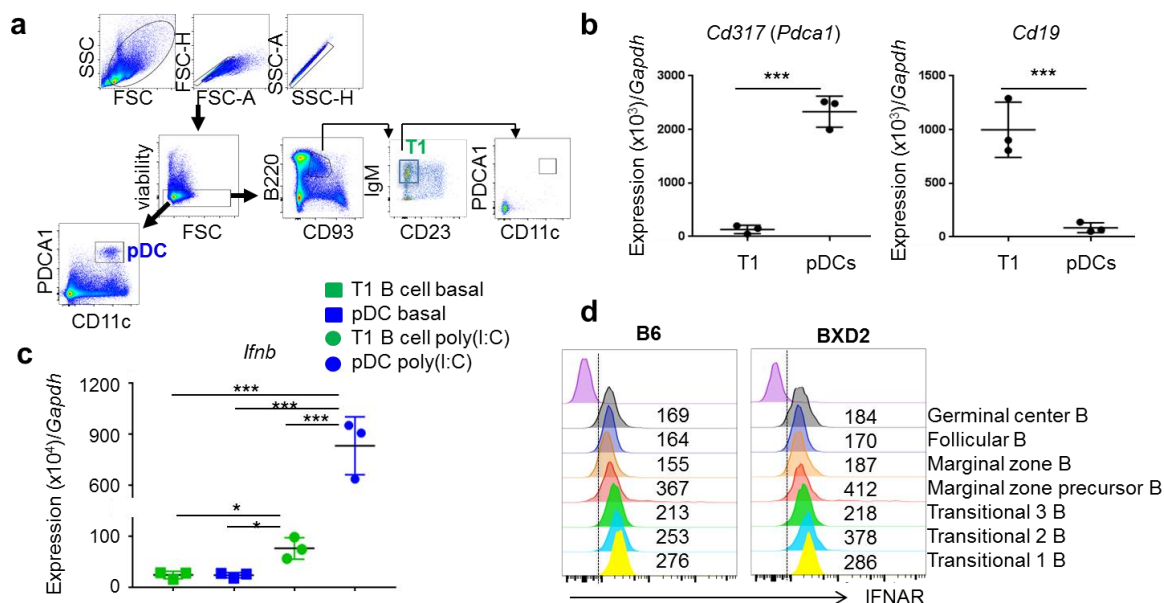
Supplementary Figure 1. Validation of IFN β expression in B cells from PBMCs of SLE patients. (a) Flow cytometry analysis of intracellular expression of IFN β from T1 B cells from a representative SLE patient. B cells were permeabilized (left), unpermeabilized (No perm) and then stained with anti-human IFN β IgG (middle) or an isotype-control primary antibody (right). (b) Flow cytometry analysis of intracellular expression of IFN β in different PBMC populations obtained from SLE patients. Top: Gating scheme for isolation or analysis of T1/T2 B cells, mature naïve B cells, CD4 T cells or plasmacytoid dendritic cells (pDCs). Bottom: Intracellular expression of IFN β on gated T1/T2 B cells, mature naïve B cells, CD4 T cells, or pDCs from a representative SLE patient with either high or low expression of IFN β in T1 B cells.



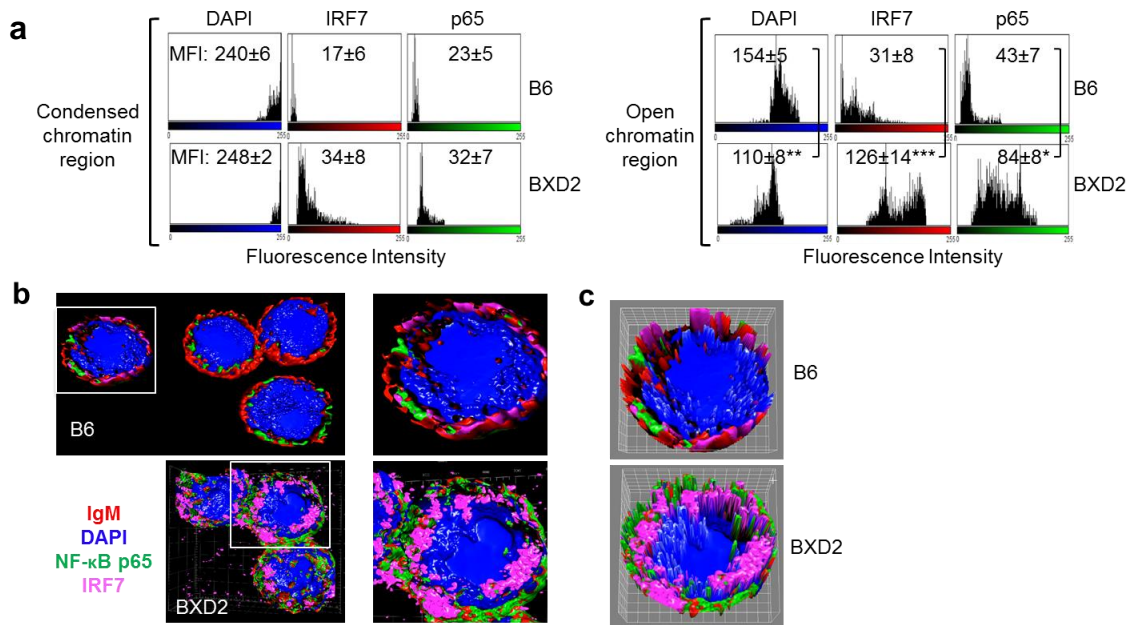
Supplementary Figure 2. Quality controls to validate sorted cell identity. qRT-PCR analysis of the expression of B cell marker gene (Cd20) and pDC marker gene (Cd303) in RNA isolated from T1/T2 B cells, pDCs and CD4 T cells from SLE samples. The results are mean \pm SD of sorted cells (n = 4, * P < 0.05 or ** P < 0.01 between the indicated comparisons, one-way ANOVA Tukey's multiple comparison test). Gating strategy to obtain these cells is as described in Supplementary Fig 1b.



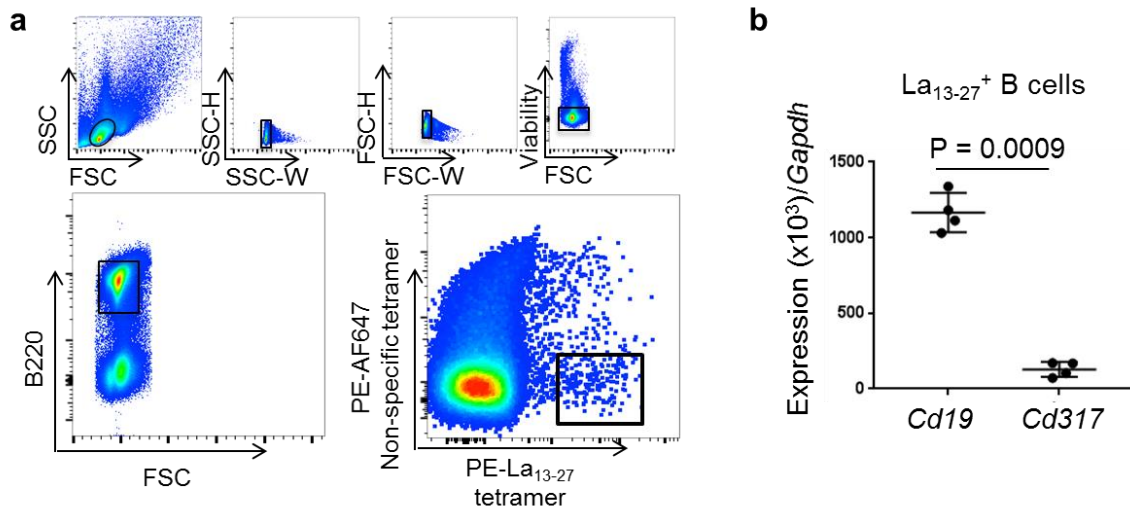
Supplementary Figure 3. Expression of intracellular IFN β in T1/T2 B cells from PBMCs of SLE patients with differential clinical characteristics. Comparison of the expression of intracellular IFN β in T1/T2 B cells from 34 SLE patients with the indicated clinical features. Intracellular IFN β in T1/T2 B cells and clinical parameters were determined in a double blinded manner. **(a)** The percentage of IFN β ⁺ T1/T2 B cells from patients who were anti-dsDNA and renal disease negative (Neg), historically positive but negative at the time of PBMC collection [Neg(+)], or positive (Pos) at the time of PBMC collection (ANOVA test, ** $P < 0.01$). **(b)** The percentage of IFN β ⁺ T1/T2 B cells from younger or older than average age (41.76-yr-old) and in male versus female SLE patients (Mann-Whitney test). **(c)** The percentage of IFN β ⁺ T1/T2 B cells from SLE patients who exhibited the indicated clinical characteristics or were under the indicated treatment. Data are mean \pm s.d. (Mann-Whitney test). Missing data points are removed due to non-determined clinical parameters in certain patients (see Supplementary Table 1). The P value for each comparison is shown (SLEDAI, Systemic Lupus Erythematosus Disease Activity Index; C3/C4, complement 3/complement 4; HCQ, hydroxychloroquine; CS, corticosteroid).



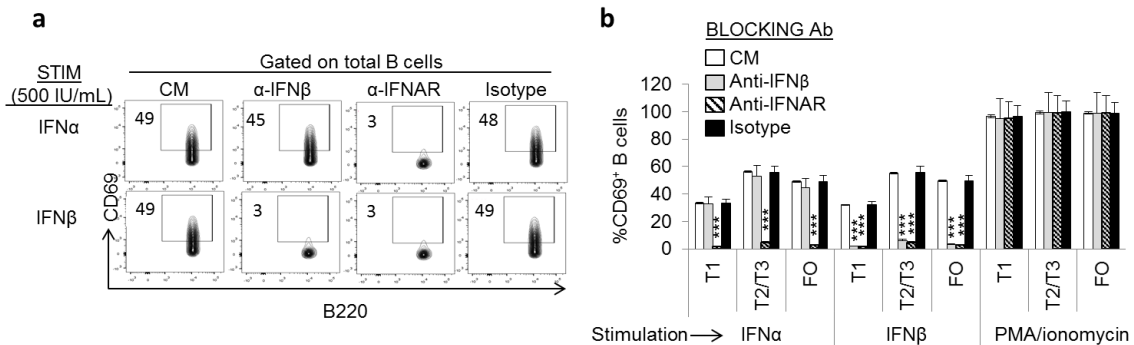
Supplementary Figure 4. Expression of IFN β gene in T1 B cells and pDCs from BXD2 mice. (a) Gating scheme for T1 B cells and pDCs to verify the absence of pDC contamination in the T1 B-cell gate. (b) qRT-PCR analysis of the expression of *Pdca1* (*Cd317*) and *Cd19* in FACS sorted T1 B cells and pDCs. The results are mean \pm s.d. of sorted cells from three individual BXD2 mice. Significance is shown above the graph (*** $P < 0.005$, unpaired t-test). (c) qRT-PCR analysis of the expression *Ifnb* in sorted T1 B cells compared to pDCs. Cells were derived from BXD2 mice that have been administered PBS (basal) or poly(I:C) *in vivo*. Mice were scarified 4 hrs post-injection (* $P < 0.05$, *** $P < 0.005$, one-way ANOVA Tukey's multiple comparison test). (d) Flow cytometry analysis of mean fluorescent intensity of IFNAR on the surface of different subpopulations of B cells from naïve B6 and BXD2 mice. All B subsets were B220⁺ cells. Each cell subset was further gated as CD93⁺IgM^{hi}CD23^{lo/-} for T1, CD93⁺IgM^{hi}CD23⁺ for T2, CD93⁺IgM^{lo}CD23⁺ for T3, CD93^{lo/-}IgM^{hi}CD23⁺CD21^{hi} for marginal zone precursor, CD93^{lo/-}IgM^{hi}CD23^{lo}CD21^{hi} for marginal zone, CD93^{lo/-}IgM^{hi}CD23^{hi}CD21^{lo} follicular and for CD93^{lo/-}GL-7⁺Fas⁺ for germinal center B cells



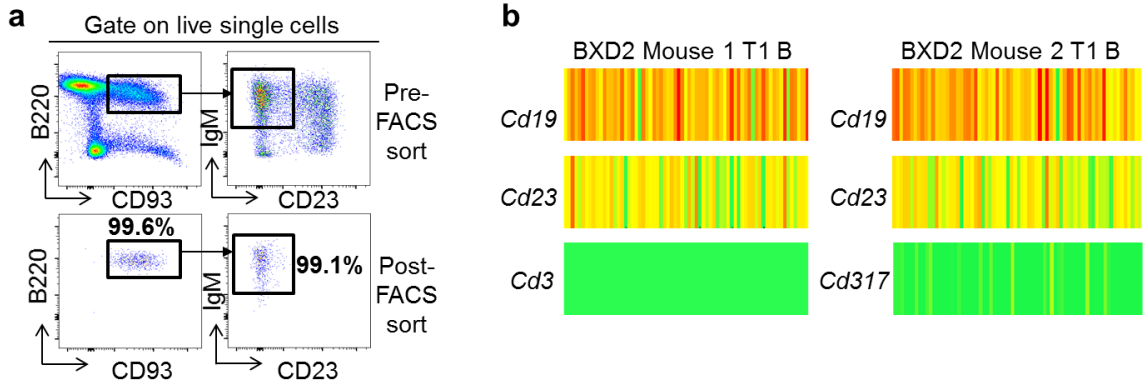
Supplementary Figure 5. Quantitation of nuclear IRF7 and three-dimensional imaging of T1 B cells. (a) ImageJ quantitation analysis showing the MFI and colocalization of IRF7 and NF-κB p65 in DAPI^{hi} condensed chromatin (squared) versus DAPI^{lo} open chromatin (circled) regions in a representative T1 B cells. Staining was carried out using FACS sorted T1 B cells obtained from the spleen of B6 and BXD2 mice (Results are from 10 cells, $n = 3$ spleens). Data are mean \pm s.e.m (* $P < 0.05$, ** $P < 0.01$, *** $P < 0.005$; by two-tailed unpaired Student's t-test). (b, c) Three-dimensional rendering of intra-nuclear expression of IRF7 and NF-κB p65 in T1 B cells isolated from B6 and BXD2 mice (b). A ZEISS LSM 880 with Airyscan confocal microscope was used for image acquisition, and ZEN microscope software was used for image processing. The original size of the images are shown on the left and digitally magnified images are shown on the right. ImageJ 3D view of the intensity of intra-nuclear IRF7 and NF-κB p65 in the selected region in each group (c).



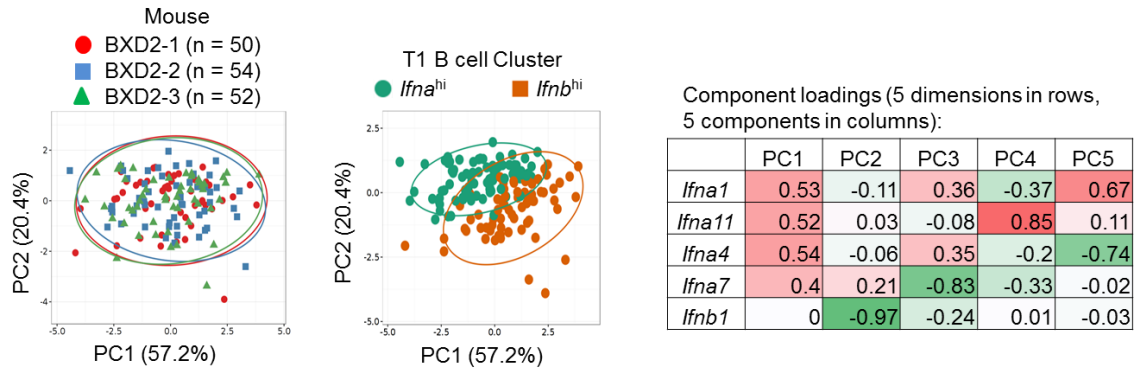
Supplementary Figure 6. La₁₃₋₂₇ reactive cells expressed high levels of *Cd19* but low levels of *Cd317*. (a) Gating strategy for isolation of La₁₃₋₂₇ tetramer reactive B cells. Cells were gated based on forward and side scatter (lymphocyte gate) and signal height and widths (doublet exclusion). B cells were selected as B220⁺ cells. Tetramer⁺ cells were identified as PE*AF647⁻ and PE peptide-tetramer⁺. (b) qRT-PCR analysis of the expression of *Cd19* and *Cd317* (*Pdca1*) in FACS sorted La₁₃₋₂₇⁺ B220⁺ B cells from the spleen of BXD2 mice (n = 4; paired Student's t-test).



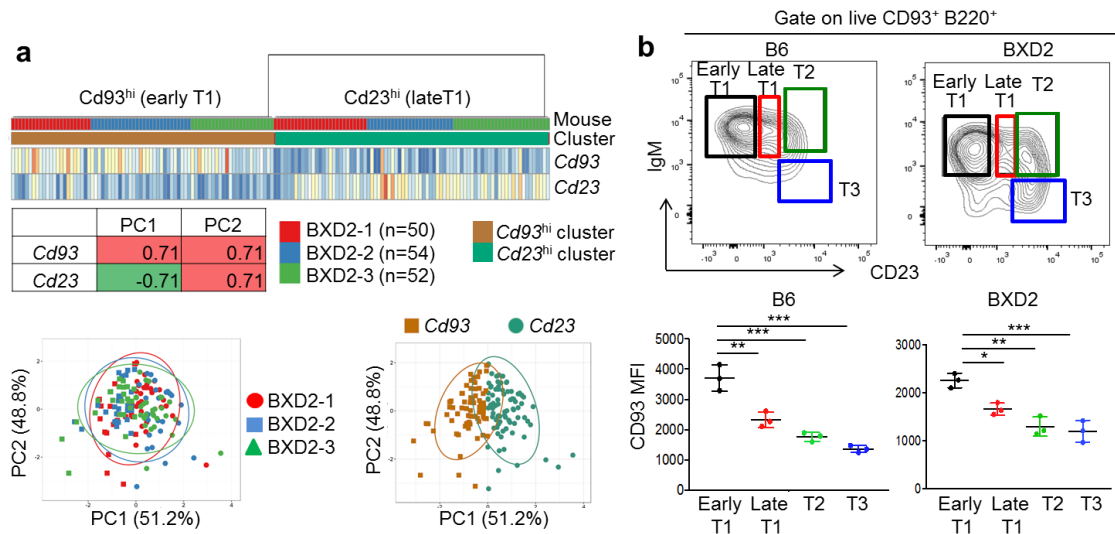
Supplementary Figure 7. Specific inhibition of IFN β by anti-IFN β antibody, or both IFN α and IFN β by IFNAR1 blockade. B cells isolated from the spleen of BXD2 mice were cultured in the presence of either control media (CM), anti-IFN β (1000 IU/mL) anti-IFNAR1 (50 μ g/mL), or antibody isotype control. Cells were immediately stimulated with 500 IU/ml IFN α or IFN β for 5 hours. **(a)** Flow cytometry analysis of the expression of CD69 in CD19⁺ B cells. The analysis was determined under specific conditions of pre-culture with anti-IFN β or anti-IFNAR blockade followed by stimulation with either IFN α (upper) or IFN β (lower). The percent stimulation is indicated by upregulation of CD69 and the percent is indicated by the boxed area. The percent is shown in the box. **(b)** Bar graph representation of percent of CD69⁺ cells in cells treated and stimulated as shown in Panel **a**. PMA is phorbol myristate acetate. The different subpopulations of cells are indicated below the bar graph and the stimulants used are indicated below these subpopulations. Results are mean \pm s.e.m (***) $P < 0.005$ versus isotype stimulated group. $n = 3$ mice per group, one-way ANOVA with Tukey's post-hoc test).



Supplementary Figure 8. Verification of the purity of T1 B cells used for single cell gene expression analysis. (a) Representative flow cytometry plots demonstrate the purity of T1 B cells (gated as live $CD93^+B220^+$ cells followed by $IgM^+CD23^{lo/-}$ gating) before and after the FACS sorting. Cells were prepared from the spleen of three 4-month-old BXD2 mice by FACS sorting. (b) Heatmap showing the expression of the indicated genes in single T1 B cells determined using the BioMark single cell qRT-PCR analysis method. Heatmap analysis was carried out using the Clustvis web tool. The expression of *Cd19* and *Cd23* was used as the marker genes for B cells. The expression levels of *Cd3* and *Cd317* (the gene encoding PDCA1) were used as marker genes for T cells and pDCs, respectively (n=50 and 54 for Mouse 1 and 2, respectively).



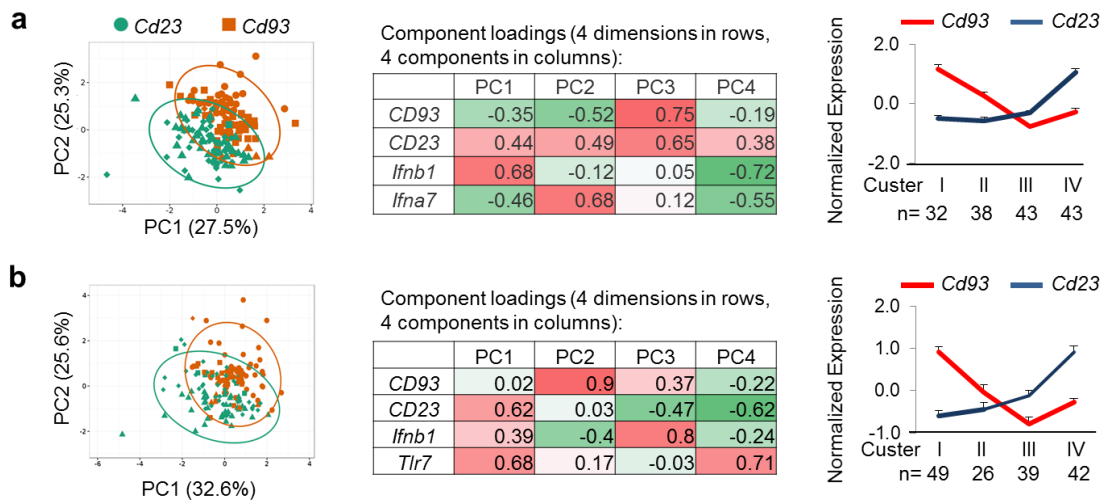
Supplementary Figure 9. Principal component analysis (PCA) of single T1 B cells based on the expression of the indicated genes. X and Y axis show principal component (PC)1 and PC2 that explain 57.2% and 20.4% of the total variance, respectively. PCA was carried out based on the expression of the indicated genes from a total of 156 individual T1 B cells isolated from 3 BXD2 mice (**left**) or based on PC1 and PC2 segregation of *Ifna1*, *Ifna11*, *Ifna4*, *Ifna7* and *Ifnb1* genes in *Ifna*^{hi} and *Ifnb*^{hi} T1 B cell subpopulations (**middle**). Prediction ellipses are such that with probability 0.95, a new observation from the same group will fall inside the ellipse. The correlation between each component and the original variables are shown in the Table in the **right**. The original data can be retrieved from <http://biit.cs.ut.ee/clustvis/?s=YkgzIkieGaEjvOi>



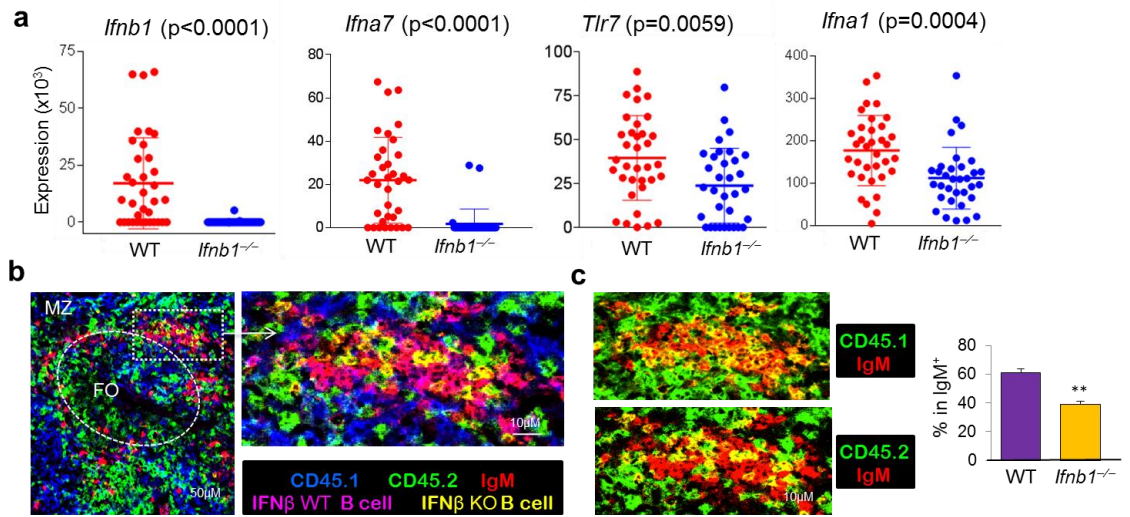
Supplementary Figure 10. Segregation of CD93 and CD23 in subsets of T1 B cells.

(a) The heatmap, component loadings table, and PCA of *Cd93*^{hi} cluster versus *Cd23*^{hi} cluster T1 B cells isolated from three BXD2 mice (n = 156 data points from three 4-month-old BXD2 mice) using the Clustvis web tool software. Prediction ellipses are such that with probability 0.95, a new observation from the same group will fall inside the ellipse. The original data can be retrieved from <http://biit.cs.ut.ee/clustvis/?s=nEZOTPHFyskUeNk>.

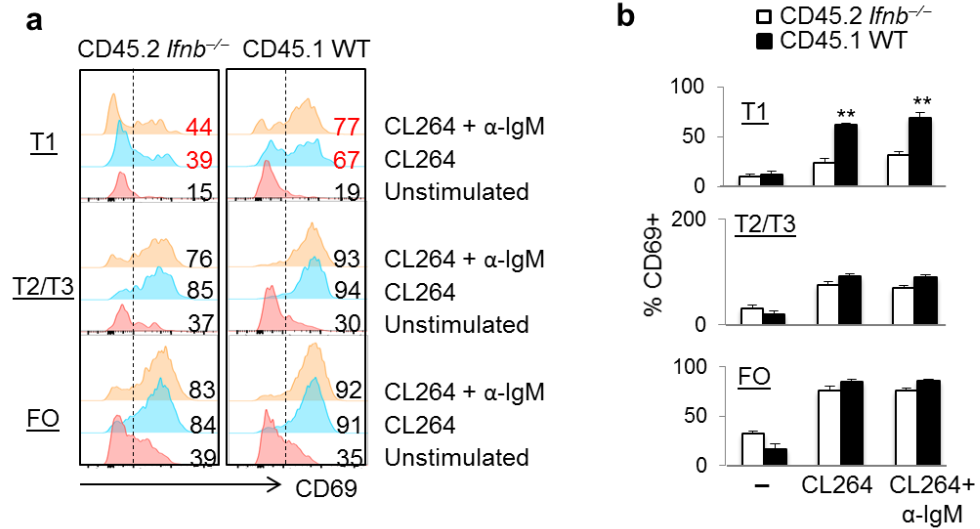
(b) Upper: Representative flow cytometry plots for subgroups of transitional B cells. Lymphocytes were first gated on CD93⁺B220⁺ followed by sub-gating based on IgM and CD23. Lower: Comparison of CD93 mean fluorescence intensity (MFI) in different subsets of transitional B cells. Cells were prepared from the spleen of three 4-month-old BXD2 mice by FACS sorting (Results are mean ± s.d.; $P < 0.05$, $P < 0.01$, Tukey's multiple comparison one-way ANOVA test).



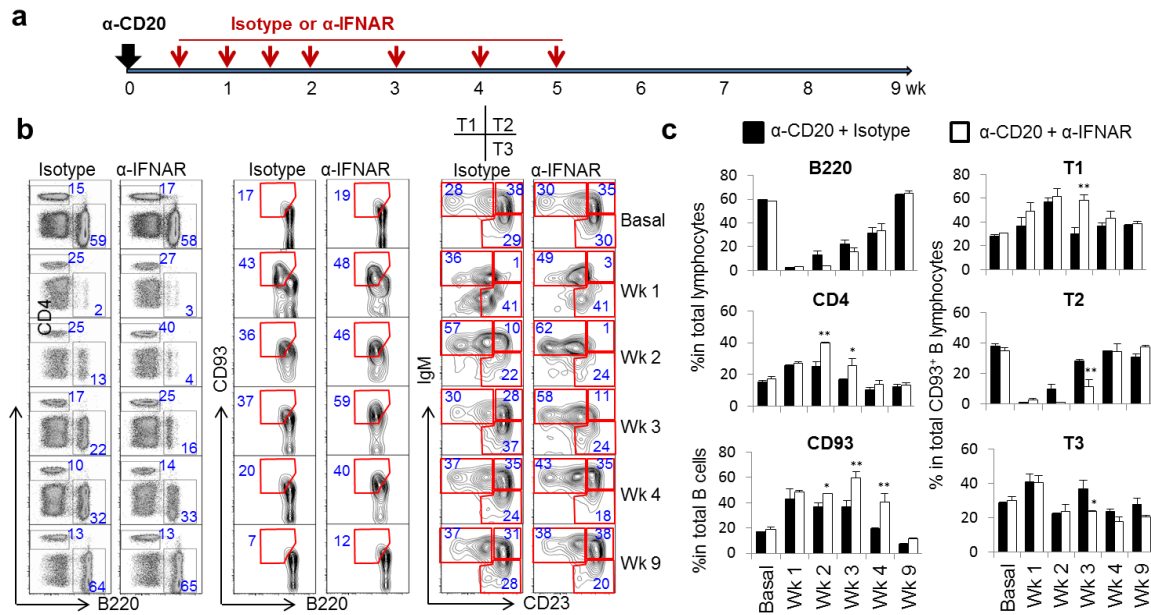
Supplementary Figure 11. PCA of single T1 B cells based on the expression of the indicated genes. (a, b) PC analysis of *Cd93*, *Cd23*, *Ifnb1* and *Ifna7* (a) or *Cd93*, *Cd23*, *Ifnb1* and *Tlr7* (b) in 156 single T1 B cells obtained from three BXD2 mice (4-mo). **Left: X and Y axis showing principal component (PC) 1 and PC2 that explain the total variance. PCA was carried out based on the segregation of PC1 and PC2 of *Cd93*^{hi} vs *Cd23*^{hi} cells. Prediction ellipses are such that with probability 0.95, a new observation from the same group will fall inside the ellipse. **Middle:** the correlation between each component and the original variables for each. **Right:** Line graph showing the expression of *Cd93* or *Cd23* in each cluster of T1 B cells. (n = 156 data points combined from three BXD2 mice). For the line graphs, Cluster I, II, III, and IV represent *Cd93*^{hi}*Cd23*^{lo}; *Cd93*^{Int}*Cd23*^{lo}, *Cd93*^{lo}*Cd23*^{Int}, and *Cd93*^{lo}*Cd23*^{hi} cells, respectively; data are shown as mean ± s.e.m). The original data can be retrieved from <http://biit.cs.ut.ee/clustvis/?s=WsDQpwrnYRSdxLf> for panel (a) and <http://biit.cs.ut.ee/clustvis/?s=SvjLZSSqPnpGBzi> for panel (b).**



Supplementary Figure 12. Endogenous IFN β production by transitional B cells is required for their development and directly stimulates production of IFN α . BM-chimeric mice were generated by reconstitution with equal numbers of BM derived from CD45.1 B6-*Ifnb*^{+/+} (WT) mice and CD45.2 B6-*Ifnb*^{-/-} mice into irradiated CD45.2 *Rag1*^{-/-} mice. Recipient mice were sacrificed at day 15 post BM transfer. **(a)** BioMark qRT-PCR analysis of the expression of the indicated gene in Fluidigm single captured T1 B cells derived from CD45.1 B6-*Ifnb*^{+/+} or CD45.2-*Ifnb*^{-/-} developed within the same double-chimeric recipient mice day 15 post BM transfer. The significance in difference of expression between the WT ($n = 35$) and KO ($n = 33$) single cells is indicated by the P value in the graph (Data are mean \pm s.d.; non-parametric Mann-Whitney test). **(b)** Left: Confocal imaging analysis of IgM⁺ CD45.1 B6-*Ifnb*^{+/+} (WT) and IgM⁺ CD45.2 *Ifnb*^{-/-} cells in the spleen sections from double-chimeric recipient mice (objective lens = 40 \times). Right: Boxed area was digitally magnified. **(c)** Left: Digitally magnified two-color IgM/CD45.1 or IgM/CD45.2 confocal image. Right: Bar graph showing the percent of IgM⁺ B cells derived from either WT BM or *Ifnb*^{-/-} BM. Data are mean \pm SEM, and all images are from a representative spleen region or a spleen follicle from each group. (** $P < 0.01$ WT vs. *Ifnb*^{-/-} $n = 2-3$ mice per group for 2 independent experiments, unpaired Student's t -test).

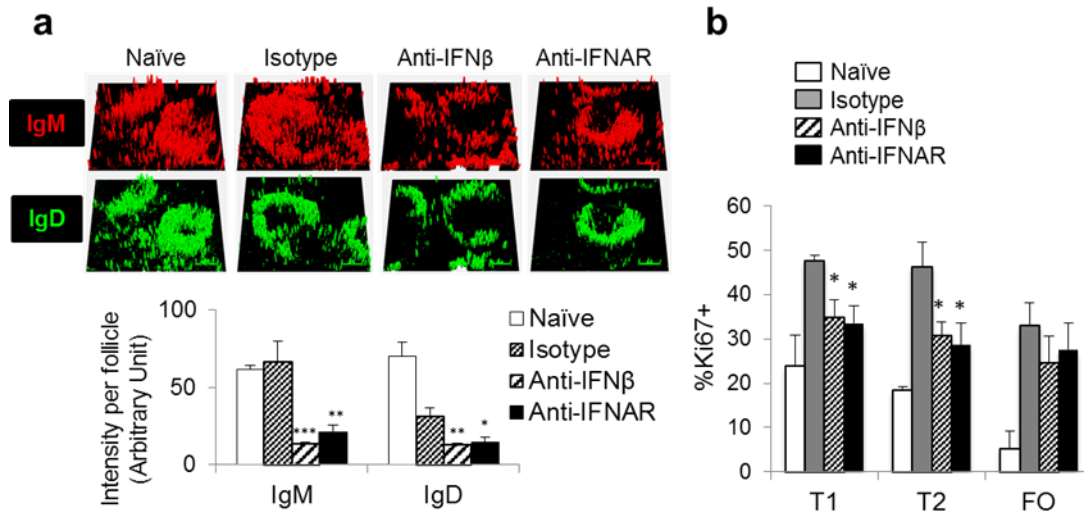


Supplementary Figure 13. B cell early activation response to TLR7 and BCR/TLR7 co-stimulation in *Ifnb*^{-/-} and *Ifnb*^{+/+} B cells. B cells isolated from the spleens of BM chimeras (irradiated recipients reconstituted 1:1 with CD45.1 *Ifnb*^{+/+} B6 and CD45.2 *Ifnb*^{-/-} BM) were co-cultured 1×10^6 cells/mL for 5 hours in the presence of a TLR7 agonist, CL264 (2 μ g/mL) or CL264 + α -IgM (2 μ g/mL each). Cells were cultured in flat bottom well plates to minimize cell - cell interaction. **(a)** FACS analysis of percent CD69⁺ T1, T2/T3 and FO-B cells 6 hours after *in vitro* stimulation with the indicated reagent(s). **(b)** Percent of CD69⁺ cells in each population of B cells stimulated by the indicated reagent(s). Data in **b** are mean \pm s.e.m (** $P < 0.01$ between *Ifnb*^{+/+} (WT) and *Ifnb*^{-/-}. $n = 2-3$ mice per group for 2 independent experiments, unpaired Student's *t*-test).



Supplementary Figure 14. Kinetics of B cell repopulation after anti-CD20 treatment and effects of IFNAR blockade with an anti-IFNAR blocking antibody.

(a) Timeline for administration of either isotype antibody control or anti-IFNAR at different times after anti-CD20 B cell depletion in male BXD2 mice (starting at 6-wk-old) (b) Flow cytometry analysis of PBMCs showing the percent of B cells in subpopulations gated first on CD4 and B220. The boxed B220⁺ subpopulation was further gated on CD93 and B220. The outlined transitional B cell population was further analyzed based on expression of IgM and CD23. The numbers represent the percent of each cell population. (c) Bar graph representation of the percent of either total lymphocytes, percent in total B cells (lower left), or the percent within the CD93⁺ B cell population (right), as indicated by B220, CD4, CD93, or T1, T2, and T3 B cells (mean ± s.e.m., * $P < 0.05$ and ** $P < 0.01$ between anti-IFNAR and isotype treated group. $n = 2$ mice per group for 2 independent experiments, unpaired Student's t -test).



Supplementary Figure 15. Anti-IFN β and anti-IFNAR inhibited B cell repopulation post anti-CD20 B-cell depletion in BXD2 mice. (a, b) Groups of BXD2 mice were treated with anti-CD20, followed by treatment with anti-IFN β (250 μ g/2x per week) anti-IFNAR (300 μ g/2x per week) or isotype-control antibody and sacrificed at 2 weeks for analysis of spleen B cell repopulation. (a) ImageJ quantification of confocal image analysis of either IgM and IgD. Upper: Distribution of B cells surrounding the follicle following repopulation at two weeks after depletion. Lower: The intensity of IgM and IgD within the follicle is quantitated by ImageJ. The bar graph represents the mean \pm s.e.m. of expression of either IgM or IgD under indicated conditions of treatment (b) Percent of Ki67⁺ B cells two weeks after B cell depletion therapy and treatment under the indicated conditions (T1, T2 and FO subpopulations as indicated). Results were analyzed by flow cytometry. The percent represents the mean \pm s.e.m. of Ki67⁺ B cells (* $P < 0.05$ and ** $P < 0.01$ versus isotype treated group. $n = 2$ mice per group for 3 independent experiments, one-way ANOVA with Tukey's post-hoc test).

GENERAL APPROACH FOR TETRAMER BASED IDENTIFICATION OF
AUTOANTIGEN REACTIVE B CELLS: CHARACTERIZATION OF LA AND
SNRNP REACTIVE B CELLS IN AUTOIMMUNE BXD2 MICE

by

JENNIE A. HAMILTON, JUN LI, QI WU, PINGAR YANG, BAO LUO, HAO LI,
JOHN E. BRADLEY, JUSTIN J. TAYLOR, TROY D. RANDALL,
JOHN D. MOUNTZ, AND HUI-CHEN HSU

Journal of Immunology, May 15;194(10):5022-34

Copyright ©

2015

by

The American Association of Immunologists, Inc.

Used by permission

Format adapted for dissertation

Abstract

Autoreactive B cells are associated with the development of several autoimmune diseases, including systemic lupus erythematosus (SLE) and rheumatoid arthritis (RA). The low frequency of these cells represents a major barrier to their analysis. Antigen-tetramers prepared from linear epitopes represent a promising strategy for the identification of small subsets of antigen-reactive immune cells. This is challenging given the requirement for identification and validation of linear epitopes and the complexity of autoantibody responses, including the broad spectrum of autoantibody specificities and the contribution of isotype to pathogenicity. We therefore tested a two-tiered peptide microarray approach, coupled with epitope mapping of known autoantigens, to identify and characterize autoepitopes using the BXD2 autoimmune mouse model. Microarray results were verified through comparison with established age-associated profiles of autoantigen specificities and autoantibody class switching in BXD2 and control (B6) mice and high-throughput ELISA and ELISPOT analyses of synthetic peptides. Tetramers were prepared from two linear peptides derived from two ribonucleic acid binding proteins (RBP): lupus La and 70 kDa U1 small nuclear ribonucleoprotein (snRNP). Flow cytometric analysis of tetramer-reactive B-cell subsets revealed a significantly higher frequency and greater numbers of RBP-reactive marginal zone precursor (MZ-P), transitional T3 and PDL-2⁺CD80⁺ memory B cells, with significantly elevated CD69 and CD86 observed in RBP⁺ MZ-P B cells in the spleens of BXD2 compared to B6 mice, suggesting a regulatory defect. This study establishes a feasible strategy for the characterization of autoantigen-specific B-cell subsets in different models of autoimmunity and, potentially, humans.

Introduction

Autoantibody production by autoreactive B cells is characteristic of many autoimmune diseases, including SLE and RA (1, 2). Studies using mouse models indicate that certain autoantibodies can drive the development of these diseases (3-5). In humans, the close association of some autoantibodies with disease activity and progression together with the therapeutic effects of B cell depletion suggests their role in clinical disease (6, 7). Although disrupted regulation of autoreactive B cells is considered central to the development of autoimmunity, the relative contributions of different subsets of B cells (8, 9) remains unclear. Progress in this area is challenged by the low frequency of the autoreactive B cells and their diversity, which encompasses the broad spectrum of autoantigens recognized, the isotype of the antibodies produced and the subtle phenotypic distinctions that differentiate B cell subsets. To date, the most commonly used approach to analysis of autoantigen-specific B cell subsets in autoimmunity has been the creation of transgenic mice in which the cells can be expanded clonally through experimental manipulation (10).

Labeled monomeric and tetrameric antigen conjugates can be used to brightly label cells on the basis of their ligand specificity (11, 12). This approach has been applied successfully to the identification and isolation of specific types of cells that occur at low frequency (13, 14). It is, however, technically difficult to construct a labeled autoantigen tetramer using most full-length antigens, as the process requires ligation of the antigen-coding material into an expression vector with a biotinylated site and, subsequently, stringent purification of the antigen. One approach to overcome this issue is the use of small, linear-peptide autoepitopes. In 2003, Newman, *et al.* described

a system in which a DNA mimotope peptide could be conjugated to phycoerythrin (PE)-labeled streptavidin (SA) and used to detect B cells reactive to this DNA mimotope in immunized BALB/c mice (15) and later in humans with SLE (16). This tetramer strategy has since been adapted for the isolation of B cells specific for various epitopes on citrullinated fibrinogen (17), HLA (18) HIV gp41 (19, 20), and tetanus toxoid C fragment (11). Recently, Taylor *et al.* used a novel detection and tetramer enrichment strategy to assess polyclonal self-antigen-specific B cells by rigorously analyzing regulation of ovalbumin (OVA) and glucose-6-phosphate isomerase (GPI) Ag-specific B cells in OVA expressing and wild-type mice (21).

Potentially, the epitope-tetramer approach represents a powerful tool for analysis of B-cell reactivity in autoimmunity, especially if it could be applied to analysis of B cells that are reactive with the predominant autoantigens that have been identified in SLE and RA. Full realization of this potential depends, however, on a feasible strategy for the identification and characterization of linear autoepitopes and the demonstration that these linear autoepitopes represent authentic, clinically relevant antigens. Since the first description of the development of large-scale autoAg arrays for autoAb determination in patient sera (22), advances in peptide microarray chip technologies have led to the development of comprehensive Ag-arrays (23, 24). We reasoned that these arrays, which contain thousands of known B-cell epitopes and their modified variants, can be used to identify authentic linear autoepitopes that are potential candidates for the generation of autoAg-tetramer panels.

To test this strategy, we used a step-wise approach to enable identification of lupus La and snRNP autoepitopes reactive with B cells from the BXD2 mouse model of

systemic autoimmunity. The emergence of the autoantibody repertoire and, importantly, its age-associated transition to the expression of pathogenic autoantibodies is well characterized in these mice (4, 25, 26). Utilization of these tetramers for FACS sorting of B cells from the spleens of BXD2 and B6 mice confirmed an expanded frequency and number of La₁₃₋₂₇ and snRNP₃₅₇₋₃₇₃ epitope-reactive, activated (CD69⁺ and CD86⁺) MZ-P B cells in BXD2 mice as compared to age-matched B6 mice and further revealed an expanded frequency and higher number of La₁₃₋₂₇ and snRNP₃₅₇₋₃₇₃ reactive transitional T3 and memory B cells. Thus, the present work validates the utilization of linear autoepitopes for analysis of the autoantibody repertoire and establishes a systematic, experimental approach to autoepitope identification and Ag tetramer-based B-cell isolation. This approach is readily adaptable to analysis of other autoimmune models and, potentially, analysis of patient-derived samples.

Materials and Methods

Mice

Female C57BL/6 (B6) and BXD2/TyJ recombinant inbred mice were obtained from The Jackson Laboratory. All mice were housed in the University of Alabama at Birmingham Mouse Facility under specific pathogen-free conditions in a room equipped with an air-filtering system. The cages, bedding, water, and food were sterilized. All mouse procedures were approved by the University of Alabama at Birmingham Institutional Animal Care and Use Committee. Sera were obtained from B6 and BXD2 mice at the specified ages by retro-orbital eye bleeding. After separation from blood, sera were stored at -80°C.

Peptide Microarray

Autoantibody profiles for linear peptides were determined using PEPperCHIP® technology (PEPperPRINT GmbH, Heidelberg, Germany). For the PEPperCHIP® Autoimmune Epitope Microarray, 2,733 autoimmune disease-associated linear B-cell epitopes were selected unbiasedly using all linear epitopes that have been curated for humans or mouse models of autoimmune diseases from the Immune Epitope Database (27) (<http://www.iedb.org/>) including 192 citrullinated peptides. Peptides shorter than 3 amino acids, peptides too long for synthesis, and peptides including non-citrulline side-chain modifications were not included on the chip. Peptides were all printed in duplicate spots and framed by a fusion tag (Flag) peptide (DYKDDDDKGG, 186 spots) and influenza virus hemagglutinin (HA) epitope tag peptide (YPYDVPDYAG, 186 spots) as controls. Controls were detected by monoclonal anti-FLAG(M2)-LL-DyLight800 and monoclonal anti-HA (12CA5)-LL-DyLight680 (1:1000) (Rockland Immunochemicals, Inc., Gilbertsville, PA).

The microarray was initially incubated with the secondary goat anti-mouse IgG (H+L) DyLight680 antibody at a dilution of 1:5000 for 60 min at room temperature to analyze background interactions with the autoimmune epitopes, ensuring that there were no background interactions due to non-specific binding of the secondary antibody to the peptides. Serum from six 8-10 month old BXD2 mice was pooled. Before serum incubation with chip, peptide arrays were first incubated for 60 min in Blocking Buffer for Near Infra Red Fluorescent Western blotting (Rockland Immunochemicals, Inc., Gilbertsville, PA). The microarray was washed twice in PBS, pH 7.4 with 0.05%

Tween 20 (PBS-T), and incubated for an additional 30 min in washing buffer. The array was then incubated overnight at 4°C with mouse sera diluted 1:1000 for anti-mouse IgG (H+L) analysis or 1:200 for gamma-chain-specific and 1:1000 for μ -chain-specific analysis in PBS-T (secondary anti-mouse Ig Abs from Rockland Immunochemicals, Inc., Gilbertsville, PA). After multiple washes in washing buffer, the microarrays were incubated for 30 min with the secondary antibody in PBS-T at room temperature. After two additional washes in washing buffer, the microarrays were rinsed with ultrapure water and dried in a stream of air.

Green/red fluorescence intensities were acquired on an LI-COR Odyssey Imager (Lincoln, NE) at scanning intensities of 7/7 in both channels (700 nm/800 nm), 0.8 - 1.0 mm offset, at a spatial resolution of 21 μ m. Staining of the Flag and HA control peptides that frame the arrays gave rise to high and homogeneous spot intensities with a coefficient of variation of <2%. PepSlide® Analyzer software was used to analyze the data. This program breaks down the fluorescence intensities of each spot into raw, foreground, and background signals, and calculates the standard deviation of the foreground median intensities. Epitopes resulting in a binding intensity greater than five standard deviations from mean chip intensity were considered as positive.

A PEPperCHIP® custom epitope microarray with 80 epitopes selected based upon the first array analysis was then prepared. Analysis of serum from individual B6 and BXD2 mice of different ages was carried out in the same fashion as the first microarray (serum dilution 1:200 for IgG analysis, 1:1000 for IgM analysis). IgG and IgM reactivity was detected by goat anti-mouse IgG conjugated DyLight800 and goat anti-mouse IgM (μ chain) conjugated to DyLight680 at 1:1000 and 1:5000 dilutions

respectively (both Rockland Immunochemicals, Inc., Gilbertsville, PA). For these analyses, epitopes resulting in a binding intensity of five-fold or greater compared to B6 control mice were considered positive.

Tetramer production

Lupus La₁₃₋₂₇ (LEAKICHQIEYYFGD) and SnRNP₃₅₇₋₃₇₃ (SHRSERERRRDRDRDRD) were produced and biotinylated at the N-terminus by Sigma-Aldrich and supplied as a lyophilized powder. Each peptide was suspended in DMSO to a stock concentration of 10 mM and diluted to 1 mM in pure dH₂O. Suspended peptides were aliquoted and stored at -80°C. Tetramers were generated by adding biotinylated peptide step-wise in 1/10 volumes to 6.7 μM streptavidin-R-phycoerythrin (SA-PE, ProZyme) at a molar ratio of 30:1 and allowed to incubate 60 min at room temperature or overnight at 4°C. Tetramers were purified on a Sephacryl S-300 FPLC size exclusion column. The tetramer fraction was concentrated using a 100-kDa molecular weight cutoff Amicon Ultra filter (Millipore). The concentration of tetramer was calculated by comparison with a standard curve of PE absorbance at 540 nM, which was measured using an Emax Precision Microplate Reader (Molecular Devices, Sunnyvale, CA).

The nonspecific tetramer control was prepared by conjugating the core fluorochrome SA-PE to AF647 (Molecular Probes) according to the manufacturer's protocol for 60 min at room temperature. The free AF647 was removed by centrifugation in a 100-kD molecular weight cut off Amicon Ultra filter (Millipore). The SA-PE*AF647 complex concentration was calculated by measuring the absorbance of

PE at 540 nm. The SA-PE*AF647 complex was then incubated with 10-fold molar excess of free biotin for 30 min at room temperature.

Tetramer enrichment

Spleens were harvested from individual mice and single-cells suspensions prepared in RPMI supplemented by 5% fetal bovine serum (FBS). Cell suspensions were prepared by gentle teasing apart of tissue with the plunger of a 3 mL syringe. Cells were passed through a cell strainer to eliminate clumps and debris and washed with RPMI. Red blood cells were lysed from the resuspended pellet with 3-5 mL ACK lysing buffer and washed twice in RPMI. Lymphocytes were resuspended to 200 μ l in anti-CD16/32 Fc block (2.4G2; BioLegend) in 2% rat serum. Next, PE*AF647-conjugated nonspecific tetramer was added at a concentration of 20-30 nM and incubated at 4°C for 5-10 minutes. PE-conjugated peptide tetramer was added at a concentration of 10-20 nM and incubated on ice for 30 min, followed by one wash in 15 ml cold fresh sorter buffer (PBS, 2 mM EDTA, 2% FBS). Tetramer-stained cells were then resuspended to a volume of 80 μ l of sorter buffer per 10^7 cells, mixed with 5-10 μ l anti-PE-conjugated magnetic microbeads (Miltenyi Biotec) per 10^7 cells and incubated on ice for 30 min, followed by one wash with 10 ml sorter buffer. In experiments where single-cell suspensions were divided into 1/2 and 1/4 mouse equivalents before tetramer labeling/enrichment, the volumes were scaled down appropriately. The cells were then resuspended in 3 ml of cold sorter buffer and passed over a magnetized LS column (Miltenyi Biotec). Bound cells were eluted according to manufacturer's instructions.

Free peptide blocking experiments were performed on unenriched samples. Free peptide (300 μ M) was allowed to incubate with cells 30 minutes prior to tetramer staining.

Flow cytometry analysis

Cell pellets from the enriched and column flow-through fractions were re-suspended in FACS buffer (PBS + 5% FBS) and incubated with surface antibodies for 30 min on ice. Surface antibodies included Pacific Blue–anti-CD19 (6D5; BioLegend) or Brilliant Violet 650–anti-CD19 (6D5; BioLegend), Brilliant Violet 605–anti-CD86 (GL-1; BioLegend), Brilliant Violet 510–anti-CD69 (H1.2F3; BioLegend), FITC–anti-CD21/35 (7E9; BioLegend), PE-Cy7–anti-F4/80 (BM8 BioLegend), PE-Cy7–anti-Thy1.2 (30-H12; BioLegend) and FITC anti-CD93 (AA4.1, Biolegend). Dead cells were excluded from analysis with APC-eFluor® 780 Organic Viability Dye (eBioscience). After cell surface staining, cells were washed twice with 3 mL FACS buffer and fixed in 1% paraformaldehyde/FACS solution for cell surface marker analysis. Cells (300,000–1 X 10⁶ /sample) were analyzed by flow cytometry. FACS data were acquired with an LSRII FACS analyzer (BD Biosciences) and analyzed with FlowJo software (Tree Star Ashland, OR). All flow cytometry analysis was carried out using a combination use of forward light scatter and side scatter height, area, and width parameters to exclude aggregated cells.

ELISA

The levels of autoantibodies specific for selected linear peptides in the sera of B6 and BXD2 mice were determined by ELISA using a NeutrAvidin High Binding Capacity-coated 96-well plate (Thermo Scientific Pierce). Briefly, biotinylated peptides

were conjugated to the plate overnight at 4°C at a concentration of 30 µM (all peptides were purchased from Sigma Aldrich). ELISAs were developed with either an HRP-labeled goat anti-mouse IgG or a goat anti-mouse IgM Ab (Southern Biotechnology Associates) and tetramethylbenzidine substrate (Sigma-Aldrich). OD₄₅₀₋₆₅₀ was measured on an Emax Microplate reader.

ELISPOT quantification of autoantibody-producing B cells

NeutrAvidin High Binding Capacity coated plates (96 well) (Thermo Scientific Pierce) were coated overnight with 50 µM of peptide at 4°C, washed, and then blocked with complete medium. Single cell suspensions of spleens isolated from B6 or BXD2 mice were prepared as described above followed by erythrocyte removal by ACK lysis. Cells were washed twice and adjusted to a final volume of 200 µl containing 1×10^5 cells/well in the presence or absence of phorbol myristate acetate (PMA; 50 ng/ml; Sigma-Aldrich) and ionomycin (750 ng/ml; Sigma-Aldrich) which stimulates the calcineurin pathway and B cell affinity maturation (28). After incubation for 24 h, plates were washed six times with PBS/0.05% Tween 20 and then incubated for 4 h with 1 µg/ml HRP-conjugated goat anti-mouse IgM mAb (Southern Biotechnology Associates) or HRP-conjugated goat anti-mouse IgG (Southern Biotechnology Associates) in PBS/5% BSA. Plates were washed six times with PBS/0.05% Tween 20, before spots were developed using 3-amino-9-ethylcarbazole. Plates were read using a CTL automatic ELISPOT reader and analyzed using Immunospot 3.1 software (CTL). All experiments were repeated in duplicate.

B cell stimulation

For some experiments, different populations of tetramer⁺, non-specific and tetramer^{neg} B cells were sorted on a FACSAria and cultured in the presence of LPS (Sigma Aldrich, 20 µg/mL) and IL-4 (100 units/mL) for four days. The supernatant was collected and used immediately or stored at -80°C until analysis of reactivity for the secreted IgG autoantibodies.

Full Length Protein and Western Blot Analysis

Full length human recombinant La was purchased from ProSpec-Tany Technogene Ltd. La protein was electrophoresed on 12% SDS polyacrylamide gels and transferred onto polyvinylidene difluoride membranes. The membranes were incubated with supernatant from cultured cells overnight at 4 °C. As a positive control, anti-La antibody (Cell Signaling Technology) was used at a dilution of 1:1000 to confirm the identity of the La protein on the blot. Anti-mouse or anti-rabbit HRP-conjugated Abs (Life Technologies) were used at a 1:250 dilution. HRP Abs were detected using a chemiluminescent substrate (Pierce).

Statistical Analyses

All results were shown as mean ± standard error of the mean (SEM). A two-tail *t* test was used when two groups were compared for statistical differences. *P* values less than 0.05 were considered significant. For microarray antigen distribution analyses, Chi squared analysis was performed, and a p-value less than 0.05 was considered significant.

Results

Identification of autoAg-derived peptides recognized by antibodies from BXD2 mice

To test whether the PEPperCHIP autoimmunity microarray could be used to identify linear autoepitopes in the sera of autoimmune mice, we used pooled sera from six BXD2 mice that all have developed spontaneous lupus-like features (8-10-month old). The microarray consists of 2,733 experimentally characterized autoimmune epitopes and 192 citrullinated variants. All of these epitopes have been associated with autoimmune disease and are cataloged in the Immune Epitope Database (IEDB) (29). The BXD2 serum peptide-reactivity profile was detected by goat-anti-mouse IgG, revealing that the majority (79%) of BXD2 reactive autoepitopes derive from three main groups: nuclear proteins, endoplasmic reticulum (ER) or mitochondrial enzymatic proteins, and matrix proteins. There was a significantly increased prevalence of reactivities to peptides deriving from nuclear Ags and ER/mitochondrial enzymatic proteins (**Fig. 1A**) and within the nuclear Ags, an increase in peptides deriving from ribonucleoprotein (RNP) Ags (**Fig. 1B**). These results are consistent with our previous MALDI-TOF-MS analysis of BXD2 autoantibody-precipitated autoantigens resolved by 2-dimensional electrophoresis, in which the major autoAgs targeted by serum from 8-10 month old BXD2 mice were identified as nuclear proteins (snRNP, Ro, histone), heat-shock proteins (GRP78 or “BiP”), enzymes (enolase, aldolase), and structural proteins (keratin, actin) (4, 26).

The identified BXD2 autoepitope profile advances knowledge concerning the autoantibody repertoire in the BXD2 mice. Common lupus associated autoantigens such as snRNP, smD1, CENP-A, and Ro52 were represented by 53, 37, 39 and 46 reported B-cell linear epitopes on the microarray, respectively (**Fig. 1C**). This extensive coverage allowed identification of multiple BXD2 positive epitopes on a given autoantigen. Antigens displaying extensive reactivity with BXD2 serum (six or greater positive epitopes) were 70 kDa U1RNP, smD1, CENP-A, and Ro52 (**Fig. 1C**). Similarly, the inclusion of citrulline-modified variants in the array content revealed that pooled BXD2 serum was reactive with a citrullinated and a non-citrullinated version of fibromodulin, fibrinogen- β and BiP peptides (**Fig. 1D**). This finding is consistent with reports that human autoantibodies recognize both an uncitrullinated and citrullinated variant of peptides deriving from common autoantigens (30, 31).

Strategies for selection of linear autoepitopes for further analysis

Given that the number of potential autoepitopes in BXD2 mice is extremely large, further analysis required development of an efficient, high throughput strategy that would generate the data required for informed selection of the linear autoepitopes of interest. A secondary microarray was printed that included linear peptides representing the predominant epitopes identified in the original screening of pooled BXD2 sera, encompassing peptides from the three major categories of proteins targeted by BXD2 autoantibodies and present in human disease (32), i.e., nuclear, matrix and enzyme/chaperone antigens (**Table 1**).

As class switching is associated with the production of pathogenic autoantibodies (33), the secondary microarrays were probed with serum from individual BXD2 mice and control normal B6 mice using an isotype-specific analysis (**Fig. 2**). In addition, because the emergence of class-switched, pathogenic autoantibodies follows a well-defined age-associated progression in BXD2 mice (4), sera from BXD2 mice of different ages and age-matched B6 controls were included in this assay. The results obtained from analysis of BXD2 sera indicated an increase in IgG autoantibodies to peptides deriving from nuclear autoantigens, with highest levels of anti-La, RNP and Ro60 in older BXD2 mice (**Fig. 2A, 2B**). The predominant nuclear peptides that were reactive with BXD2 sera were associated with a cluster of key antigens, including La, the U1snRNP complex, Ro60, CENP-A/E, DNA topoisomerase, and RNA polymerase II (**Fig. 2A**). Epitopes derived from matrix proteins fibrinogen- β and fibromodulin (**Fig. 2C**) and enzyme proteins BiP and clusterin (**Fig. 2D**) were positive in most BXD2 mice.

In contrast to the IgG autoantibodies, which were detected largely in BXD2 mice only, IgM autoantibodies were broadly present in both B6 and BXD2 mice (**Fig. 2, Supplementary Fig. 1**). These results are consistent with the previously described age-associated emergence of class-switched Ro60, followed by heat-shock proteins including BiP, and finally histone and DNA autoantibodies in BXD2 mice (4).

Verification of epitopes using synthesized peptides.

To verify that the peptides discovered by screening the epitope microarray are authentic epitopes, selected peptides were synthesized with an N-terminal biotin (**Table 2**). These biotinylated peptides were analyzed for reactivity with IgM and IgG

autoantibodies in the sera of B6 and BXD2 mice by standard ELISA and ELISPOT analyses. For these assays, we used high-binding capacity (HBC) neutravidin coated 96-well plates for anti-peptide antibody detection. Using this modified ELISA, we found significantly higher levels of IgG autoantibodies directed against all tested linear epitopes from BiP, histone, CENP-A, La, snRNP as well as structural antigen epitopes fibrinogen- β -cit and fibromodulin-cit in the sera of 7-9 month-old BXD2 compared to younger BXD2 mice and normal B6 mice (**Fig. 3A, 3B**). Also, consistent with the microarray data, we found IgM autoantibody reactivity with all peptides tested and, for most peptides, a lack of elevation in the levels of these autoantibodies between young or old B6 mice compared to young or old BXD2 mice (**Fig. 3C**).

Using the modified ELISPOT, we also were able to enumerate anti-peptide antibody producing B cells from the spleens of 5-6 month old B6 and BXD2 mice, and observed a significantly increased number of IgG producing B cells from BXD2 mice that were reactive with La₁₃₋₂₇, histone H1b₂₀₅₋₂₁₉, and snRNP₃₅₇₋₃₇₃, which was increased by stimulation with PMA + ionomycin (**Fig. 4D**). There were, however, little to no detectable IgG producing autoantibody-reactive B cells from B6 mice (**Fig. 4D**). For IgM isotype ELISPOT analysis, under unstimulated condition, there was a significantly lower number of IgM spots for H1b₂₀₅₋₂₁₉ and snRNP₃₅₇₋₃₇₃ in BXD2 compared to B6 mice (**Fig. 4E**).

Construction of tetramers and strategy for gating analysis

From the above assays, the La₁₃₋₂₇ epitope was selected for construction of an autoepitope tetramer using a protocol modified from Taylor et al (21). Briefly, a 10-20

fold molar excess of biotinylated peptide was conjugated to R-phycoerythrin (PE)-labeled streptavidin (SA). To exclude cells binding irrelevant epitopes on PE or streptavidin, a non-specific tetramer was also produced by conjugating Alexa Fluor 647 (AF647) to SA-PE loaded with biotin to block free binding sites. For all tetramer experiments, single-cell suspensions were co-stained with the non-specific biotin-PE*AF647 tetramer and the peptide-PE tetramer to discriminate between peptide-binding and non-specific binding (21). Lymphocytes were gated by forward and side scatter, followed by exclusion of doublets, non-viable cells, and non-B cells. The resulting two-dimensional plot with biotin-PE*AF647 non-specific tetramer on the y-axis and the peptide PE-tetramer on the x-axis yields a small population of La₁₃₋₂₇ binding B cells (**Fig. 4A**). To test the specificity of tetramer-labeled B cells, cells were pre-incubated with free peptide prior to tetramer staining. Pre-incubation of cells with La₁₃₋₂₇ but not irrelevant OVA₃₂₃₋₃₃₉ peptide, resulted in a significant decrease in La₁₃₋₂₇ tetramer-stained cells (**Fig. 4B, 4C**).

Because epitope specific B cells are rare events within the B6 and BXD2 polyclonal repertoire (**Fig. 4D**, left panels), tetramer-stained cells were enriched with magnetic anti-PE beads and a magnetized MACS column using the protocol described by Taylor et al (21). While most cells obtained in the final enriched fraction bind nonspecifically to the column or Biotin-PE*AF647 tetramer, a smaller number of cells bind only the peptide-PE tetramer. This tetramer enrichment strategy enables isolation and analysis of rare peptide-specific B cells with significantly increased sensitivity as compared to a similar analysis of pre-enriched B cells and column flow-thru fractions

(**Fig. 4D, 4E**). A similar method was used to generate, enrich and determine the B-cell binding specificity of a second snRNP₃₅₇₋₃₇₃ tetramer (**Supplementary Fig. 2**).

Increased La₁₃₋₂₇ and snRNP₃₅₇₋₃₇₃ reactive in selective B cell subsets in BXD2 mice

Identifying a BXD2 autoepitope repertoire for tetramer design enables study of epitope-reactive B cells in non-transgenic autoimmune mice. We therefore tested this approach in a proof-of-principle study designed to determine if autoantigen-reactive B cells are skewed towards separate B-cell subsets in B6 and BXD2 mice. Based on results from the aforementioned analyses, epitopes derived from La and snRNP were selected. These two RNA binding protein autoantigens are targets of human SLE autoantigens (6) and are present in apoptotic debris (34, 35). Tetramer-reactive cell populations were gated as described in Figure 4. There were comparable percentages of La₁₃₋₂₇ or snRNP₃₅₇₋₃₇₃ reactive B cells in the spleen of 6-8-mo-old B6 and BXD2 mice (**Fig. 5A**), though the total numbers of La₁₃₋₂₇⁺ or snRNP₃₅₇₋₃₇₃⁺ B cells were significantly higher in the spleen of BXD2 mice (**Fig. 5B**) as a result of splenomegaly in these mice (36).

We have shown previously that IgM^{hi}CD21^{hi}CD23^{hi} marginal zone precursor (MZ-P) B cells can capture and present Ags derived from mOVA apoptotic debris to directly stimulate OT-II TCR- specific CD4 T cells (37). We also have shown previously that splenic MZ-P B cells are increased in BXD2 mice and can capture and transport TNP-ficoll directly into the GC of BXD2 mice (38). As both MZ and MZ-P B cells are increasingly implicated in the pathogenesis of SLE (9, 39, 40) and both populations are critical in BXD2 autoreactive GC development (41), we analyzed expression of IgM, CD21, and CD23, markers (42) to delineate subsets of B cell that

were reactive to La₁₃₋₂₇ and snRNP₃₅₇₋₃₇₃ peptides. From these analyses, both the IgM^{hi}CD21^{hi} containing the MZ and MZ-P B subsets, and IgM^{lo/-}CD21^{lo/-} B cell containing the FO B subset were represented in the tetramer⁺ population (**Fig. 5C**). There was an increased percent of La₁₃₋₂₇ and snRNP₃₅₇₋₃₇₃ reactive FO B cells in the BXD2 mouse compared to B6 mouse. Furthermore, within the IgM^{hi}CD21^{hi} population that contains both IgM^{hi}CD21^{hi}CD23^{lo/-} MZ and IgM^{hi}CD21^{hi}CD23⁺ MZ-P, there was a significant increase in the percentage of La₁₃₋₂₇ and snRNP₃₅₇₋₃₇₃ tetramer-reactive CD23^{hi} MZ-P B cells in BXD2 mice (**Fig. 5C**). There were also significantly increased numbers of La₁₃₋₂₇⁺ and snRNP₃₅₇₋₃₇₃⁺ MZ-P B cells in the BXD2 mouse spleen (**Fig. 5D**). These results are consistent with our previous finding that BXD2 mice have a higher frequency and greater number of FO and MZ-P B cells than B6 mice (41) and further demonstrate that a fraction of these cells exhibit reactivity to La₁₃₋₂₇ and snRNP₃₅₇₋₃₇₃ epitopes.

In vivo studies by other investigators have shown that counter selection against autoreactivity may take place at the transitional stage of B-cell development (43, 44). We further used CD93 (AA4) marker in combination with CD23 and sIgM staining to determine if there is abnormal deletion or selection of a transitional T1, T2 or T3 population of B cells within tetramer⁺ B cells in BXD2 mice. The results show that while T1 is the dominant La₁₃₋₂₇⁺ or snRNP₃₅₇₋₃₇₃⁺ population of CD93⁺ transitional B cells from B6 mouse spleens, there was abnormal skewing of La₁₃₋₂₇⁺ and snRNP₃₅₇₋₃₇₃⁺ B cells to the T3 population in BXD2 mice (**Fig. 5E, 5F**). Such abnormal expansion of T3 transitional B cells is also observed in the total B cell population in BXD2 mice (**Supplementary Fig. 3A, 3B**).

Increased activation and maturation of La₁₃₋₂₇ reactive B cells in BXD2 mice

The unusual expansion of MZ-P B cells and otherwise anergic T3 B cells (45) in BXD2 mice suggests that specific activation signals must exist to lead to expansion of these antigen-specific B cells. We showed previously that type I IFN-mediated upregulation of CD69 and down-regulation of SIP1 results in their inward migration from the MZ into the follicle (39) where higher CD86 expression enables CD4 T-helper cell stimulation (46). We therefore analyzed if the La₁₃₋₂₇-reactive and snRNP₃₅₇₋₃₇₃-reactive MZ-P B cells exhibited an activation phenotype characterized by CD69 and CD86 expression. Compared to B6 mice, there was a significant upregulation of CD69 and CD86 in the tetramer⁺ MZ-P B cell population in BXD2 mice (**Fig. 6A, 6B**). Similar analysis of these markers in the tetramer⁺ IgM^{lo/-} CD21^{lo/-} compartment, containing mainly FO and potentially GC B cells, revealed a slight increase in CD86, but not CD69 expression on both La₁₃₋₂₇ and snRNP₃₅₇₋₃₇₃ reactive cells (**Fig. 6A, 6B**). These results demonstrate that autoantigen La₁₃₋₂₇ and snRNP₃₅₇₋₃₇₃ specific MZ-P B cells in BXD2 mice exhibit upregulation of CD69 and CD86.

As ELISPOT analysis demonstrated significantly elevated numbers of IgG anti-La₁₃₋₂₇ and anti-snRNP₃₅₇₋₃₇₃ producing B cells, one important question is whether tetramer⁺ B cells from BXD2 mice can mature into IgG secreting cells reactive with the peptide epitope and the whole self-Ag when under appropriate stimulation. This was tested by sorting of La₁₃₋₂₇⁺ B cells, non-specific PE*AF647⁺La₁₃₋₂₇^{+/-}, and double negative PE*AF647^{neg}La₁₃₋₂₇^{neg} B cell subsets, followed by stimulation of these cells *in*

vitro with LPS + IL-4. We first tested cell culture supernatant reactivity against the La₁₃₋₂₇⁺ peptide and an irrelevant histone H1b peptide (His₂₀₅₋₂₁₉). ELISA results verified that La₁₃₋₂₇⁺ B cells indeed produced significantly higher levels of IgG antibodies that reacted specifically with the La₁₃₋₂₇⁺ peptide, and not an irrelevant His₂₀₅₋₂₁₉ peptide. In contrast, the non-specific PE*AF647⁺La₁₃₋₂₇^{+/-} B cells produced low levels of antibodies for both His₂₀₅₋₂₁₉ and La₁₃₋₂₇ (**Fig. 6C**). The selective production of full-length 47 kDa La/SSB reactive IgG antibodies by LPS + IL-4 stimulated La₁₃₋₂₇⁺ B cells but not other subsets of B cells was also verified using a western immunoblotting analysis using whole recombinant La/SSB (**Fig. 6D**).

Finally, we applied the current tetramer approach to determine if, *in vivo*, BXD2 mice indeed exhibited elevated numbers of mature and mutated B cells. This was carried out by analyzing the presence of CD80⁺PD-L2⁺ memory B cells within the La₁₃₋₂₇ and snRNP₃₅₇₋₃₇₃ reactive populations. B cells upregulating these two molecules have been shown to be enriched in isotype-switched cells and in highly mutated cells, even when IgM bearing (47). Using this classification, La₁₃₋₂₇ and snRNP₃₅₇₋₃₇₃ tetramer reactive B cells in BXD2 mice displayed a significantly higher frequency of CD80⁺PD-L2⁺ B cells compared to the counterpart B cells from B6 mice (**Fig. 6E, 6F**). There was also an increased frequency of CD80⁺PD-L2⁺ B cells in tetramer⁺ cells compared to non-tetramer gated total B cells from BXD2 mice (**Fig. 6E, 6F**). Together, these results indicate that this tetramer approach can be used to identify abnormal development of autoreactive B cells at various developmental stages.

Discussion

In this study, we demonstrate a step-wise approach to enable enrichment, isolation and characterization of autoantigen-reactive B cells in a mouse model that spontaneously develops autoantibody-mediated systemic autoimmune disease (4, 48). We demonstrate that an IEDB based peptide array of 2,733 autoimmune disease associated B-cell epitopes can reveal linear epitopes on known autoantigens in BXD2 mice. Further, the age-related emergence of class-switched autoantibodies identified using the peptide arrays paralleled previous observations using standard whole Ag ELISA assays (4). Moreover, the serum reactivity of a panel of these identified autoepitopes was confirmed using ELISA and ELISPOT analysis of synthetic peptides. Peptide reactive tetramer B cells can also be stimulated to produce IgG antibodies that react with the full-length protein antigen.

The peptides identified as BXD2 autoepitopes by the epitope array assay indicate which of these may be considered to be immunodominant. Potentially, this apparent immunodominance may simply reflect the array assay conditions. However, the reactivity pattern of BXD2 autoantibodies showed a preference towards nuclear and RNP autoantigens. Since initial observations of autoantigen clustering in apoptotic blebs (49), there has been growing awareness that chemical and structural modifications to autoantigens during cell death and neutrophil NETosis may provide B cells with access to normally concealed epitopes that may drive an aberrant adaptive immune response (50-52). Multiple studies have demonstrated that the majority of autoantigens targeted in systemic autoimmune diseases are substrates for granzymes, particularly granzyme B (53-55), and La itself is cleaved during apoptosis (56, 57). Similarly, the

70 kDa fragment of U1snRNP, another hallmark autoAg in patients with SLE, is specifically cleaved by the caspase-3 during apoptosis. This cleavage converts the molecule into a truncated 40-kDa fragment and a smaller 96-residue C-terminal fragment (35, 58), containing the snRNP₃₅₇₋₃₇₃ epitope identified here as a major BXD2 autoAg. Notably, this particular epitope is located in a structurally disordered region of the protein, a characteristic which may influence antigen capture, processing, presentation and immune dominance during cellular processes, including apoptosis (59). The peptide array identification of these autoepitopes is consistent with our previous observations of defective apoptotic body clearance and the ability of MZ-P B cells to directly capture antigen derived from uncleared apoptotic debris in BXD2 mice (37).

The present peptide array results also provide a clear picture of the transition from autoreactive IgM to IgG in BXD2 mice and confirm that this transition is absent for most linear autoepitopes in B6 mice, as we have described previously for full-length autoantigens (4). The autoreactive IgG in BXD2 mice are highly pathogenic and form immune complexes that deposit in the kidney and joints (4). It should be noted, however, that the current studies were focused on the identification of antigen-specific subsets of autoreactive B cells. It has not yet been confirmed that the peptide-specific IgG autoantibodies that we identified are capable of forming pathogenic immune complexes or eliciting tissue damage.

The IgM autoantibody pattern, which is often overlooked, also revealed some interesting features. Although both B6 and BXD2 produce broadly autoreactive IgM, the IgM repertoire in both mice does exhibit specificity in that only some autoAg, but not all, are recognized. Thus, in both strains, IgM appears to recognize a similar set of

key autoAgs. These results are consistent with the observation that autoreactive and polyreactive autoantibodies are present both healthy and autoimmune humans (44, 60, 61), an observation not limited to IgM but occurring commonly even within the IgG memory B-cell pool (62, 63). These results suggest that BCR ability to recognize and engage self-Ag does not necessarily cause disease. However, within a permissive environment, as in the BXD2 mouse, even small perturbations in B-cell development, selection, or phenotype may drive normally benign autoreactivity toward an auto-toxic response. They further support the concept that while normal individuals may manifest some degree of autoimmunity to a set of self-antigens, this is benign as long as the regulatory capacity is intact (64).

Consistent with the detection of IgM autoantibodies in both B6 and BXD2 mice, most of the autoAg tetramer⁺ B cells that are obtained directly from the spleen of a mouse are IgM⁺. The most likely reason for this is that there is a larger population of splenic B cells that express both surface and secretory IgM compared to a relatively small number of IgG B cells that express both surface and secretory IgG (65). However, in the spleen of BXD2 mouse, there is a decreased percent of IgM^{hi} B cells, compared to spleen B cells of B6 mouse B cells, both in the pan-B cell population (38) as well as the Ag specific tetramer⁺ B cell population (Figure 5C).

Analysis of B cell subsets using the tetramer strategy enabled us to identify key differences between normal B6 and autoimmune BXD2 mice, and such observations may be highly applicable for characterization of autoreactive B cells in human disease, as tetramer⁺ B cells that exhibit abnormal phenotypes can be detected in well-defined B cell subsets in human PBMCs (66). While La₁₃₋₂₇ and snRNP₃₅₇₋₃₇₃ reactive IgM^{hi} B

cells from B6 mice are primarily the CD21^{hi}CD23^{lo} MZ B cells, the majority of these B cells in BXD2 mice display the CD21^{hi}CD23^{hi} MZ-P B cell phenotype. Furthermore, these Ag⁺ MZ-P B cells are skewed toward a hyper-reactive CD86⁺CD69⁺ phenotype in BXD2. In mice, B cells with regulatory function have been observed within the transitional, B1 and marginal zone compartments (67). We have previously shown that while the expression of *Il10* and *Tgfb* was significantly higher, the expression of *Il6* was significantly lower in MZ-P B cells of B6 mice, compared to MZ-P B cells BXD2 mice (37). Consistent with this, CD23⁺CD21^{hi}CD1d^{hi} B cells have been reported as the key pathogenic B cells in other mouse models of autoimmunity (68, 69). In contrast, Evans *et al.* demonstrated that MZ-P B cells from spleens of healthy naïve DBA/1 mice adoptively transferred into immunized DBA/1 mice significantly prevented and ameliorated disease (70). This and other reports (71) of MZ-P-like B cell regulatory functions suggest that, in the non-autoimmune state, these cells may indeed serve a regulatory role. Regulatory roles of human B cells are less understood, but transitional B cells with an IL-10-mediated regulatory function have similarly been reported to be defective in patients with SLE (39). Increased CD80⁺ and CD86⁺ B cells also coincide with the observation that naïve populations of B cells from SLE patients appear to be activated (72).

Analysis of the CD93⁺ transitional population of La₁₃₋₂₇⁺ or snRNP₃₅₇₋₃₇₃⁺ B cells in BXD2 mice further revealed that there is an abnormal expansion of T3 transitional B cells, a phenotype that has not been identified in other autoimmune mouse models (45). T3 B cells generally are considered not strictly transitional but anergic B cells maintaining self-tolerance through rapid turnover *in vivo* (73, 74). Interestingly, self-Ag

stimulation has been shown to promote regression of mature B cells into the T3 compartment (74, 75). Thus, expansion of these cells coupled with abnormal T-cell help (25, 76) may present a risk for B-cell tolerance loss to La₁₃₋₂₇ or snRNP₃₅₇₋₃₇₃ in BXD2 mice.

Consistent with the possible B-cell tolerance defects that can occur before or at the MZ-P B cell stage in BXD2 mice, there was a 10-fold increase in numbers of CD80⁺PD-L2⁺ tetramer⁺ B cells in the spleen of BXD2 mice compared to B6 mice, further suggesting that there is at least an additional checkpoint defect leading to differentiation of these memory-like tetramer⁺ B cells in BXD2 mice. The percentage and number of B cells with this CD80⁺ PD-L2⁺ phenotype is enriched five to six fold in the La₁₃₋₂₇⁺ and snRNP₃₅₇₋₃₇₃ population compared to that within the total splenic B cells. Thus, the results suggest the specific Ag stimulation can lead to expansion of Ag-specific memory B cell population in BXD2 mice. Notably, CD80⁺ PD-L2⁺ memory B cells have been shown to differentiate rapidly into antibody producing B cells upon re-challenge without the need to go through another GC response (77). The present results may thus help to identify mechanisms related to the high titers of IgG autoantibody production in BXD2 mice.

The present proof-of-principle study establishes that the approach described in this work should provide a platform for integrating autoantibody profiles with underlying B-cell defects. The ability to collect and compare comprehensive global autoantibody profiles coupled with the sensitivity and specificity of the tetramer approach provides a feasible strategy to address other clinically relevant questions. The approach described in this work provides a platform for integrating autoantibody

profiles with underlying B cell defects to identify and isolate B cells that recognize autoantigen epitopes.

References

1. Li, Q. Z., C. Xie, T. Wu, M. Mackay, C. Aranow, C. Putterman, and C. Mohan. 2005. Identification of autoantibody clusters that best predict lupus disease activity using glomerular proteome arrays. *J Clin Invest* 115: 3428-3439.
2. Ferucci, E. D., D. S. Majka, L. A. Parrish, M. B. Moroldo, M. Ryan, M. Passo, S. D. Thompson, K. D. Deane, M. Rewers, W. P. Arend, D. N. Glass, J. M. Norris, and V. M. Holers. 2005. Antibodies against cyclic citrullinated peptide are associated with HLA-DR4 in simplex and multiplex polyarticular-onset juvenile rheumatoid arthritis. *Arthritis Rheum* 52: 239-246.
3. Cheng, Q., I. M. Mumtaz, L. Khodadadi, A. Radbruch, B. F. Hoyer, and F. Hiepe. 2013. Autoantibodies from long-lived 'memory' plasma cells of NZB/W mice drive immune complex nephritis. *Ann Rheum Dis* 72: 2011-2017.
4. Hsu, H. C., T. Zhou, H. Kim, S. Barnes, P. Yang, Q. Wu, J. Zhou, B. A. Freeman, M. Luo, and J. D. Mountz. 2006. Production of a novel class of polyreactive pathogenic autoantibodies in BXD2 mice causes glomerulonephritis and arthritis. *Arthritis Rheum* 54: 343-355.
5. Burlingame, R. W., M. L. Boey, G. Starkebaum, and R. L. Rubin. 1994. The central role of chromatin in autoimmune responses to histones and DNA in systemic lupus erythematosus. *J Clin Invest* 94: 184-192.
6. Arbuckle, M. R., M. T. McClain, M. V. Rubertone, R. H. Scofield, G. J. Dennis, J. A. James, and J. B. Harley. 2003. Development of autoantibodies before the clinical onset of systemic lupus erythematosus. *N Engl J Med* 349: 1526-1533.

7. Sanz, I. 2014. Rationale for B cell targeting in SLE. *Semin Immunopathol* 36: 365-375.
8. Anolik, J., and I. Sanz. 2004. B cells in human and murine systemic lupus erythematosus. *Curr Opin Rheumatol* 16: 505-512.
9. Palanichamy, A., J. Barnard, B. Zheng, T. Owen, T. Quach, C. Wei, R. J. Looney, I. Sanz, and J. H. Anolik. 2009. Novel human transitional B cell populations revealed by B cell depletion therapy. *J Immunol* 182: 5982-5993.
10. Shlomchik, M. J. 2008. Sites and stages of autoreactive B cell activation and regulation. *Immunity* 28: 18-28.
11. Franz, B., K. F. May, Jr., G. Dranoff, and K. Wucherpfennig. 2011. Ex vivo characterization and isolation of rare memory B cells with antigen tetramers. *Blood* 118: 348-357.
12. Goodnow, C. C. 1992. Transgenic mice and analysis of B-cell tolerance. *Annu Rev Immunol* 10: 489-518.
13. Doucett, V. P., W. Gerhard, K. Owler, D. Curry, L. Brown, and N. Baumgarth. 2005. Enumeration and characterization of virus-specific B cells by multicolor flow cytometry. *J Immunol Methods* 303: 40-52.
14. Townsend, S. E., C. C. Goodnow, and R. J. Cornall. 2001. Single epitope multiple staining to detect ultralow frequency B cells. *J Immunol Methods* 249: 137-146.
15. Newman, J., J. S. Rice, C. Wang, S. L. Harris, and B. Diamond. 2003. Identification of an antigen-specific B cell population. *J Immunol Methods* 272: 177-187.

16. Jacobi, A. M., J. Zhang, M. Mackay, C. Aranow, and B. Diamond. 2009. Phenotypic characterization of autoreactive B cells--checkpoints of B cell tolerance in patients with systemic lupus erythematosus. *PLoS One* 4: e5776.
17. van de Stadt, L. A., P. A. van Schouwenburg, S. Bryde, S. Kruithof, D. van Schaardenburg, D. Hamann, G. Wolbink, and T. Rispens. 2013. Monoclonal anti-citrullinated protein antibodies selected on citrullinated fibrinogen have distinct targets with different cross-reactivity patterns. *Rheumatology (Oxford)* 52: 631-635.
18. Zachary, A. A., D. Kopchaliiska, R. A. Montgomery, and M. S. Leffell. 2007. HLA-specific B cells: I. A method for their detection, quantification, and isolation using HLA tetramers. *Transplantation* 83: 982-988.
19. Morris, L., X. Chen, M. Alam, G. Tomaras, R. Zhang, D. J. Marshall, B. Chen, R. Parks, A. Foulger, F. Jaeger, M. Donathan, M. Bilska, E. S. Gray, S. S. Abdool Karim, T. B. Kepler, J. Whitesides, D. Montefiori, M. A. Moody, H. X. Liao, and B. F. Haynes. 2011. Isolation of a human anti-HIV gp41 membrane proximal region neutralizing antibody by antigen-specific single B cell sorting. *PLoS One* 6: e23532.
20. Holl, T. M., G. Yang, M. Kuraoka, L. Verkoczy, S. M. Alam, M. A. Moody, B. F. Haynes, and G. Kelsoe. 2014. Enhanced antibody responses to an HIV-1 membrane-proximal external region antigen in mice reconstituted with cultured lymphocytes. *J Immunol* 192: 3269-3279.
21. Taylor, J. J., R. J. Martinez, P. J. Titcombe, L. O. Barsness, S. R. Thomas, N. Zhang, S. D. Katzman, M. K. Jenkins, and D. L. Mueller. 2012. Deletion and

- energy of polyclonal B cells specific for ubiquitous membrane-bound self-antigen. *J Exp Med* 209: 2065-2077.
22. Robinson, W. H., C. DiGennaro, W. Hueber, B. B. Haab, M. Kamachi, E. J. Dean, S. Fournel, D. Fong, M. C. Genovese, H. E. de Vegvar, K. Skriner, D. L. Hirschberg, R. I. Morris, S. Muller, G. J. Pruijn, W. J. van Venrooij, J. S. Smolen, P. O. Brown, L. Steinman, and P. J. Utz. 2002. Autoantigen microarrays for multiplex characterization of autoantibody responses. *Nat Med* 8: 295-301.
23. Price, J. V., D. J. Haddon, D. Kemmer, G. Delepine, G. Mandelbaum, J. A. Jarrell, R. Gupta, I. Balboni, E. F. Chakravarty, J. Sokolove, A. K. Shum, M. S. Anderson, M. H. Cheng, W. H. Robinson, S. K. Browne, S. M. Holland, E. C. Baechler, and P. J. Utz. 2013. Protein microarray analysis reveals BAFF-binding autoantibodies in systemic lupus erythematosus. *J Clin Invest* 123: 5135-5145.
24. Cohen, I. R. 2013. Autoantibody repertoires, natural biomarkers, and system controllers. *Trends Immunol* 34: 620-625.
25. Hsu, H. C., P. Yang, J. Wang, Q. Wu, R. Myers, J. Chen, J. Yi, T. Guentert, A. Tousson, A. L. Stanus, T. V. Le, R. G. Lorenz, H. Xu, J. K. Kolls, R. H. Carter, D. D. Chaplin, R. W. Williams, and J. D. Mountz. 2008. Interleukin 17-producing T helper cells and interleukin 17 orchestrate autoreactive germinal center development in autoimmune BXD2 mice. *Nat Immunol* 9: 166-175.
26. Hsu, H. C., P. Yang, Q. Wu, J. H. Wang, G. Job, T. Guentert, J. Li, C. R. Stockard, T. V. Le, D. D. Chaplin, W. E. Grizzle, and J. D. Mountz. 2011. Inhibition of the catalytic function of activation-induced cytidine deaminase

- promotes apoptosis of germinal center B cells in BXD2 mice. *Arthritis Rheum* 63: 2038-2048.
27. Kim, Y., J. Ponomarenko, Z. Zhu, D. Tamang, P. Wang, J. Greenbaum, C. Lundegaard, A. Sette, O. Lund, P. E. Bourne, M. Nielsen, and B. Peters. 2012. Immune epitope database analysis resource. *Nucleic Acids Res* 40: W525-530.
28. Winslow, M. M., E. M. Gallo, J. R. Neilson, and G. R. Crabtree. 2006. The calcineurin phosphatase complex modulates immunogenic B cell responses. *Immunity* 24: 141-152.
29. Vita, R., L. Zarebski, J. A. Greenbaum, H. Emami, I. Hoof, N. Salimi, R. Damle, A. Sette, and B. Peters. 2010. The immune epitope database 2.0. *Nucleic Acids Res* 38: D854-862.
30. Brink, M., M. Hansson, J. Ronnelid, L. Klareskog, and S. Rantapaa Dahlqvist. 2014. The autoantibody repertoire in periodontitis: a role in the induction of autoimmunity to citrullinated proteins in rheumatoid arthritis? Antibodies against uncitrullinated peptides seem to occur prior to the antibodies to the corresponding citrullinated peptides. *Ann Rheum Dis* 73: e46.
31. Shoda, H., K. Fujio, M. Shibuya, T. Okamura, S. Sumitomo, A. Okamoto, T. Sawada, and K. Yamamoto. 2011. Detection of autoantibodies to citrullinated BiP in rheumatoid arthritis patients and pro-inflammatory role of citrullinated BiP in collagen-induced arthritis. *Arthritis Res Ther* 13: R191.
32. Plotz, P. H. 2003. The autoantibody repertoire: searching for order. *Nat Rev Immunol* 3: 73-78.

33. Weinstein, J. S., S. G. Hernandez, and J. Craft. 2012. T cells that promote B-Cell maturation in systemic autoimmunity. *Immunol Rev* 247: 160-171.
34. Reed, J. H., M. W. Jackson, and T. P. Gordon. 2008. B cell epitopes of the 60-kDa Ro/SSA and La/SSB autoantigens. *J Autoimmun* 31: 263-267.
35. Degen, W. G., Y. Aarssen, G. J. Pruijn, P. J. Utz, and W. J. van Venrooij. 2000. The fate of U1 snRNP during anti-Fas induced apoptosis: specific cleavage of the U1 snRNA molecule. *Cell Death Differ* 7: 70-79.
36. Mountz, J. D., P. Yang, Q. Wu, J. Zhou, A. Tousson, A. Fitzgerald, J. Allen, X. Wang, S. Cartner, W. E. Grizzle, N. Yi, L. Lu, R. W. Williams, and H. C. Hsu. 2005. Genetic segregation of spontaneous erosive arthritis and generalized autoimmune disease in the BXD2 recombinant inbred strain of mice. *Scand J Immunol* 61: 128-138.
37. Li, H., Q. Wu, J. Li, P. Yang, Z. Zhu, B. Luo, H. C. Hsu, and J. D. Mountz. 2013. Cutting Edge: defective follicular exclusion of apoptotic antigens due to marginal zone macrophage defects in autoimmune BXD2 mice. *J Immunol* 190: 4465-4469.
38. Wang, J. H., J. Li, Q. Wu, P. Yang, R. D. Pawar, S. Xie, L. Timares, C. Raman, D. D. Chaplin, L. Lu, J. D. Mountz, and H. C. Hsu. 2010. Marginal zone precursor B cells as cellular agents for type I IFN-promoted antigen transport in autoimmunity. *J Immunol* 184: 442-451.
39. Blair, P. A., L. Y. Norena, F. Flores-Borja, D. J. Rawlings, D. A. Isenberg, M. R. Ehrenstein, and C. Mauri. 2010. CD19(+)CD24(hi)CD38(hi) B cells exhibit

- regulatory capacity in healthy individuals but are functionally impaired in systemic Lupus Erythematosus patients. *Immunity* 32: 129-140.
40. Landolt-Marticorena, C., R. Wither, H. Reich, A. Herzenberg, J. Scholey, D. D. Gladman, M. B. Urowitz, P. R. Fortin, and J. Wither. 2011. Increased expression of B cell activation factor supports the abnormal expansion of transitional B cells in systemic lupus erythematosus. *J Rheumatol* 38: 642-651.
 41. J, W. 2010. Marginal Zone Precursor B Cells as Cellular Agents for Type I IFN Promoted Antigen Transport in Autoimmunity. *Journal of Immunology* 184: 442-51.
 42. Allman, D., and S. Pillai. 2008. Peripheral B cell subsets. *Curr Opin Immunol* 20: 149-157.
 43. Meffre, E., and H. Wardemann. 2008. B-cell tolerance checkpoints in health and autoimmunity. *Curr Opin Immunol* 20: 632-638.
 44. Wardemann, H., S. Yurasov, A. Schaefer, J. W. Young, E. Meffre, and M. C. Nussenzweig. 2003. Predominant autoantibody production by early human B cell precursors. *Science* 301: 1374-1377.
 45. Teague, B. N., Y. Pan, P. A. Mudd, B. Nakken, Q. Zhang, P. Szodoray, X. Kim-Howard, P. C. Wilson, and A. D. Farris. 2007. Cutting edge: Transitional T3 B cells do not give rise to mature B cells, have undergone selection, and are reduced in murine lupus. *J Immunol* 178: 7511-7515.
 46. Wang, J. H., Q. Wu, P. Yang, H. Li, J. Li, J. D. Mountz, and H. C. Hsu. 2011. Type I interferon-dependent CD86(high) marginal zone precursor B cells are potent T cell costimulators in mice. *Arthritis Rheum* 63: 1054-1064.

47. Tomayko, M. M., N. C. Steinel, S. M. Anderson, and M. J. Shlomchik. 2010. Cutting edge: Hierarchy of maturity of murine memory B cell subsets. *J Immunol* 185: 7146-7150.
48. Hsu, H. C., Y. Wu, P. Yang, Q. Wu, G. Job, J. Chen, J. Wang, M. A. Accavitti-Loper, W. E. Grizzle, R. H. Carter, and J. D. Mountz. 2007. Overexpression of activation-induced cytidine deaminase in B cells is associated with production of highly pathogenic autoantibodies. *J Immunol* 178: 5357-5365.
49. Rosen, A. 1995. Novel packages of viral and self-antigens are generated during apoptosis. *J Exp Med* 181: 1557-1561.
50. Radic, M., T. Marion, and M. Monestier. 2004. Nucleosomes are exposed at the cell surface in apoptosis. *J Immunol* 172: 6692-6700.
51. van Bavel, C. C., J. W. Dieker, Y. Kroeze, W. P. Tamboer, R. Voll, S. Muller, J. H. Berden, and J. van der Vlag. 2011. Apoptosis-induced histone H3 methylation is targeted by autoantibodies in systemic lupus erythematosus. *Ann Rheum Dis* 70: 201-207.
52. Khandpur, R., C. Carmona-Rivera, A. Vivekanandan-Giri, A. Gizinski, S. Yalavarthi, J. S. Knight, S. Friday, S. Li, R. M. Patel, V. Subramanian, P. Thompson, P. Chen, D. A. Fox, S. Pennathur, and M. J. Kaplan. 2013. NETs are a source of citrullinated autoantigens and stimulate inflammatory responses in rheumatoid arthritis. *Sci Transl Med* 5: 178ra140.
53. Darrah, E., and A. Rosen. 2010. Granzyme B cleavage of autoantigens in autoimmunity. *Cell Death Differ* 17: 624-632.

54. Casciola-Rosen, L., F. Andrade, D. Ulanet, W. B. Wong, and A. Rosen. 1999. Cleavage by granzyme B is strongly predictive of autoantigen status: implications for initiation of autoimmunity. *J Exp Med* 190: 815-826.
55. Dudek, N. L., S. Maier, Z. J. Chen, P. A. Mudd, S. I. Mannering, D. C. Jackson, W. Zeng, C. L. Keech, K. Hamlin, Z. J. Pan, K. Davis-Schwarz, J. Workman-Azbill, M. Bachmann, J. McCluskey, and A. D. Farris. 2007. T cell epitopes of the La/SSB autoantigen in humanized transgenic mice expressing the HLA class II haplotype DRB1*0301/DQB1*0201. *Arthritis Rheum* 56: 3387-3398.
56. Rutjes, S. A., P. J. Utz, A. van der Heijden, C. Broekhuis, W. J. van Venrooij, and G. J. Pruijn. 1999. The La (SS-B) autoantigen, a key protein in RNA biogenesis, is dephosphorylated and cleaved early during apoptosis. *Cell Death Differ* 6: 976-986.
57. Huang, M., H. Ida, M. Kamachi, N. Iwanaga, Y. Izumi, F. Tanaka, K. Aratake, K. Arima, M. Tamai, A. Hida, H. Nakamura, T. Origuchi, A. Kawakami, N. Ogawa, S. Sugai, P. J. Utz, and K. Eguchi. 2005. Detection of apoptosis-specific autoantibodies directed against granzyme B-induced cleavage fragments of the SS-B (La) autoantigen in sera from patients with primary Sjogren's syndrome. *Clin Exp Immunol* 142: 148-154.
58. Kattah, N. H., M. G. Kattah, and P. J. Utz. 2010. The U1-snRNP complex: structural properties relating to autoimmune pathogenesis in rheumatic diseases. *Immunol Rev* 233: 126-145.
59. Pavlovic, M. D., D. R. Jandrljic, and N. S. Mitic. 2014. Epitope distribution in ordered and disordered protein regions. Part B - Ordered regions and disordered

- binding sites are targets of T- and B-cell immunity. *J Immunol Methods* 407: 90-107.
60. Shaw, P. X., C. S. Goodyear, M. K. Chang, J. L. Witztum, and G. J. Silverman. 2003. The autoreactivity of anti-phosphorylcholine antibodies for atherosclerosis-associated neo-antigens and apoptotic cells. *J Immunol* 170: 6151-6157.
61. Silverman, G. J. 2011. Regulatory natural autoantibodies to apoptotic cells: pallbearers and protectors. *Arthritis Rheum* 63: 597-602.
62. Tiller. 2007. Autoreactivity in human IgG+ memory B cells. *Immunity* 26: 205-213.
63. Nagele, E. P., M. Han, N. K. Acharya, C. DeMarshall, M. C. Kosciuk, and R. G. Nagele. 2013. Natural IgG autoantibodies are abundant and ubiquitous in human sera, and their number is influenced by age, gender, and disease. *PLoS One* 8: e60726.
64. Fattal, I., N. Shental, D. Mevorach, J. M. Anaya, A. Livneh, P. Langevitz, G. Zandman-Goddard, R. Pauzner, M. Lerner, M. Blank, M. E. Hincapie, U. Gafter, Y. Naparstek, Y. Shoenfeld, E. Domany, and I. R. Cohen. 2010. An antibody profile of systemic lupus erythematosus detected by antigen microarray. *Immunology* 130: 337-343.
65. Morbach, H., E. M. Eichhorn, J. G. Liese, and H. J. Girschick. 2010. Reference values for B cell subpopulations from infancy to adulthood. *Clin Exp Immunol* 162: 271-279.

66. Kaminski, D. A., C. Wei, Y. Qian, A. F. Rosenberg, and I. Sanz. 2012. Advances in human B cell phenotypic profiling. *Front Immunol* 3: 302.
67. Fillatreau, S., D. Gray, and S. M. Anderton. 2008. Not always the bad guys: B cells as regulators of autoimmune pathology. *Nat Rev Immunol* 8: 391-397.
68. Moshkani, S., Kuzin, II, F. Adewale, J. Jansson, I. Sanz, E. M. Schwarz, and A. Bottaro. 2012. CD23+ CD21(high) CD1d(high) B cells in inflamed lymph nodes are a locally differentiated population with increased antigen capture and activation potential. *J Immunol* 188: 5944-5953.
69. Li, J., I. Kuzin, S. Moshkani, S. T. Proulx, L. Xing, D. Skrombolas, R. Dunn, I. Sanz, E. M. Schwarz, and A. Bottaro. 2010. Expanded CD23(+)/CD21(hi) B cells in inflamed lymph nodes are associated with the onset of inflammatory-erosive arthritis in TNF-transgenic mice and are targets of anti-CD20 therapy. *J Immunol* 184: 6142-6150.
70. Evans, J. G., K. A. Chavez-Rueda, A. Eddaoudi, A. Meyer-Bahlburg, D. J. Rawlings, M. R. Ehrenstein, and C. Mauri. 2007. Novel suppressive function of transitional 2 B cells in experimental arthritis. *J Immunol* 178: 7868-7878.
71. Yanaba, K., J. D. Bouaziz, K. M. Haas, J. C. Poe, M. Fujimoto, and T. F. Tedder. 2008. A regulatory B cell subset with a unique CD1dhiCD5+ phenotype controls T cell-dependent inflammatory responses. *Immunity* 28: 639-650.
72. Chang, N. H., T. McKenzie, G. Bonventi, C. Landolt-Marticorena, P. R. Fortin, D. Gladman, M. Urowitz, and J. E. Wither. 2008. Expanded population of activated antigen-engaged cells within the naive B cell compartment of patients with systemic lupus erythematosus. *J Immunol* 180: 1276-1284.

73. Allman, D., R. C. Lindsley, W. DeMuth, K. Rudd, S. A. Shinton, and R. R. Hardy. 2001. Resolution of three nonproliferative immature splenic B cell subsets reveals multiple selection points during peripheral B cell maturation. *J Immunol* 167: 6834-6840.
74. Merrell, K. T., R. J. Benschop, S. B. Gauld, K. Aviszus, D. Decote-Ricardo, L. J. Wysocki, and J. C. Cambier. 2006. Identification of anergic B cells within a wild-type repertoire. *Immunity* 25: 953-962.
75. Liubchenko, G. A., H. C. Appleberry, V. M. Holers, N. K. Banda, V. C. Willis, and T. Lyubchenko. 2012. Potentially autoreactive naturally occurring transitional T3 B lymphocytes exhibit a unique signaling profile. *J Autoimmun* 38: 293-303.
76. Ding, Y., J. Li, P. Yang, B. Luo, Q. Wu, A. J. Zajac, O. Wildner, H. C. Hsu, and J. D. Mountz. 2014. Interleukin-21 promotes germinal center reaction by skewing the follicular regulatory T cell to follicular helper T cell balance in autoimmune BXD2 mice. *Arthritis Rheumatol* 66: 2601-2612.
77. Zuccarino-Catania, G. V., S. Sadanand, F. J. Weisel, M. M. Tomayko, H. Meng, S. H. Kleinstein, K. L. Good-Jacobson, and M. J. Shlomchik. 2014. CD80 and PD-L2 define functionally distinct memory B cell subsets that are independent of antibody isotype. *Nat Immunol* 15: 631-637.

Footnotes

1. Corresponding author: Hui-Chen Hsu, Ph.D, Shelby 311, 1825 University Blvd, Birmingham, AL 35294, USA, Phone: 205-934-8909, Fax: 205-996-6788, E-mail: Rhue078@uab.edu
2. This work was supported by a grant from Arthritis Foundation (to J.L.), Rheumatology Research Foundation, the Department of Veterans Affairs Merit Review Grant 1I01BX000600-01, the National Institutes of Health Grants 1AI 071110, and P30 AR048311 (to J.D.M.), and 1RO1 AI083705 (to H-C.H.). Flow cytometry data acquisition was carried out at the University of Alabama at Birmingham Comprehensive Flow Cytometry Core (supported by NIH grants P30-AR-048311 and P30-AI-027767). We thank Dr. Fiona Hunter for critical review of this manuscript.
3. Abbreviations used in this paper: SLE, systemic lupus erythematosus; RA, rheumatoid arthritis; RBP, ribonucleic acid binding protein; snRNP, small nuclear ribonucleoprotein; MZ-P, marginal zone precursor; SA, streptavidin; RNP, ribonucleoprotein; GC, germinal center; FO, follicular.

Table 1. List of autoantigen epitopes used for reactivity comparisons between B6 and BXD2 mice

Category A. Nuclear			Category B. Matrix		
AggResidue	Peptide	Uniprot ID	AggResidue	Peptide	Uniprot ID
La3-27	LEAKICHQIEYFFGD*	P05455	Collagen α -1(II) 558-569	GARGLTGRPGDA	P02458
UlsnRNP-70s17-713	SHRSERERRRDRDRD*	P08621	Collagen α -1(II) [cit] 558-569	GAZGLTGZPGDA	P02458
UlsnRNP-70s112-128	YDTTESKLRREFEYVGP*	P08621	COMP472-488	DDNDNGVPDSZDNCZLV	P49747
UlsnRNP-70s45-234	SREEDKERER	P08621	COMP [cit] 472-488	DDNDNGVPDSRDNCRLV	P49747
UlsnRNP-70s60-74	AETREERMERKRRE	P08621	Fibrinogen- α 296-410	DSPGSGNARPNPDW	P02671
UlsnRNP-70s41-157	GKPRGYAFIEYEHERDM	P08621	Fibrinogen- α [cit] 396-410	DSPGSGNAPZNPNDW	P02671
UlsnRNP-70s107-123	VARVNYDTTESKLRREF	P08621	fibrinogen α 183-197	SCSRALAREVDLKDY	P02671
UlsnRNP-SmD197-109	RGRGRGRGRGRGR	P62314	Fibrinogen- α [cit] 183-197	SCSZALAZEVDLKDY	P02671
HNRNPA2B131-43	ETTESLRNYEQ	P22626	Fibrinogen- α 27-43	FLAEGGGVGRPRVVERH	P02671
p70s19-533	GSLVDFEKLVPYPPDYN	P12956	Fibrinogen- α [cit] 27-43	FLAEGGGVZGPRVVERH	P02671
Ro52197-207	LQELEKDEREQ	P19474	Fibrinogen β 420-434	PRKQCSKEDGGGWY*	P02675
Ro52180-196	AEFVQKKNFLVEEQRQ	P19474	Fibrinogen- β [Cit] 420-434	PZKQCSKEDGGGWY*	P02675
Ro5218-234	LAQSQALQELISELDR	P19474	Fibrinogen- β 433-447	WYNRCHAAANPNGRYY	P02675
Ro5218-27	EVTCPICLDPFVEPV	P19474	Fibrinogen- β [Cit] 433-447	WYNZCHAAANPNGRYY	P02675
Ro60480-487	ALALREYR	P10155	Fibrinogen- β 60-74	RPAPPISGGGYRAR	P02675
Ro60505-518	GFTIADPDRGMLD	P10155	Fibrinogen- β [cit] 60-74	ZPAPPISGGGYZAZ	P02675
CENP-A-110-24	PEAPRRRSPSPPTTP	P49450	Fibromodulin49-265	LYMEHNNVYTPVDSYFR*	Q06828
CENP-A-222-21	PTPGPSRRGP*	P49450	Fibromodulin [cit] 249-265	LYMEHNNVYTPVDSYFZ*	Q06828
CENP-A-397-411	AAEAFLVHLFEDAYL*	P49450	Filaggrin527-340	EQSRDGSRHPR.SHD	P20930
CENP-A-47-16	SRKPEAPRRR	P49450	filaggrin [cit] 327-340	EQSRDGSZHPR.SHD	P20930
CENP-E121-135	PDREFLLRVSYMEIY	Q02224	Filaggrin1363-1385	QSADSSRHSGSGH	P20930
CENP-B193-207	SATETSLLWYDFLPDQ	P07199	filaggrin [cit] 1363-1385	QSADSSZHSGS GH	P20930
Histone H1b205-219	KPKAAKPKKAAAKK*	P10412	Filaggrin63-276	TGTS TGGRQGS HHE	Q08388
Histone H1b145-160	ATPKKSAKKTPKKAKK	P10412	filaggrin [cit] 263-276	TGTS TGGZQGS HHE	Q08388
Histone H1b171-186	KSPKKAKAAKPKKAPK	P10412	Vimentin184-200	RLREKLQEEMILQREAE	P08670
Histone H2b52-61	IMNSFVTDIFERIASASRL	P62807	Vimentin [cit] 184-200	ZLZEKLQEEMILQZEEAE	P08670
Histone H2b [cit]62-81	IMNSFVTDIFEZIASEASZL	P62807			
DNA Topo220-243	PPYEPLPENVKFYD	P11387			
DNA Topo197-211	KEEEQKWKWWEERY	P11387			
RNA Pol 3 RPC11320-1334	SFEKTAHDLFDAAFY	O14802			
RNA Pol 3 RPC2357-371	NTFRLMRRAGVYNEF	Q9NW08			

Category C. Enzyme/Chaperone		
AggResidue	Peptide	Uniprot ID
BCKDHB18-27	GAEGHWRRLP	P21953
HSP65113-127	EGMRFDKGYISGYFV	E5FHX3
HSP60444-460	LLRVIPALDSLTPANED	P10809
Bip-1325-341	TTINDQNRLTPEEIERM*	P11021
Bip-1[cit]1325-341	TTINDQNRLTPEEIERM*	P11021
Bip-2398-314	ALSSHQARIEIESFYE*	P11021
Bip-2[cit] 298-314	ALSSHQAZIEIESFYE*	P11021
Bip249-265	GDTHLGGEDFDQRVMEH	P11021
Bip530-546	QNRLTPEEIERMVDNAE	P11021
Citrate synthase54-	DPRYTCQREF	O75390
Clusterin67-376	NWVSRLANLTQGEDQYY	P10909
Clusterin [cit] 367-376	NWVSRLANLTQGEDQYY	P10909
α -Enolase154-270	SGKYLDLDFKSPDDPSRY	P06733
α -Enolase 1 [cit] 254-270	SGKYLDLDFKSPDDPSZY	P06733
GAD65-2507-2523	WYPPSLRLTLEDNEERM	Q05329
GAD65-2564-580	PAATHQDIDFLIEIER	Q05329
GPI72-88	AKSRGVEAARERMFNGE	P06744
GPI-[cit]72-88	AKSZGVEAAEZFNFNGE	P06744
GPI437-453	MRGKSTEEARKELQAAG	P06744
GPI-[cit]437-453	MZGKSTEEAZKELQAAG	P06744
MPO197-211	RWLPAEYEDGFSLPY	P05164
MPO261-275	NQIAVDEIRERLFEQ	P05164
PAD-4141-157	WGPGCGGAILLVNCDRD	Q9UM07

*Grey highlight, used in ELISA, ELISPOT, and/or tetramer analysis
[cit] or Z = citrullinated arginine

Peptide (Residue)	Abbreviation	Sequence	Confirmed by
Nuclear or stress-response related proteins			
Bip-1 ₅₂₅₋₅₄₁	Bip-1	TITNDQNRLTPEEIERM	E
Bip-1[cit] ₅₂₅₋₅₄₁	Bip-1-cit	TITNDQNZLTPEEIERM	E
Bip-2 ₂₉₈₋₃₁₄	Bip-2	ALSSQHQARIEIESFYE	E
Bip-2[cit] ₂₉₈₋₃₁₄	Bip-2	ALSSQHQAZIEIESFYE	E
Histone H1b ₂₀₅₋₂₁₉	H1b	KPKAAKPKKAAAKKK	E, ES
CENP-A2 ₂₂₋₃₁	CENP-A2	PTPGPSRRGP	E
CENP-A2 ₉₇₋₁₁₁	CENP-A3	AAEAFLVHLFEDAYL	E
CENP-A4 ₇₋₁₆	CENP-A4	SRKPEAPRRR	E
La ₁₃₋₂₇	La	LEAKICHQIEYYFGD	E, ES, T
U1 snRNP Sm-D ₁₉₇₋₁₀₉	snRNP-1	RGRGRGRGRGRGR	E
70 kDa U1snRNP ₃₅₇₋₃₇₃	snRNP-2	SHRSERERRRDRDRDRD	E, ES, T
70 kDa U1snRNP ₁₁₂₋₁₂₈	snRNP-3	YDTTESKLRREFEVYGP	E
Structural proteins			
Fibrinogen B ₄₂₀₋₄₃₄	Fib-β	PRKQCSKEDGGGWY	E
Fibrinogen B ₄₂₀₋₄₃₄ -[cit]	Fib-β-cit	PZKQCSKEDGGGWY	E
Fibromodulin ₂₄₉₋₂₆₅	FMOD	LYMEHNNVYTVPDSYFR	E
Fibromodulin ₂₄₉₋₂₆₅ -[cit]	FMOD-cit	LYMEHNNVYTVPDSYFZ	E

Table 2. Summary of epitopes used for ELISA, ELISPOT, and tetramer analyses
E=ELISA, ES=ELISPOT, T= Tetramer, [cit] or Z=citrullinated arginine
E=ELISA, ES=ELISPOT, T= Tetramer, [cit] or Z=citrullinated arginine

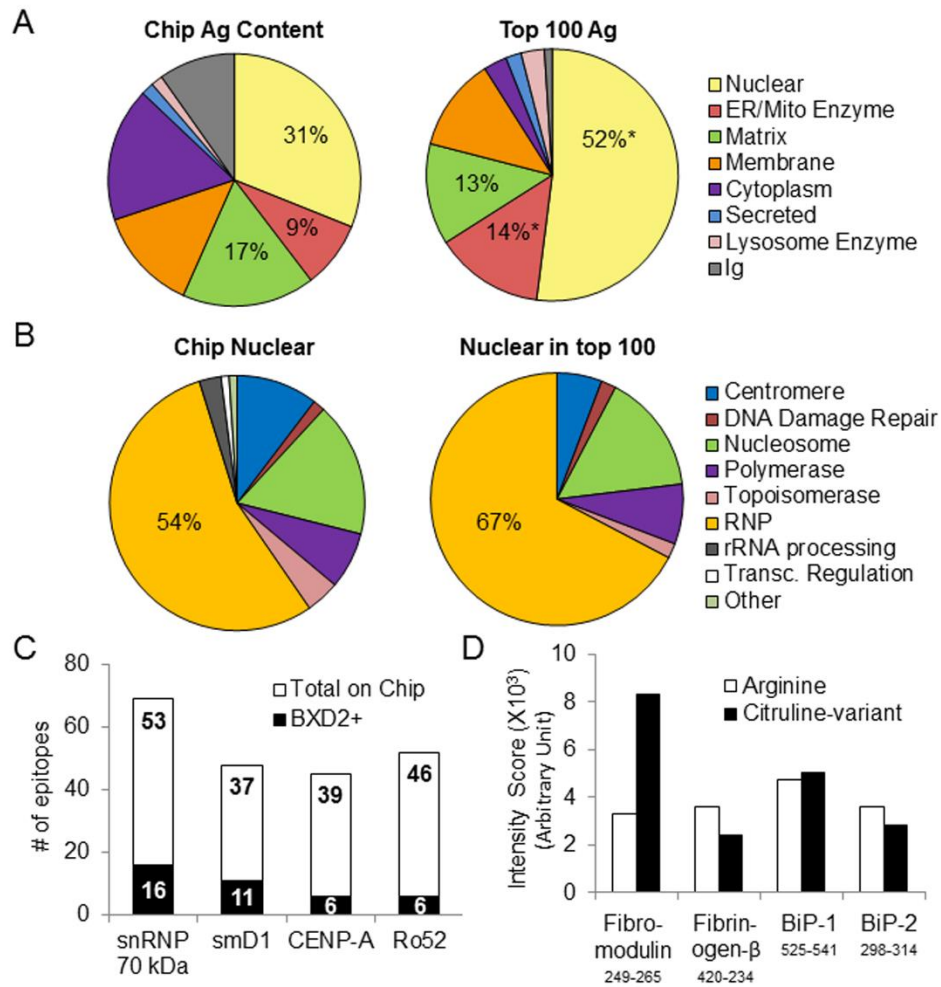


Fig. 1. Autoantibody binding to peptide epitopes in BXD2 mice. An array containing 2,733 database derived linear peptide epitopes associated with autoimmune disease was probed with pooled sera (n=6). **(A)** Antigen content distribution of entire chip compared to top 100 BXD2 positive epitopes, where positive is defined as greater than five-fold above the mean intensity score. **(B)** Sub-classification of total chip nuclear antigens compared to top 100 BXD2 nuclear epitopes. **(C)** Number of BXD2 positive epitopes deriving from the indicated autoantigen. **(D)** BXD2 autoantibody binding intensity to un-citrullinated and citrulline modified peptides deriving from the indicated autoantigen. * $P < 0.05$ between the antigen content distribution of the top 100 BXD2 epitopes vs. the distribution of the entire epitope microarray.

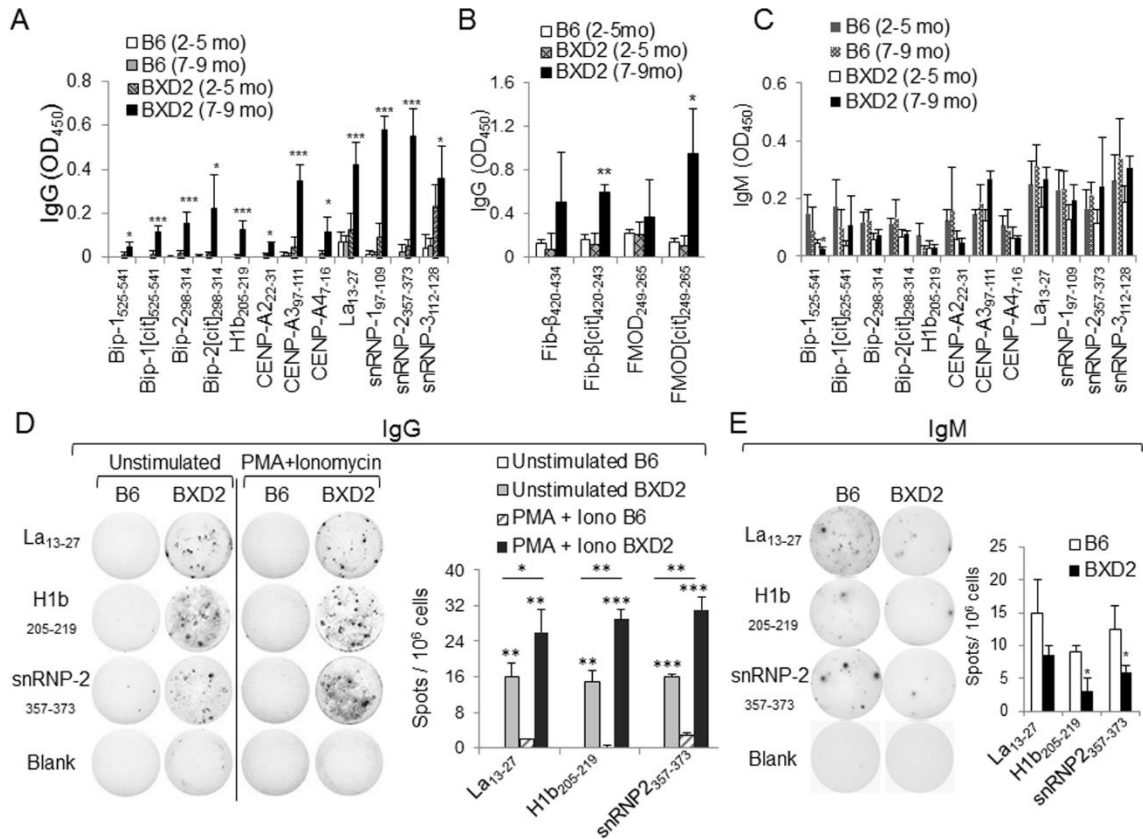


Fig. 3. Verification of synthesized peptides. **(A-C)** ELISA of **(A)** IgG autoantibodies specific to BiP, histone, centromere, and ribonucleoprotein peptide epitopes; **(B)** IgG autoantibodies specific to fibrinogen and fibromodulin peptide epitopes, and **(C)** IgM autoantibodies specific to BiP, histone, centromere, and ribonucleoprotein peptide epitopes in the sera of B6 and BXD2 mice at the indicated ages. All data are the mean \pm SEM of at least four mice per group. **(D, E)** ELISPOT assay of the **(D)** IgG or **(E)** IgM isotype autoantibody-producing B cells from B6 or BXD2 mice. Total spleen cells from 5-6 month-old B6 or BXD2 mice were cultured *in vitro* unstimulated (or stimulated with PMA + ionomycin in the IgG specific ELISPOT) on neutravidin ELISPOT plates coated with Lupus La₁₃₋₂₇, histone H1b₂₀₅₋₂₁₉ or snRNP₃₅₇₋₃₇₃. Right, mean \pm SEM number of **(D)** IgG or **(E)** IgM autoantibody-forming spots. Results are data from 3-5 mice and at least two independent experiments. For all panels, * $P < 0.05$; ** $P < 0.01$; *** $P < 0.005$ versus control group (normal B6 mice or the indicated comparison).

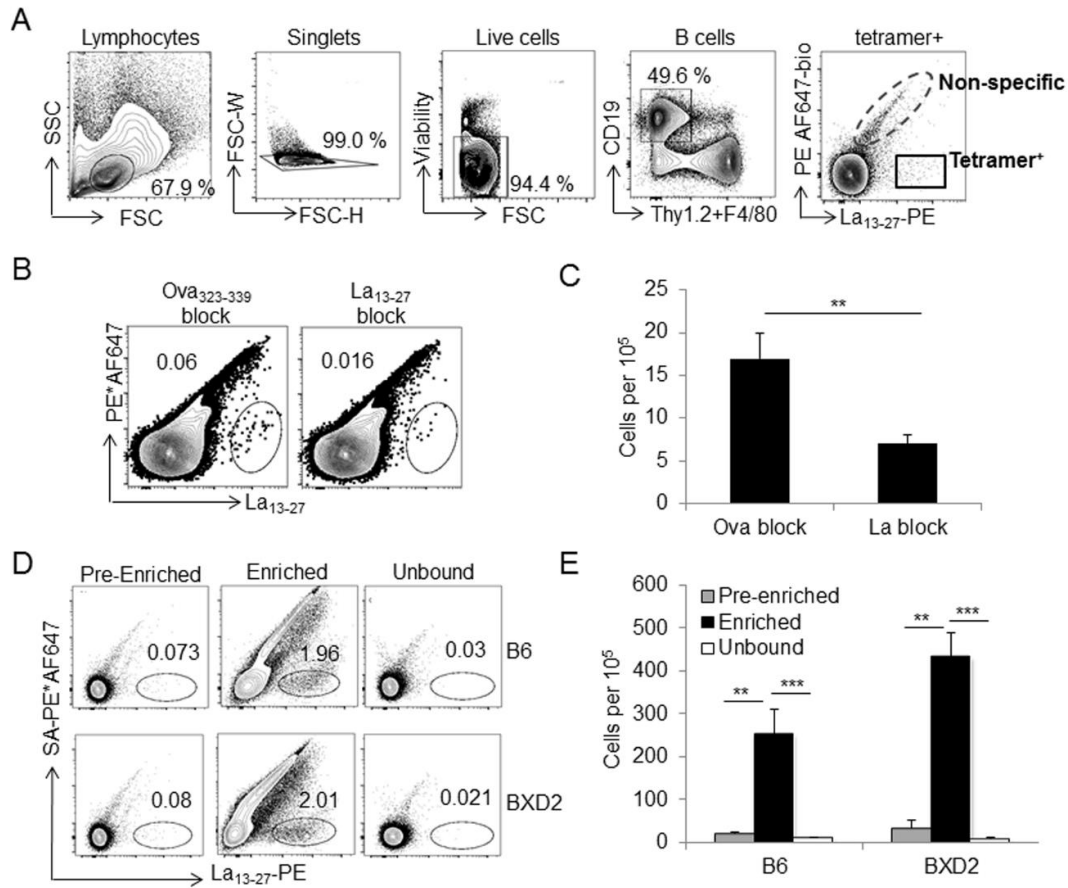


Fig. 4. Tetramer enrichment and gating strategy. **(A)** Gating strategy for tetramer experiments. Cells were gated based on forward and side scatter (lymphocyte gate) and signal height and widths (doublet exclusion). B cells were selected as CD19⁺ F4/80⁻ Thy1.2⁻. Tetramer⁺ cells were identified as PE*AF647⁺ and PE peptide-tetramer⁺. The experiment and gating strategy shown are representative of similar tetramer experiments. **(B, C)** Cells were incubated with 300 μ M of monomeric La₁₃₋₂₇ or 300 μ M OVA₃₂₃₋₃₃₉ peptide 30 min before La₁₃₋₂₇ tetramer labeling. Representative tetramer gated plots analyzed by flow cytometry **(B)**, and bar graph showing the average of cell counts under each blocking condition (per 10⁵ events analyzed) **(C)**. ***P* < 0.01 compared to OVA₃₂₃₋₃₃₉ peptide blocked cells. **(D, E)** Enrichment of tetramer⁺ B cells using anti-PE microbeads. Representative plots of enriched, pre-enriched, and flow-through fractions of La₁₃₋₂₇⁺ cells **(D)**, and cell counts for plots shown in panel D (per 10⁵ events analyzed) **(E)**. ***P* < 0.01; ****P* < 0.005 compared to enriched or unbound fractions (N=3-5 from at least 2 independent experiments).

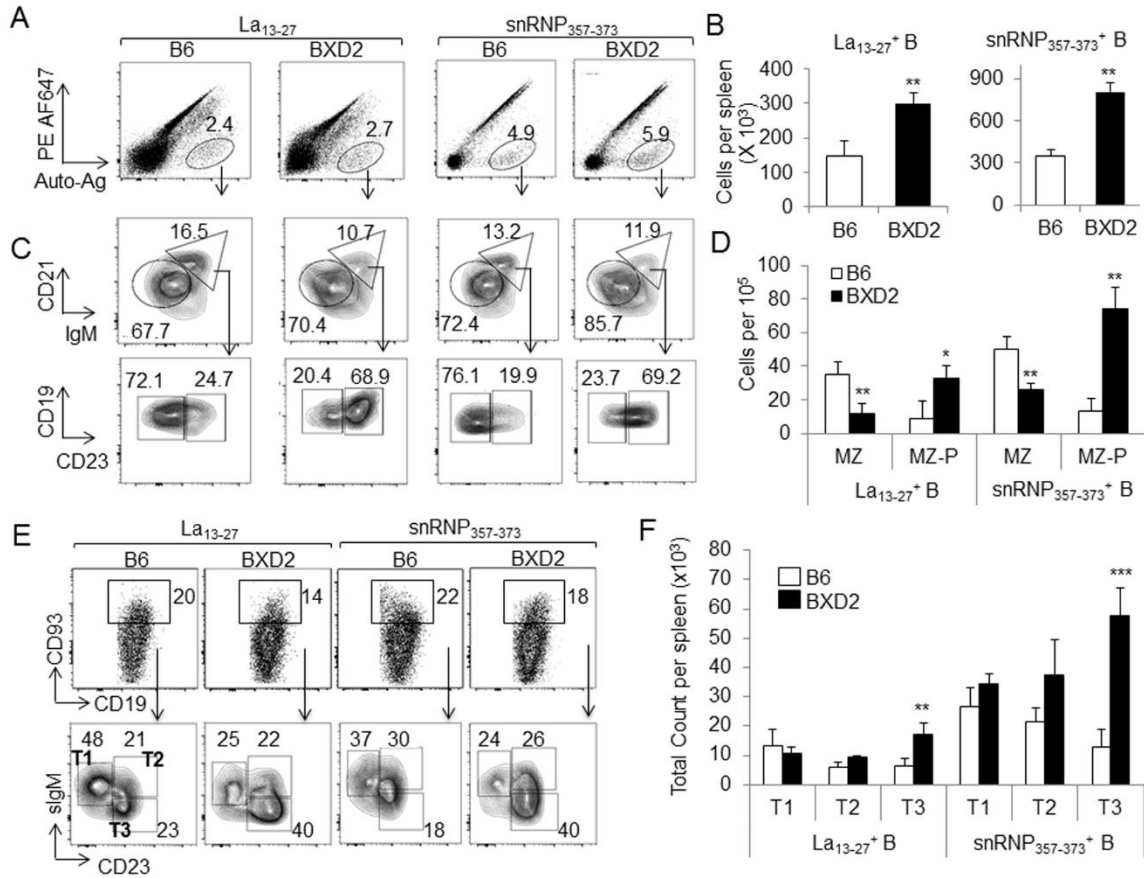


Fig. 5. Increased La₁₃₋₂₇ and snRNP₃₅₇₋₃₇₃ tetramer⁺ MZ-P and T3 B cells in BXD2 mice. **(A)** Spleen cells from 6-8 month old B6 and BXD2 mice were tetramer stained and enriched for FACS analysis of the frequency and number of La₁₃₋₂₇ or snRNP₃₅₇₋₃₇₃ tetramer⁺ B cells. **(B)** Cell counts for La₁₃₋₂₇ and snRNP₃₅₇₋₃₇₃ tetramer⁺ cells in total single cell suspension derived from the spleens of B6 and BXD2 mice. **(C)** La₁₃₋₂₇ and snRNP₃₅₇₋₃₇₃ tetramer⁺ cells were further analyzed for the frequency of IgM^{hi}CD21^{hi} B cells or IgM^{lo/-}CD21^{lo/-} B cells (top panels). The IgM^{hi}CD21^{hi} B cells were further gated into IgM^{hi}CD21^{hi} CD23⁻ MZ and IgM^{hi}CD21^{hi} CD23⁺ MZ-Ps (bottom panels), and the frequency of MZ or MZ-P B cells within this population is shown. **(D)** Cell counts for La₁₃₋₂₇ and snRNP₃₅₇₋₃₇₃ tetramer⁺ MZ and MZ-P cells in spleens of B6 and BXD2 mice (per 10⁵ events analyzed). **(E)** FACS analysis showing the frequency of La₁₃₋₂₇ and snRNP₃₅₇₋₃₇₃ tetramer⁺ transitional B cell subsets. **(F)** Cell counts for La₁₃₋₂₇ and snRNP₃₅₇₋₃₇₃ tetramer⁺ T1, T2, and T3 B cells in spleens of B6 and BXD2 mice. Each panel is representative of 3-5 mice and at least two independent experiments. **P* < 0.05 and ***P* < 0.01 between B6 and BXD2.

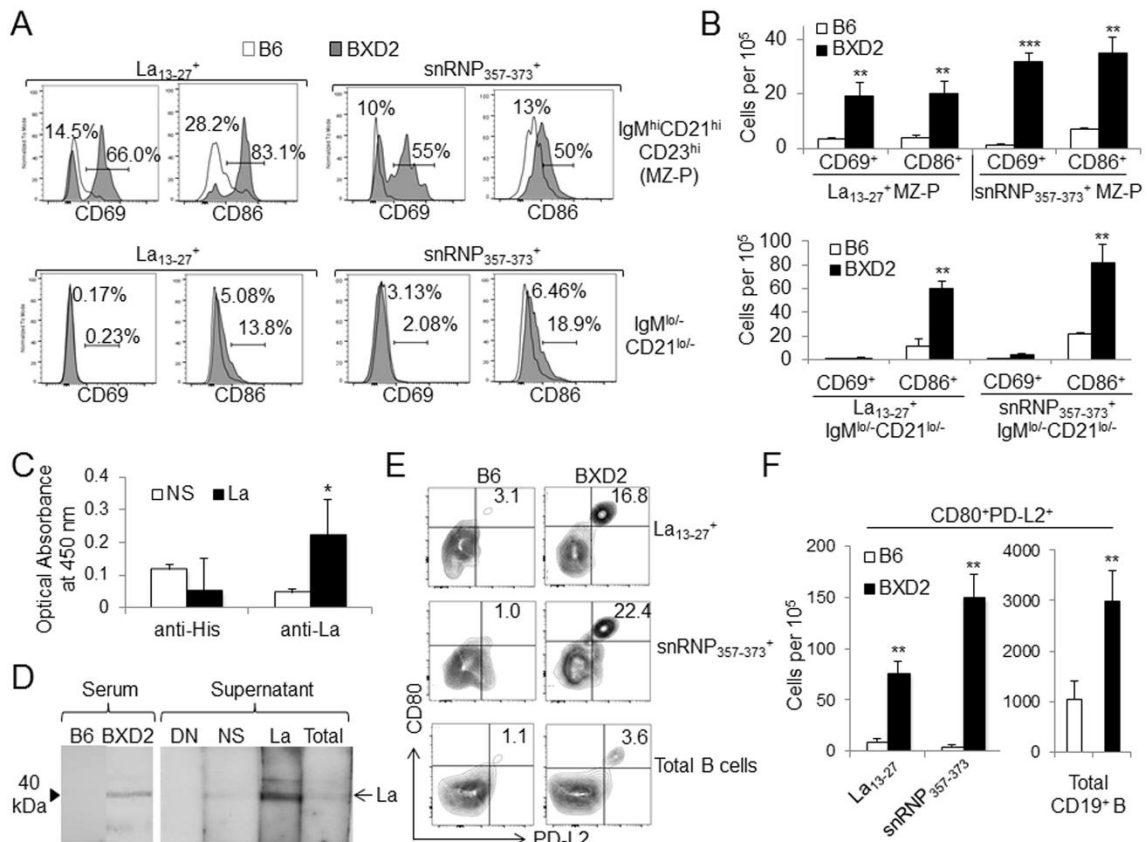
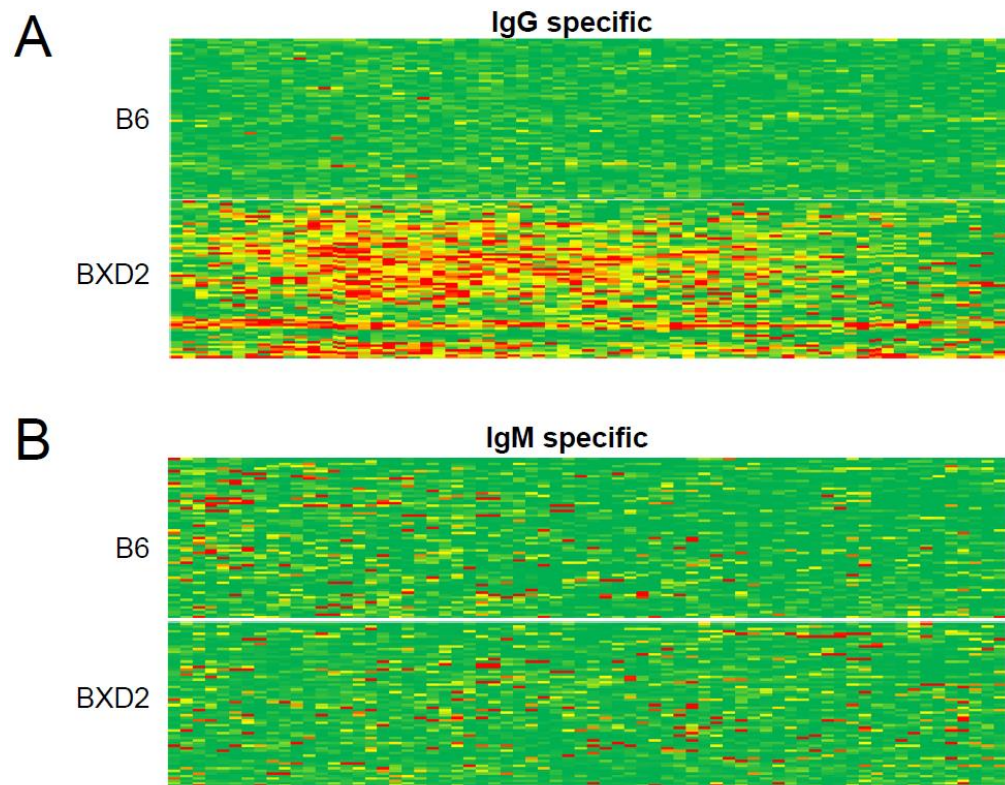
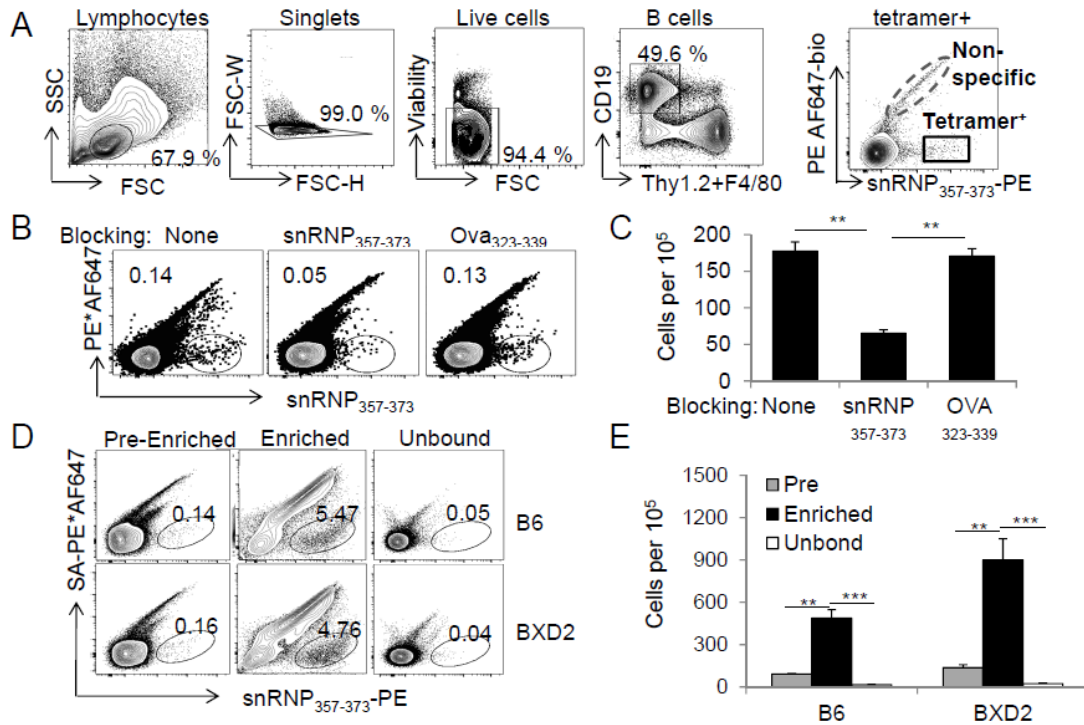


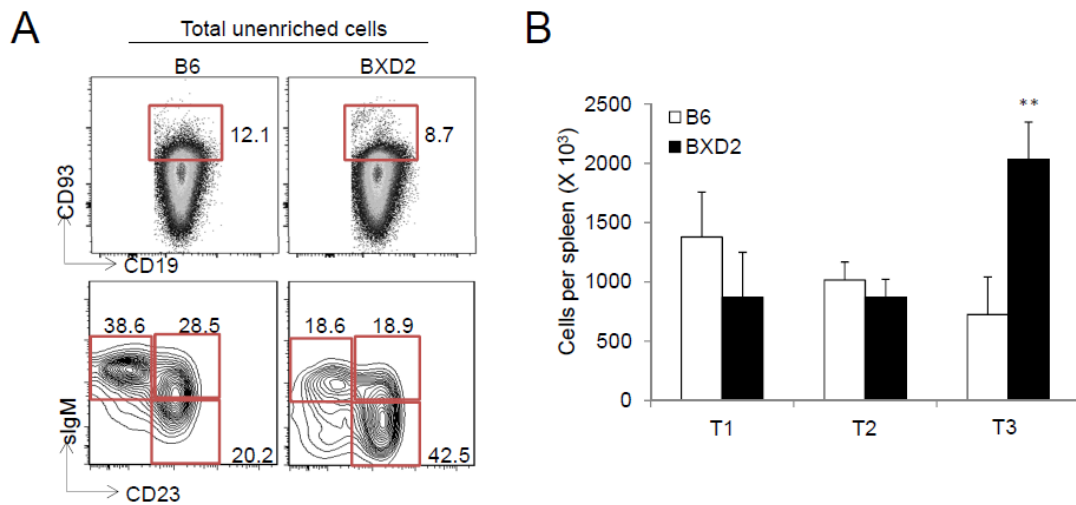
Fig. 6. Increased percentage of activated tetramer⁺ MZ-P and CD80⁺PD-L2⁺ memory B cells in BXD2 mouse spleens. **(A)** Flow cytometry analysis of expression of CD69⁺ and CD86⁺ cells in La₁₃₋₂₇⁺ and snRNP₃₅₇₋₃₇₃⁺ MZ-P (top) and IgM^{lo/-}CD21^{lo/-} (bottom) B cells from B6 and BXD2 mice. **(B)** Cell counts for histograms in panel A (per 10⁵ events analyzed). **(C)** ELISA analysis using supernatant collected from LPS + IL-4 stimulated sorted cell culture as the primary antibody to probe against Histone H1b₂₀₅₋₂₁₉ or La₁₃₋₂₇ peptide. NS = supernatant produced by non-specific tetramer⁺ B cells; La = supernatant produced by La₁₃₋₂₇⁺ B cells. **(D)** Western blotting analysis using B6 or BXD2 serum (1:50) or supernatant from LPS + IL-4 stimulated sorted cell culture as the primary antibody to probe against recombinant La antigen. DN = double tetramer negative supernatant; NS = non-specific tetramer⁺ supernatant; La = La₁₃₋₂₇⁺ supernatant. **(E)** La₁₃₋₂₇ (top) and snRNP₃₅₇₋₃₇₃ (middle) tetramer⁺ cells and total CD19⁺ B cells (bottom) were analyzed for the frequency of CD80⁺PD-L2⁺ memory B cells. **(F)** Mean cell counts for plots shown in E (per 10⁵ events analyzed). Data are representative of 2-3 mice from at least two independent experiments. **P* < 0.05; ***P* < 0.01, and ****P* < 0.005 between B6 and BXD2.



Supplementary Figure 1. Global autoantibody binding profile to peptide epitopes in BXD2 compared to B6 mice. Peptide microarray chips were probed with serum (1:200) from pooled 6-8 month old B6 or BXD2 mice to reveal IgG (A) and with serum (1:000) for IgM (B) autoantibody binding profiles to peptide autoepitopes derived from the Immune Epitope Database.



Supplementary Figure 2. Tetramer enrichment and gating strategy. **(A)** Gating strategy for tetramer experiments. Cells were gated based on forward and side scatter (lymphocyte gate) and signal height and widths (doublet exclusion). B cells were selected as CD19⁺ F4/80⁻ Thy1.2⁻. Tetramer⁺ cells were identified as PE*AF647⁻ and peptide-tetramer⁺. The experiment and gating strategy shown are representative of similar tetramer experiments in which the percentage of tetramer⁺ cells ranged from 0.3 to 5%. **(B, C)** Cells were incubated with 300 μ M of monomeric snRNP₃₅₇₋₃₇₃ or 300 μ M OVA₃₂₃₋₃₃₉ peptide 30 min before snRNP₃₅₇₋₃₇₃ tetramer labeling. Representative tetramer gated plots analyzed by flow cytometry **(B)**, and bar graph showing the average of cell counts under each blocking condition (per 105 events analyzed) **(C)**. ** $P < 0.01$ compared to un-blocked or OVA₃₂₃₋₃₃₉ peptide blocked cells. **(D, E)** Enrichment of tetramer⁺ B cells using anti-PE microbeads. Representative plots of enriched, pre-enriched, and flow-through fractions of La13-27⁺ cells **(D)**, and cell counts for plots shown in panel D (per 105 events analyzed) **(E)**. ** $P < 0.01$; *** $P < 0.005$ compared to enriched or unbound fractions (N=3-5 from 2 independent experiments)



Supplementary Figure 3. Transitional B cell subsets in total splenocytes from B6 and BXD2 mice. **(A)** FACS analysis showing the frequency of transitional B cell subsets T1, T2, and T3 in B6 and BXD2 mice. **(B)** Cell counts for T1, T2, and T3 B cells in spleens of B6 and BXD2 mice. Panels are representative of 2-3 mice from two independent experiments. Each panel is representative of 3-5 mice and at least two independent experiments. $**P < 0.01$ between B6 and BXD2.

DISCUSSION

Newly generated B cells that escape negative selection in the BM migrate to the spleen. It is here that these “transitional” T1 B cells acquire immune competence [32] and potentially come into contact with systemic products including “non-self” pathogens or “self” apoptotic debris. The present research suggests that during this formative stage of B cell development, B cell produced IFN β can influence the activity and development of these cells. One unique aspect of these studies is the identification of IFN β at the RNA and protein level in B cells isolated *ex vivo* from naïve autoimmune mice without artificial stimulation. Our results highlight the autocrine activity of IFN β produced specifically by immature T1 B cells, a formative stage of B cell development in mice and humans [31, 48].

pDCs vs. B Cells

Currently, pDCs are the main consideration in studies of type I IFN production in SLE. Certainly, the ability of pDCs to produce type I IFN that acts on multiple cell types including B cells is well documented [104, 105]. It is of course difficult to prove a causative association between pDCs and lupus in human SLE patients. Studies that have measured the phenotype and frequency of circulating pDC in SLE patients revealed various abnormalities, but no consistent trend among different studies [199, 200]. The leading hypothesis is that the scarcity of pDCs in the circulation of SLE patients is due to their recruitment to tissues of SLE patients [105, 107-109]. However, the data that

these cells produce type I IFN at these sites is lacking. The present work found that in BXD2 lupus mice and humans with SLE, freshly isolated pDCs show evidence of IFN gene and protein expression, but at levels equivalent to B lymphocytes (Figure 1). It is surprising that so few studies in the literature include measurement of pDC type I IFN expression. One recent study reported a consistent result that freshly isolated type I IFN expression in pooled pDCs from SLE patients was only modestly increased (<2 fold) in SLE patients vs. healthy controls [72]. Interestingly, a more recent study found consistent results that circulating pDCs from SLE patients did not produce elevated type I IFN compared to healthy controls, though pDCs from STING patients did exhibit increased type I IFN production [110].

While pDCs appear to be important in later stages of SLE [107, 108], questions remain including what is the source of type I IFN acting on B cells early in disease? Are there certain patient populations where B cell endogenous type I IFN may drive autoAb formation? Are there specific therapeutic windows where B cell derived type I IFN or type II IFN may preferentially modulate the B cell responses? The present research strongly implicates the importance of non-pDC cellular sources of type I IFN in SLE pathogenesis. Our studies suggest that type I IFN production by B cells is an important mechanism for autoreactive B cell development. In contrast to B cells, pDCs lack a specific antigen receptor capable of delivering TLR ligands to endosomal compartments. Thus, it has been proposed that pDCs are unlikely to be the primary sensors of nuclear antigens [115]. Instead, pDCs appear to be stimulated “downstream” of B cell activation and autoantibody production and immune complex formation [114-116]. This is consistent with the studies demonstrating that autoAbs precede disease by up to a

decade [6] suggesting a model where B cell tolerance is lost gradually early in disease progression, and pDC activation occurs in later stages of disease [107, 108]. Consistent with this, our data and the data of others suggest that B cell endogenous IFN may promote early B cell tolerance loss and autoAb formation, while pDC mediated end-organ damage is a feature of later disease stages [107, 108].

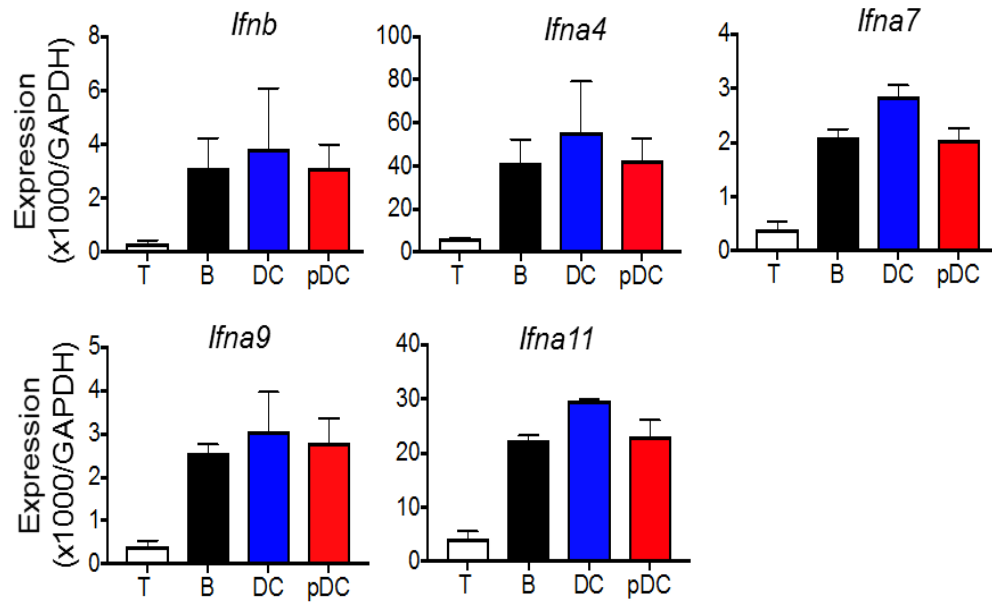


Figure 1. Type I IFN expression in BXD2 mice. 2-3 month old BXD2 female mice were sacrificed and spleens were collected for FACS sorting of the indicated cell population. Following RNA isolation, *Ifnb* and *Ifna* gene expression was determined.

There is a large body of literature that confirms pDCs produce large amounts of type I IFN following viral stimulation or stimulation with viral nucleic acid mimics [201]. Consistent with results from others [202], when we injected the mice with poly(I:C), sorted spleen pDCs produce >10 fold more IFN genes than B cells (Figure 2). However, it is intriguing that the BXD2 mice develop an IFNAR dependent autoimmune disease in the absence of such exogenous stimulation [23]. This is reminiscent of another lupus mouse model that developed anti-nuclear autoAbs and a large expansion

of pDCs in the absence of increased pDC produced type I IFN [111]. These observations suggest a role for other sources of type I IFN. This is not mere speculation, as T1 B cell endogenous IFN β had a significant impact on B cell gene expression, development and survival as described above in the manuscript. Thus, a major theme of this work is that a more precise understanding of cell-type specific [79] and IFN-subtype specific contributions to autoimmunity including IFN α vs IFN β downstream immune-modulation [102] will be important to take into consideration in future design of IFN-targeted therapies that will be suited to individual patients. Moreover, understanding the mechanisms of action of the different type I IFNs in more detail would aid effective therapeutic design in settings where a defined cell type is to be targeted.

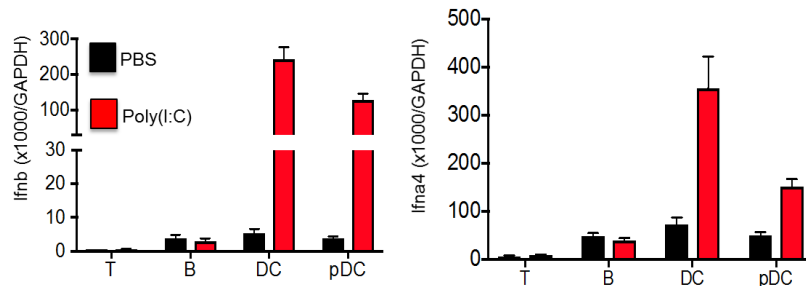


Figure 2. Functional verification of sorted DC populations. 2-3 month old BXD2 female mice were injected with HMW poly(I:C) LyoVec to activate the RIG1 and MDA5 cytosolic RNA sensing pathways. After 4 hours, mice were sacrificed and spleens were collected for FACS sorting of the indicated cell population. Following RNA isolation, *Ifna4* and *Ifnb* gene expression was determined.

B cells and IFN Production

Several previous studies identified B cells as prominent type I IFN producing and responding cells [70, 203, 204]. An early observation in human B cells was that the IFN receptor is highly expressed on peripheral blood B cells [204]. B cells were also found to be the most significant producers of type I IFN following interaction with

foreign cells [203], and recently transitional B cells from a subset of lupus patients were shown to secrete high levels of IFN α [70]. Our findings that IFN- β is expressed at the RNA and protein level in early T1 B cells in BXD2 mice and lupus patients are consistent with these previous studies and suggests that rapid type I IFN production by B cells may be of extreme importance in initiating B cell mediated host defense mechanisms. In addition, our findings that IFN- β was required for autoreactive B cell activation and survival suggests that tight transcriptional control of B cell IFN- α and IFN- β is critical for maintenance of B cell tolerance.

The transcription factors that govern type I IFN production are cell type dependent. In B cells, type I IFN production is IRF3 dependent [205], whereas induction of IFN- α and IFN- β mRNA upon viral infection was normal in IRF3 $-/-$ pDCs but impaired in IRF7 $-/-$ pDCs [150]. IRF3 is constitutively expressed in the cytoplasm of cells, and when activated translocates to the nucleus where it can associate with NF κ B P65 to induce transcription primarily at the IFN- β locus, but also the IFN α 4 locus [206]. IRF7, which is normally expressed at low levels in lymphoid cells but is induced by type I IFN, is activated downstream of the same pathways that activate IRF3, and preferentially stimulates IFN- α gene transcription [150]. In the early phase of infection or endogenous Ag stimulation, therefore, recognition of nucleic acids can induce IRF3 activation and IFN- β production. IFN- β induction of IRF7 then enables a feed-forward loop involving amplification of IFN- α gene transcription [207, 208]. This suggests that targeting of IRF3 may be an effective strategy to block B cell IFN- β induction, whereas IRF7 blockade may be more effective to block amplification of the IFN- α genes. Analysis of IRF3, IRF7, and IFN expression in single T1 B cells revealed that induction

of IRF7 expression is rare as compared to IRF3 and IFN α 4, suggesting that IRF7 induction is a tightly controlled event in the type I IFN circuit (Figure 3).

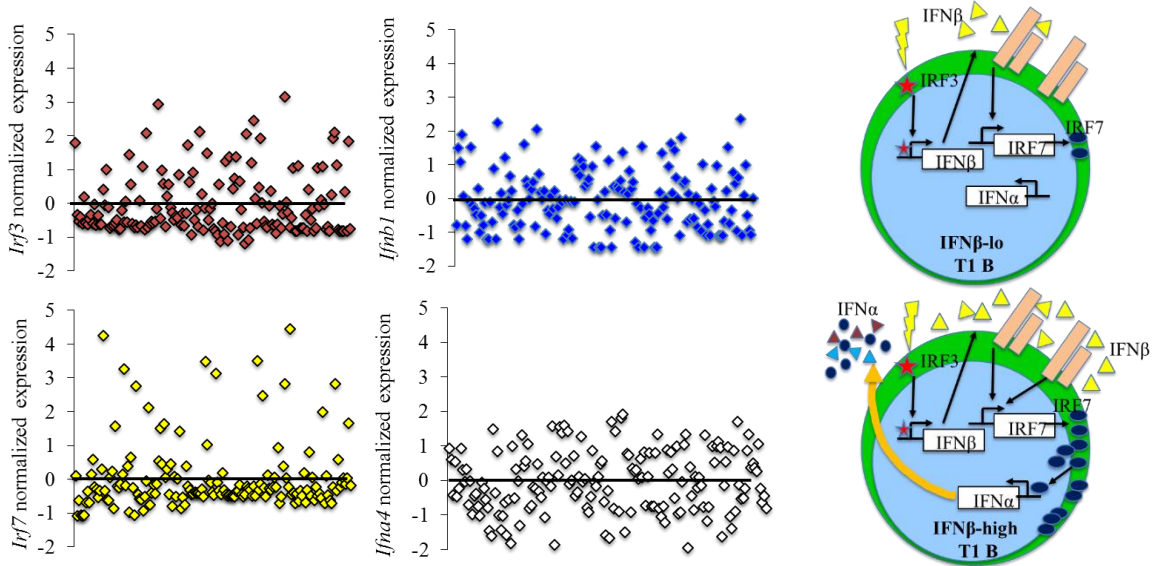


Figure 3. Variability in IFN and IRF genes in T1 B cells from BXD2 mice. Left, IRF7 induction is limited to a few outlier T1 B cells, while IRF3 exhibits an expression pattern similar to *Ifnb1* and *Ifna4*. Dots represent normalized expression of the indicated genes in single cells. Right, model for the generation of IRF7 high IFN α -high T1 B cells through overexpression of IFN β through IRF3

Significance of B cell type I IFN Heterogeneity

The present work identified heterogeneous expression of *Ifnb* and *Ifna* genes in T1 B cells isolated from naive autoimmune BXD2 mice. The tuning of *Ifnb1* expression involves variable expression across individual cells, as demonstrated for viral infections of various myeloid cell types [209-213]. One outcome of *Ifnb* heterogeneity across cells is that first responder cells can shape the IFN β response to stimulation, and dysregulation in *Ifnb1* expression may lead to hyper-activation of the type I IFN system [213]. In the present studies, it is important to note that the expression patterns in T1 B cells are not artificially induced but represent a snapshot of in vivo gene expression.

What is the significance of this heterogeneity in BXD2 mice? Multiple papers have studied heterogeneity in the type I IFN induction, though most if not all of these previous studies involved myeloid cells infected in vitro and did not study the induction of IFN genes themselves, but rather focused on IFN-response genes. For a given cell type, the various murine IFN- α subtypes have been shown to all exhibit antiviral or stimulatory effects, though with variable induction kinetics and potencies. This suggests that the heterogeneous induction of various IFN- α subtypes does not confer specific biological activities but enables specific expression patterns. The sequential induction of type I IFNs where genes are induced with early, intermediate, or late kinetics is an important point. Cytokines act locally in autocrine and paracrine fashion; thus certain early IFN subtypes may communicate the new appearance of an infection, informing naïve bystanders to induce other early genes that may control the infection. Late subtypes may signal to nearby cells that amplification of the response is necessary to clear an infection (Figure 4). Thus, the integration of the type I IFNs sensed by single T1 B cells may tune immune responses of the T1 B cells themselves and other cell-types.

The data described here suggest that coordinated expression of the different type I IFN genes is a prominent feature of T1 B cell development in the spleen of autoimmune mice. In the spleens of BXD2 mice, T1 B cells segregated into *Ifna*^{hi} and *Ifnb*^{hi} sub-populations. An important question is do these populations represent distinct effector populations, different stages of B cell development, or different stages in the evolution of the type I IFN response or all of these at once? In support of different developmental stages, clustering of cells based on *Cd23* and *Cd93* revealed distinct

expression patterns of IFN genes and *Tlr7* in early vs. late T1 B cells. In the early T1 subset (*Cd93^{hi}Cd23^{lo}*), *Ifnb* expression was significantly higher than *Ifna7*. However, marked elevation of *Ifna7* and *Tlr7* expression occurred in T1 B cells that had down-regulated early B cell marker *Cd93*. This and in vitro experiments demonstrating the requirement of autocrine IFN β for TLR7 responses in T1 B cells suggests that autocrine IFN β driven TLR7 expression may be important in TLR7 competence of T1 B cells. What stimulates this B cell endogenous IFN β - TLR7 pathway? In B6 mice, spontaneous germinal centers are known to form in the absence of exogenous stimuli, but TLR7-deficient B6 mice showed a complete absence of spontaneous germinal center B cells [214]. This was B cell intrinsic and TLR7 specific as μ MT mice receiving BM cells from TLR7 KO, but not TLR9 KO mice failed to form germinal centers [214]. The present work suggests that B cell produced IFN β enhancement of TLR7 responses is a prominent feature of T1 B cells and is critical for shaping B cell responses to endogenous antigen.

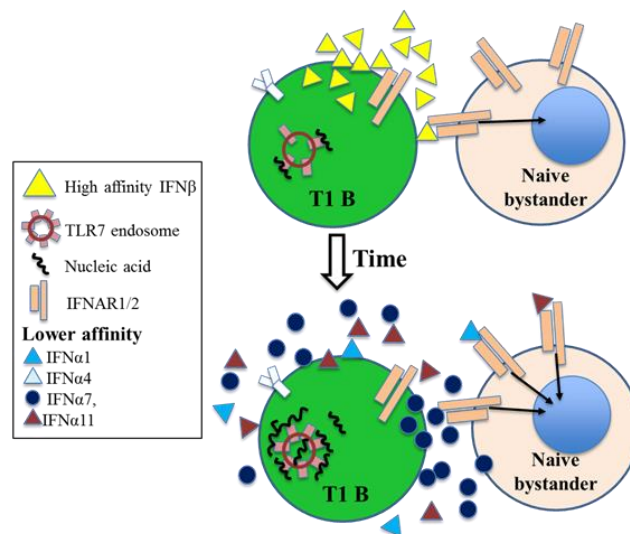


Figure 4. Model for interaction of T1 B cell IFN communication network

The heterogeneity in type I IFN expression may also represent different stages of a type I IFN response. IFN β is known to enable expression of certain IFN α subtypes [215], though this is complex and dependent on various factors such as the strength and multiplicity of the interferonogenic stimulus and the IFN α subtype [215]. Thus the *Ifnb*-low T1 B cells with upregulated IFN α genes represent IFN β -responding cells *in vivo*. One advantage of the single cell gene expression analysis is it reveals which genes are co-expressed. IFN β transcription is induced with immediate early kinetics due to its lack of dependency on the transcription factor IRF7; rather IRF3 is sufficient to induce IFN β . The IFN α genes *Ifna1* and *Ifna4* have also been reported to be early response genes. Interestingly, single cell analysis of *Ifnb*, *Ifna1* and *Ifna4* revealed that although these three genes have early induction kinetics, the early IFN α genes are not induced in the same cell where IFN β is induced (Figure 5). However, *Ifna1* and *Ifna4* exhibited higher co-expression with *Ifnb* as compared to *Ifna7* and *Ifna11*, which is consistent with previous observations that *Ifna1* and *Ifna4* are early response genes. No IFN α gene showed significant co-expression with *Ifnb* suggesting that in most cells the activation of different type I IFN α loci vs. the IFN β locus do not occur simultaneously (Figure 5).

An important focus of future studies using single cell RNA-seq would have greater ability to identify other IFN β -response genes which may be essential to the genesis of a type I IFN cascade and thus potential targets for diseases involving type I IFN dysregulation. We propose that the endogenous expression of different type 1 interferons at the T1 subpopulation establishes initial trajectories for these T1 B cells that can influence their subsequent developmental potential, which would be highly dependent upon exogenous signals through the B cell receptor or TLR signaling.

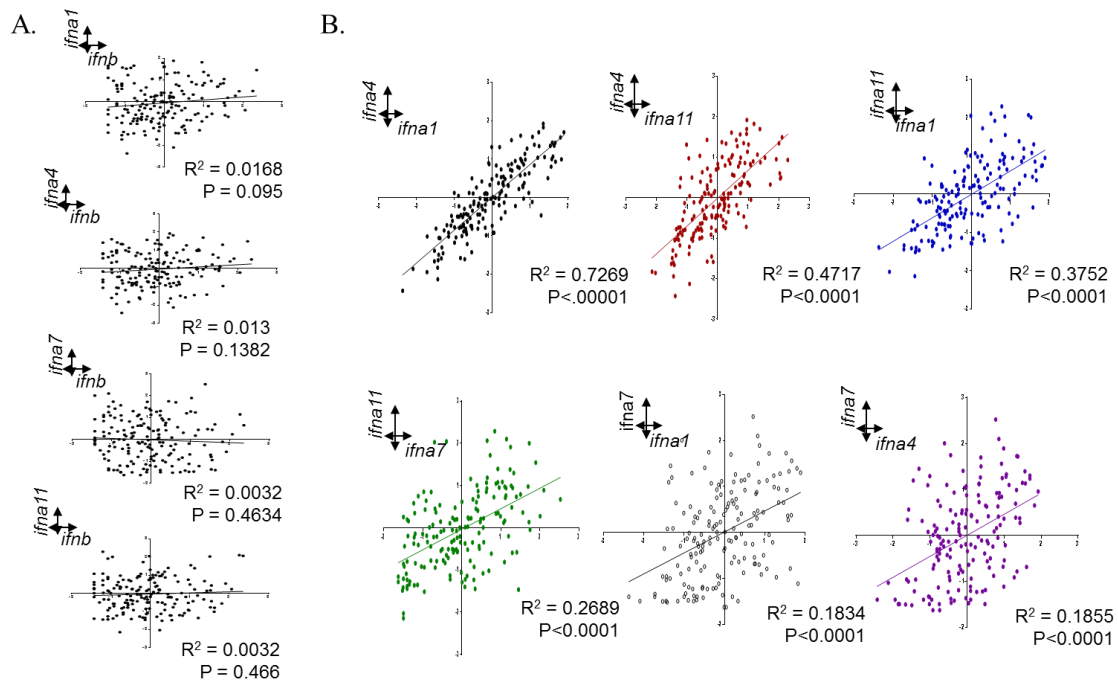


Figure 5. Correlation plots showing co-expression of type I IFN genes. Each dot represents the normalized expression of the indicated gene in a single cell (n=167).

IFN β in Mouse Autoimmunity

There are several lupus prone mouse models that develop systemic autoimmune disease as a result of complex interactions of multiple genetic loci. These include the NZB/W, SLE1.2.3 and BXD2 mice [22, 216]. Baccala *et al.* is the only study to date which has specifically investigated the role of IFN- β in the development of disease in a lupus-prone mouse, using NZB/W IFN- β -/- mice [217]. These investigators suggested that IFN- β was not required for anti-chromatin Abs or renal disease in NZB/W mice. Baccala *et al.* did not report on any other autoAb specificities besides anti-chromatin [217]. However, our data show that in BXD2 lupus-prone mice, IFN- β specifically promotes anti-DNA, anti-histone, and anti-La autoAbs and renal disease. Additionally,

SLE patients with high intracellular IFN- β in our study were more likely to have high anti-Sm and renal disease. Our findings are not the first to report an association with transitional B cell cytokine production and an immune-mediated renal dysfunction [71]. Cherukuri *et al.* recently reported that the T1/T2 B cell ratio and associated cytokine production strongly correlated with renal allograft dysfunction.

A role for abnormal B cell activity in the development of renal disease in NZB/W mice was recently implicated by successful amelioration of renal disease using a Btk specific inhibitor. Interestingly, this study found that the reduced renal disease in Btk inhibited NZB/W mice was associated with gene expression signatures essential for splenic B cell terminal differentiation [218]. In the BXD2 mice, we showed that over-production of IFN- β was most pronounced in the T1 B cell subset that developmentally precedes mature B cell fate commitment. It is not known whether NZB/W mice also exhibit over-expression of IFN- β and in what cell types. However, the lack of a phenotype reported in Baccala *et al.* may be due to genetic background differences leading to a unique type I IFN dysregulation or developmental compensatory effects of other IFNs in mice that developed without IFN- β from birth [217]. In human cells, constitutively expressed IRF-3 was shown to activate predominantly IFN- α 1 and IFN- β , while IRF-7 expression subsequently induced multiple other IFN- α genes [219]. Similarly, in mice, IFN- β is the earliest IFN response gene, where IFN- α 1 and IFN- α 4 were subsequently induced with relatively early kinetics (relative to other “late” type I IFNs) [207, 220]. It is possible in a global IFN- β knockout mouse, the induction requirements of other specific IFN- α subtypes are such that they can be induced early and may compensate for the lack of IFN- β in global IFN- β ko mice.

In the present study, we sought to control for this possibility using competitive reconstitution experiments in which we reconstituted B6 RAG1^{-/-} mice with a 1:1 ratio of Ifnb^{-/-} to Ifnb^{+/+} B6 mice. These studies revealed that development of germinal center, La⁺ autoreactive, and IgG class switched anti-DNA, anti-La and anti-Histone autoAb producing B cells were highly dependent upon endogenous IFN- β (Figure 6). Single-cell examination of Ifnb^{-/-} vs. Ifnb^{+/+} T1 B cells further revealed distinct gene expression signatures associated with endogenous IFN β , including significantly lower expression of CD86, TLR7, and PKR, and type I IFN genes as described in the manuscript above.

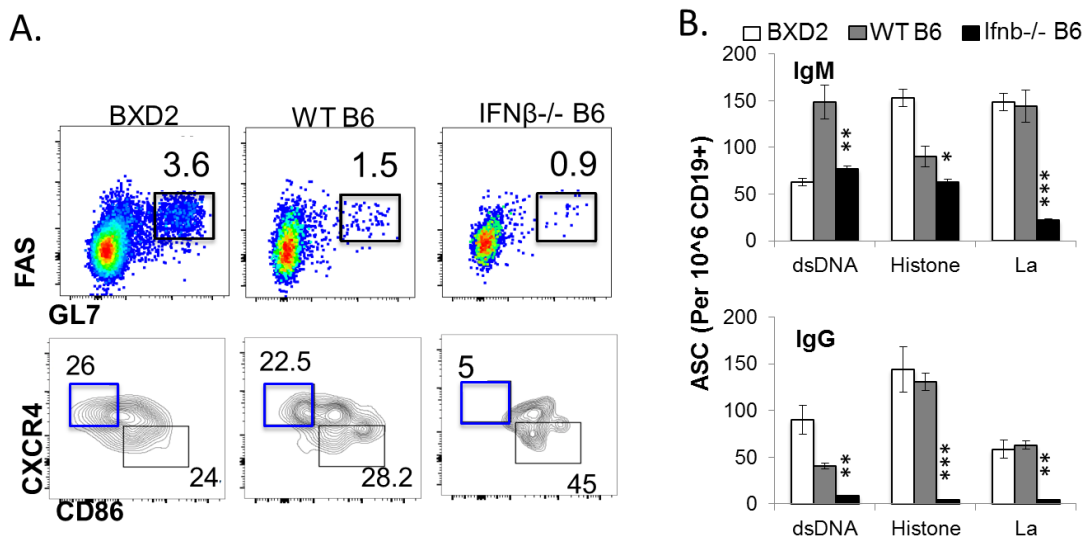


Figure 6. B cell endogenous IFN- β is required for autoAb formation. (A) The percentage of GC and CXCR4⁺CD86^{lo} GC B cells derived from Ifnb^{-/-} and Ifnb^{+/+}. (B). Quantification of autoAb secreting B cells derived from Ifnb^{-/-} and Ifnb^{+/+}.

IFN β in Human SLE

In B cells, IRF3 dependent type I IFN production enhanced CD138 (Syndecan-1) expression and IgM production and was required for IgG2a production following CpG-B stimulation, implicating B cell produced type I IFN in autoantibody production and the pathogenesis of certain autoimmune diseases. Consistent with this, examination of human lupus T1 B cells in this study revealed that patients who had higher T1 B cell endogenous IFN- β also had significantly increased CD19^{lo}CD27⁺CD38^{hi} plasma cells (Figure 7). It is possible that some new emigrant B cells from the bone marrow may develop directly into antibody secreting cells following stimulation with endogenous nucleic acid antigens. Indeed, an expansion of T1 B cells was observed in TLR7 transgenic mice, and these T1 B cells had a phenotype resembling antibody-secreting plasmablasts. In addition, SLE patients who had higher T1 B cell endogenous IFN- β also had a significantly increased IgD⁻CD27⁻ “double negative” population of CD19⁺ B cells (Figure 7). The identity of these cells is not known, but they are potentially an effector memory population capable upon recall responses [221]. Clearly there is an advantage for cells to induce certain type I IFNs at the right time and environment in a highly regulated cascade (with IFN- β being the first type I IFN induced [222]). We propose that in lupus-prone BXD2 mice and some SLE patients, blockade of IFN- β can dampen the type I IFN pathway without completely shutting it down making it a desirable therapeutic treatment in some patients.

Our findings that IFN β in SLE patients correlates positively with percentages of 9G4 autoreactive mature naïve B cells implicate B cell IFN β as both a potential biomarker and effector of disease. Furthermore, SLE patients who have had anti-Sm

antibodies and who exhibited active renal disease at the time of sample collection also exhibited significantly increased frequency of IFN β + T1 B cells. SLE patients who were positive for anti-DNA also showed increased frequency of IFN β + T1/T2 B cells. The data suggest that higher IFN β expression by B cells is associated with the development of autoreactive B cells and renal disease. In addition, African American patients in our studies were significantly enriched in B cell IFN β expression, suggesting that polymorphisms in the IFN β enhanceosome or other upstream factors may predispose this population to development of higher IFN β expression by B cells. Therefore, for SLE, endogenous expression of IFN β in transitional B cells is highly associated with the most classical clinical and laboratory features (AA race, nephritis and anti-Sm). The clinical and laboratory features of the BXD2 mouse model of lupus also shares strong similarities to SLE [14, 15, 17]. In addition to the plasma cell population, the IgD-CD27- double negative (DN) population was also increased in IFN- β -high SLE patients. Importantly, these two phenotypes are both associated with increased SLE severity [221].

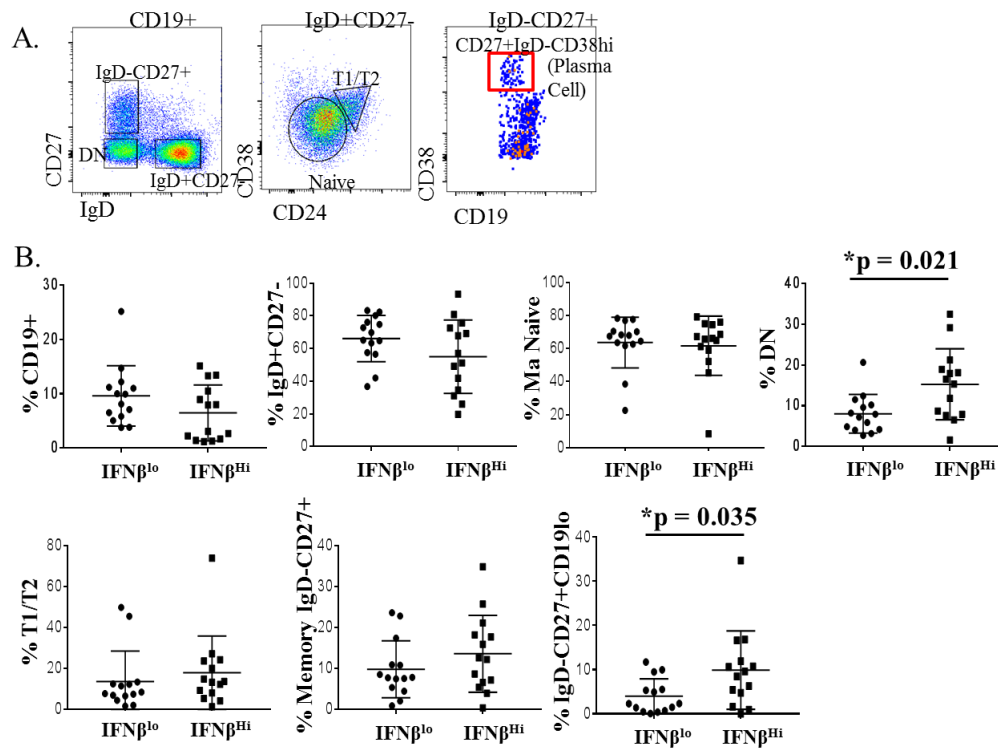


Figure 7. T1 B cell endogenous IFN β is associated with expansions in the plasma cell and IgD-CD27- double negative populations in SLE. A) Gating strategy for human PBMC analysis. B) The percentages of the indicated B cell subset in SLE patients segregated based on T1/T2 B cell IFN β^{lo} or IFN β^{hi} .

While IFN β has been found to be important in RA, the cross talk between type I IFNs and TNF α , the major pathogenic cytokine in RA, is a key consideration [223, 224]. The balance of type I IFN and TNF α may be a determining factor in the dysregulated immune response. When the type I IFN arm prevails, IFN-driven autoimmunity such as SLE may occur, while RA may develop when TNF α dysregulation is dominant, which is consistent with early observations by Ivashkiv that a fraction of RA patients treated with anti-TNF α therapy develop antinuclear antibodies and even sometimes lupus-like syndromes [225]. The present work is consistent with the growing recognition that transitional B cells are prominent producers of regulatory cytokines [69, 71] which can

have a profound effect on immune responses. The ratio of transitional B produced IL-10 to TNF- α was reduced in patients with allograft rejection [226], and more recently, dysregulation in these regulatory transitional B cells was strongly associated with subsequent deterioration in renal allograft function [71]. Our findings may also be relevant in the context of Sjogren's syndrome, another disease which is primarily due to B cell infiltration and inflammation in the salivary gland and has been associated with type I IFN [227-229]. A better understanding of this disease could be obtained by analyzing B cell heterogeneity as related to IFN β -IFNAR network, especially as recent work has shown that the patterns of IFN activity were heterogeneous in Sjogren's syndrome [227]. A more precise understanding and ability to define different pathways of type I IFN dysregulation within a group of clinically similar patients should lead to improved targeted therapies in SLE and potentially other autoimmune diseases.

Conclusion

Together, these data highlight the role of IFN β in shaping T1 B cell responses in the mouse spleen, including their survival and responses to TLR7. Notably, they indicate that these effects are mediated through the endogenous expression of IFN β in T1 B cells. This mechanism suggests that endogenous IFN β -expressing T1 B cells are initially autonomous and that their expression of IFN β plays a key role in regulating their responsiveness to external factors, including externally-derived type 1 IFNs and TLR7. In lupus, overexpression of IFN β in T1 B cells may promote the development of autoreactive mature B cells leading to the generation of polyreactive self-antigen-reactive mature B cells. The present data from SLE patients further suggests a need for

future human lupus studies into type I IFN dysregulation that pioneer beyond the view of pDC produced IFN α . These results also provide a mechanistic basis for development of more effective therapies to dampen the type I IFN cascade by specifically targeting the high-affinity IFN β or the enhanceosome components that promote its induction in a subgroup of lupus patients.

GENERAL LIST OF REFERENCES

1. Sharma, S., et al., *Widely divergent transcriptional patterns between SLE patients of different ancestral backgrounds in sorted immune cell populations.* J Autoimmun, 2015. **60**: p. 51-8.
2. Tsokos, G.C., *Systemic lupus erythematosus.* N Engl J Med, 2011. **365**(22): p. 2110-21.
3. Crow, M.K., *Type I interferon in the pathogenesis of lupus.* J Immunol, 2014. **192**(12): p. 5459-68.
4. Moroni, G., et al., *"Nephritic flares" are predictors of bad long-term renal outcome in lupus nephritis.* Kidney Int, 1996. **50**(6): p. 2047-53.
5. Ching, K.H., et al., *Two major autoantibody clusters in systemic lupus erythematosus.* PLoS One, 2012. **7**(2): p. e32001.
6. Arbuckle, M.R., et al., *Development of autoantibodies before the clinical onset of systemic lupus erythematosus.* N Engl J Med, 2003. **349**(16): p. 1526-33.
7. Grammer, A.C. and P.E. Lipsky, *B cell abnormalities in systemic lupus erythematosus.* Arthritis Res Ther, 2003. **5 Suppl 4**: p. S22-7.
8. Wakeland, E.K., et al., *Delineating the genetic basis of systemic lupus erythematosus.* Immunity, 2001. **15**(3): p. 397-408.
9. Deng, Y. and B.P. Tsao, *Genetic susceptibility to systemic lupus erythematosus in the genomic era.* Nat Rev Rheumatol, 2010. **6**(12): p. 683-92.
10. Deapen, D., et al., *A revised estimate of twin concordance in systemic lupus erythematosus.* Arthritis Rheum, 1992. **35**(3): p. 311-8.

11. Chan, O.T., M.P. Madaio, and M.J. Shlomchik, *The central and multiple roles of B cells in lupus pathogenesis*. Immunol Rev, 1999. **169**: p. 107-21.
12. Manjarrez-Orduno, N., T.D. Quach, and I. Sanz, *B cells and immunological tolerance*. J Invest Dermatol, 2009. **129**(2): p. 278-88.
13. Shlomchik, M.J., *Sites and stages of autoreactive B cell activation and regulation*. Immunity, 2008. **28**(1): p. 18-28.
14. Mountz, J.D., et al., *Genetic segregation of spontaneous erosive arthritis and generalized autoimmune disease in the BXD2 recombinant inbred strain of mice*. Scand J Immunol, 2005. **61**(2): p. 128-38.
15. Li, H., et al., *Interferon-induced mechanosensing defects impede apoptotic cell clearance in lupus*. J Clin Invest, 2015. **125**(7): p. 2877-90.
16. Li, H., et al., *Cutting Edge: defective follicular exclusion of apoptotic antigens due to marginal zone macrophage defects in autoimmune BXD2 mice*. J Immunol, 2013. **190**(9): p. 4465-9.
17. Wang, J.H., et al., *Extension of the germinal center stage of B cell development promotes autoantibodies in BXD2 mice*. Arthritis Rheum, 2013. **65**(10): p. 2703-12.
18. Hsu, H.C., et al., *Interleukin 17-producing T helper cells and interleukin 17 orchestrate autoreactive germinal center development in autoimmune BXD2 mice*. Nat Immunol, 2008. **9**(2): p. 166-75.
19. Hsu, H.C., et al., *Overexpression of activation-induced cytidine deaminase in B cells is associated with production of highly pathogenic autoantibodies*. J Immunol, 2007. **178**(8): p. 5357-65.

20. Hsu, H.C., et al., *Inhibition of the catalytic function of activation-induced cytidine deaminase promotes apoptosis of germinal center B cells in BXD2 mice.* Arthritis Rheum, 2011. **63**(7): p. 2038-48.
21. Wang, J.H., et al., *Marginal zone precursor B cells as cellular agents for type I IFN-promoted antigen transport in autoimmunity.* J Immunol, 2010. **184**(1): p. 442-51.
22. Mountz, J.D., et al., *Cytokine regulation of B-cell migratory behavior favors formation of germinal centers in autoimmune disease.* Discov Med, 2011. **11**(56): p. 76-85.
23. Wang, J.H., et al., *Type I interferon-dependent CD86(high) marginal zone precursor B cells are potent T cell costimulators in mice.* Arthritis Rheum, 2011. **63**(4): p. 1054-64.
24. Cambier, J.C., et al., *B-cell anergy: from transgenic models to naturally occurring anergic B cells?* Nat Rev Immunol, 2007. **7**(8): p. 633-43.
25. Melchers, F., *Checkpoints that control B cell development.* J Clin Invest, 2015. **125**(6): p. 2203-10.
26. Pelanda, R. and R.M. Torres, *Central B-cell tolerance: where selection begins.* Cold Spring Harb Perspect Biol, 2012. **4**(4): p. a007146.
27. Goodnow, C.C., *Transgenic mice and analysis of B-cell tolerance.* Annu Rev Immunol, 1992. **10**: p. 489-518.
28. Nemazee, D.A. and K. Burki, *Clonal deletion of B lymphocytes in a transgenic mouse bearing anti-MHC class I antibody genes.* Nature, 1989. **337**(6207): p. 562-6.

29. Grandien, A., et al., *Negative selection of multireactive B cell clones in normal adult mice*. Eur J Immunol, 1994. **24**(6): p. 1345-52.
30. Wardemann, H., et al., *Predominant autoantibody production by early human B cell precursors*. Science, 2003. **301**(5638): p. 1374-7.
31. Loder, F., et al., *B cell development in the spleen takes place in discrete steps and is determined by the quality of B cell receptor-derived signals*. J Exp Med, 1999. **190**(1): p. 75-89.
32. Chung, J.B., M. Silverman, and J.G. Monroe, *Transitional B cells: step by step towards immune competence*. Trends Immunol, 2003. **24**(6): p. 343-9.
33. Carsetti, R., G. Kohler, and M.C. Lamers, *Transitional B cells are the target of negative selection in the B cell compartment*. J Exp Med, 1995. **181**(6): p. 2129-40.
34. Merrell, K.T., et al., *Identification of anergic B cells within a wild-type repertoire*. Immunity, 2006. **25**(6): p. 953-62.
35. Goodnow, C.C., et al., *Altered immunoglobulin expression and functional silencing of self-reactive B lymphocytes in transgenic mice*. Nature, 1988. **334**(6184): p. 676-82.
36. Mason, D.Y., M. Jones, and C.C. Goodnow, *Development and follicular localization of tolerant B lymphocytes in lysozyme/anti-lysozyme IgM/IgD transgenic mice*. Int Immunol, 1992. **4**(2): p. 163-75.
37. Cooke, M.P., et al., *Immunoglobulin signal transduction guides the specificity of B cell-T cell interactions and is blocked in tolerant self-reactive B cells*. J Exp Med, 1994. **179**(2): p. 425-38.

38. Healy, J.I., et al., *Different nuclear signals are activated by the B cell receptor during positive versus negative signaling*. *Immunity*, 1997. **6**(4): p. 419-28.
39. Yurasov, S., et al., *Defective B cell tolerance checkpoints in systemic lupus erythematosus*. *J Exp Med*, 2005. **201**(5): p. 703-11.
40. Yurasov, S., et al., *Persistent expression of autoantibodies in SLE patients in remission*. *J Exp Med*, 2006. **203**(10): p. 2255-61.
41. Menard, L., et al., *The PTPN22 allele encoding an R620W variant interferes with the removal of developing autoreactive B cells in humans*. *J Clin Invest*, 2011. **121**(9): p. 3635-44.
42. Kolhatkar, N.S., et al., *Altered BCR and TLR signals promote enhanced positive selection of autoreactive transitional B cells in Wiskott-Aldrich syndrome*. *J Exp Med*, 2015. **212**(10): p. 1663-77.
43. Su, T.T. and D.J. Rawlings, *Transitional B lymphocyte subsets operate as distinct checkpoints in murine splenic B cell development*. *J Immunol*, 2002. **168**(5): p. 2101-10.
44. Srivastava, B., et al., *Characterization of marginal zone B cell precursors*. *J Exp Med*, 2005. **202**(9): p. 1225-34.
45. Allman, D., et al., *Resolution of three nonproliferative immature splenic B cell subsets reveals multiple selection points during peripheral B cell maturation*. *J Immunol*, 2001. **167**(12): p. 6834-40.
46. Carsetti, R., M.M. Rosado, and H. Wardmann, *Peripheral development of B cells in mouse and man*. *Immunol Rev*, 2004. **197**: p. 179-91.

47. Sims, G.P., et al., *Identification and characterization of circulating human transitional B cells*. *Blood*, 2005. **105**(11): p. 4390-8.
48. Palanichamy, A., et al., *Novel human transitional B cell populations revealed by B cell depletion therapy*. *J Immunol*, 2009. **182**(10): p. 5982-93.
49. Melchers, F., et al., *Positive and negative selection events during B lymphopoiesis*. *Curr Opin Immunol*, 1995. **7**(2): p. 214-27.
50. Rolink, A.G., et al., *Selection events operating at various stages in B cell development*. *Curr Opin Immunol*, 2001. **13**(2): p. 202-7.
51. Hammad, H., et al., *Transitional B cells commit to marginal zone B cell fate by Taok3-mediated surface expression of ADAM10*. *Nat Immunol*, 2017. **18**(3): p. 313-320.
52. Khan, W.N., et al., *Defective B cell development and function in Btk-deficient mice*. *Immunity*, 1995. **3**(3): p. 283-99.
53. Benatar, T., et al., *Immunoglobulin-mediated signal transduction in B cells from CD45-deficient mice*. *J Exp Med*, 1996. **183**(1): p. 329-34.
54. Fruman, D.A., et al., *Impaired B cell development and proliferation in absence of phosphoinositide 3-kinase p85alpha*. *Science*, 1999. **283**(5400): p. 393-7.
55. Xu, S., et al., *B cell development and activation defects resulting in xid-like immunodeficiency in BLNK/SLP-65-deficient mice*. *Int Immunol*, 2000. **12**(3): p. 397-404.
56. Khan, W.N., *B cell receptor and BAFF receptor signaling regulation of B cell homeostasis*. *J Immunol*, 2009. **183**(6): p. 3561-7.

57. Schiemann, B., et al., *An essential role for BAFF in the normal development of B cells through a BCMA-independent pathway*. Science, 2001. **293**(5537): p. 2111-4.
58. Hsu, B.L., et al., *Cutting edge: BLyS enables survival of transitional and mature B cells through distinct mediators*. J Immunol, 2002. **168**(12): p. 5993-6.
59. Batten, M., et al., *BAFF mediates survival of peripheral immature B lymphocytes*. J Exp Med, 2000. **192**(10): p. 1453-66.
60. Gross, J.A., et al., *TACI-Ig neutralizes molecules critical for B cell development and autoimmune disease. impaired B cell maturation in mice lacking BLyS*. Immunity, 2001. **15**(2): p. 289-302.
61. Andrews, S.F. and D.J. Rawlings, *Transitional B cells exhibit a B cell receptor-specific nuclear defect in gene transcription*. J Immunol, 2009. **182**(5): p. 2868-78.
62. Petro, J.B., et al., *Transitional type 1 and 2 B lymphocyte subsets are differentially responsive to antigen receptor signaling*. J Biol Chem, 2002. **277**(50): p. 48009-19.
63. Hoek, K.L., et al., *Transitional B cell fate is associated with developmental stage-specific regulation of diacylglycerol and calcium signaling upon B cell receptor engagement*. J Immunol, 2006. **177**(8): p. 5405-13.
64. Petro, J.B. and W.N. Khan, *Phospholipase C-gamma 2 couples Bruton's tyrosine kinase to the NF-kappaB signaling pathway in B lymphocytes*. J Biol Chem, 2001. **276**(3): p. 1715-9.

65. Lee, J., et al., *Identification and characterization of a human CD5+ pre-naive B cell population*. J Immunol, 2009. **182**(7): p. 4116-26.
66. Chang, N.H., et al., *Expanded population of activated antigen-engaged cells within the naive B cell compartment of patients with systemic lupus erythematosus*. J Immunol, 2008. **180**(2): p. 1276-84.
67. Blair, P.A., et al., *CD19(+)CD24(hi)CD38(hi) B cells exhibit regulatory capacity in healthy individuals but are functionally impaired in systemic Lupus Erythematosus patients*. Immunity, 2010. **32**(1): p. 129-40.
68. Evans, J.G., et al., *Novel suppressive function of transitional 2 B cells in experimental arthritis*. J Immunol, 2007. **178**(12): p. 7868-78.
69. Nova-Lamperti, E., et al., *IL-10-produced by human transitional B-cells down-regulates CD86 expression on B-cells leading to inhibition of CD4+T-cell responses*. Sci Rep, 2016. **6**: p. 20044.
70. Ward, J.M., et al., *Human effector B lymphocytes express ARID3a and secrete interferon alpha*. J Autoimmun, 2016. **75**: p. 130-140.
71. Cherukuri, A., et al., *Reduced human transitional B cell T1/T2 ratio is associated with subsequent deterioration in renal allograft function*. Kidney Int, 2017. **91**(1): p. 183-195.
72. Menon, M., et al., *A Regulatory Feedback between Plasmacytoid Dendritic Cells and Regulatory B Cells Is Aberrant in Systemic Lupus Erythematosus*. Immunity, 2016. **44**(3): p. 683-97.
73. McNab, F., et al., *Type I interferons in infectious disease*. Nat Rev Immunol, 2015. **15**(2): p. 87-103.

74. Pestka, S., C.D. Krause, and M.R. Walter, *Interferons, interferon-like cytokines, and their receptors*. Immunol Rev, 2004. **202**: p. 8-32.
75. Humphray, S.J., et al., *DNA sequence and analysis of human chromosome 9*. Nature, 2004. **429**(6990): p. 369-74.
76. Hardy, M.P., et al., *Characterization of the type I interferon locus and identification of novel genes*. Genomics, 2004. **84**(2): p. 331-45.
77. Uze, G., G. Lutfalla, and K.E. Mogensen, *Alpha and beta interferons and their receptor and their friends and relations*. J Interferon Cytokine Res, 1995. **15**(1): p. 3-26.
78. van Boxel-Dezaire, A.H., et al., *Major differences in the responses of primary human leukocyte subsets to IFN-beta*. J Immunol, 2010. **185**(10): p. 5888-99.
79. Zula, J.A., et al., *The role of cell type-specific responses in IFN-beta therapy of multiple sclerosis*. Proc Natl Acad Sci U S A, 2011. **108**(49): p. 19689-94.
80. Schreiber, G. and J. Piehler, *The molecular basis for functional plasticity in type I interferon signaling*. Trends Immunol, 2015. **36**(3): p. 139-49.
81. Lavoie, T.B., et al., *Binding and activity of all human alpha interferon subtypes*. Cytokine, 2011. **56**(2): p. 282-9.
82. Novick, D., B. Cohen, and M. Rubinstein, *The human interferon alpha/beta receptor: characterization and molecular cloning*. Cell, 1994. **77**(3): p. 391-400.
83. Owczarek, C.M., et al., *Cloning and characterization of soluble and transmembrane isoforms of a novel component of the murine type I interferon receptor, IFNAR 2*. J Biol Chem, 1997. **272**(38): p. 23865-70.

84. Hertzog, P.J. and B.R. Williams, *Fine tuning type I interferon responses*. Cytokine Growth Factor Rev, 2013. **24**(3): p. 217-25.
85. Wilmes, S., et al., *Receptor dimerization dynamics as a regulatory valve for plasticity of type I interferon signaling*. J Cell Biol, 2015. **209**(4): p. 579-93.
86. Kalie, E., et al., *The stability of the ternary interferon-receptor complex rather than the affinity to the individual subunits dictates differential biological activities*. J Biol Chem, 2008. **283**(47): p. 32925-36.
87. Domanski, P., et al., *A region of the beta subunit of the interferon alpha receptor different from box 1 interacts with Jak1 and is sufficient to activate the Jak-Stat pathway and induce an antiviral state*. J Biol Chem, 1997. **272**(42): p. 26388-93.
88. Yan, H., et al., *Molecular characterization of an alpha interferon receptor 1 subunit (IFNaR1) domain required for TYK2 binding and signal transduction*. Mol Cell Biol, 1996. **16**(5): p. 2074-82.
89. Stark, G.R. and J.E. Darnell, Jr., *The JAK-STAT pathway at twenty*. Immunity, 2012. **36**(4): p. 503-14.
90. Ivashkiv, L.B. and L.T. Donlin, *Regulation of type I interferon responses*. Nat Rev Immunol, 2014. **14**(1): p. 36-49.
91. van Boxel-Dezaire, A.H., M.R. Rani, and G.R. Stark, *Complex modulation of cell type-specific signaling in response to type I interferons*. Immunity, 2006. **25**(3): p. 361-72.
92. Kaur, S., S. Uddin, and L.C. Plataniias, *The PI3' kinase pathway in interferon signaling*. J Interferon Cytokine Res, 2005. **25**(12): p. 780-7.

93. Plataniias, L.C., *The p38 mitogen-activated protein kinase pathway and its role in interferon signaling*. *Pharmacol Ther*, 2003. **98**(2): p. 129-42.
94. Ruuth, K., et al., *Interferon-alpha promotes survival of human primary B-lymphocytes via phosphatidylinositol 3-kinase*. *Biochem Biophys Res Commun*, 2001. **284**(3): p. 583-6.
95. *Autoimmune thyroid disease in interferon-treated patients*. *Lancet*, 1985. **2**(8446): p. 100-1.
96. Kim, T., et al., *Serum levels of interferons in patients with systemic lupus erythematosus*. *Clin Exp Immunol*, 1987. **70**(3): p. 562-9.
97. Niewold, T.B., et al., *Age- and sex-related patterns of serum interferon-alpha activity in lupus families*. *Arthritis Rheum*, 2008. **58**(7): p. 2113-9.
98. Ko, K., et al., *Activation of the Interferon Pathway is Dependent Upon Autoantibodies in African-American SLE Patients, but Not in European-American SLE Patients*. *Front Immunol*, 2013. **4**: p. 309.
99. Kirou, K.A., et al., *Activation of the interferon-alpha pathway identifies a subgroup of systemic lupus erythematosus patients with distinct serologic features and active disease*. *Arthritis Rheum*, 2005. **52**(5): p. 1491-503.
100. Feng, X., et al., *Association of increased interferon-inducible gene expression with disease activity and lupus nephritis in patients with systemic lupus erythematosus*. *Arthritis Rheum*, 2006. **54**(9): p. 2951-62.
101. Petri, M., et al., *Longitudinal expression of type I interferon responsive genes in systemic lupus erythematosus*. *Lupus*, 2009. **18**(11): p. 980-9.

102. Chiche, L., et al., *Modular transcriptional repertoire analyses of adults with systemic lupus erythematosus reveal distinct type I and type II interferon signatures*. *Arthritis Rheumatol*, 2014. **66**(6): p. 1583-95.
103. Asselin-Paturel, C., et al., *Mouse type I IFN-producing cells are immature APCs with plasmacytoid morphology*. *Nat Immunol*, 2001. **2**(12): p. 1144-50.
104. Eloranta, M.L., G.V. Alm, and L. Ronnblom, *Disease mechanisms in rheumatology--tools and pathways: plasmacytoid dendritic cells and their role in autoimmune rheumatic diseases*. *Arthritis Rheum*, 2013. **65**(4): p. 853-63.
105. Ronnblom, L. and G.V. Alm, *The natural interferon-alpha producing cells in systemic lupus erythematosus*. *Hum Immunol*, 2002. **63**(12): p. 1181-93.
106. Barbalat, R., et al., *Nucleic acid recognition by the innate immune system*. *Annu Rev Immunol*, 2011. **29**: p. 185-214.
107. Fiore, N., et al., *Immature myeloid and plasmacytoid dendritic cells infiltrate renal tubulointerstitium in patients with lupus nephritis*. *Mol Immunol*, 2008. **45**(1): p. 259-65.
108. Tucci, M., et al., *Glomerular accumulation of plasmacytoid dendritic cells in active lupus nephritis: role of interleukin-18*. *Arthritis Rheum*, 2008. **58**(1): p. 251-62.
109. Farkas, L., et al., *Plasmacytoid dendritic cells (natural interferon- alpha/beta-producing cells) accumulate in cutaneous lupus erythematosus lesions*. *Am J Pathol*, 2001. **159**(1): p. 237-43.
110. Rodero, M.P., et al., *Detection of interferon alpha protein reveals differential levels and cellular sources in disease*. *J Exp Med*, 2017. **214**(5): p. 1547-1555.

111. Pau, E., et al., *TLR tolerance reduces IFN-alpha production despite plasmacytoid dendritic cell expansion and anti-nuclear antibodies in NZB bicongenic mice*. PLoS One, 2012. **7**(5): p. e36761.
112. Bekeredjian-Ding, I.B., et al., *Plasmacytoid dendritic cells control TLR7 sensitivity of naive B cells via type I IFN*. J Immunol, 2005. **174**(7): p. 4043-50.
113. Swanson, C.L., et al., *Type I IFN enhances follicular B cell contribution to the T cell-independent antibody response*. J Exp Med, 2010. **207**(7): p. 1485-500.
114. Bave, U., G.V. Alm, and L. Ronnblom, *The combination of apoptotic U937 cells and lupus IgG is a potent IFN-alpha inducer*. J Immunol, 2000. **165**(6): p. 3519-26.
115. Christensen, S.R. and M.J. Shlomchik, *Regulation of lupus-related autoantibody production and clinical disease by Toll-like receptors*. Semin Immunol, 2007. **19**(1): p. 11-23.
116. Lovgren, T., et al., *Induction of interferon-alpha production in plasmacytoid dendritic cells by immune complexes containing nucleic acid released by necrotic or late apoptotic cells and lupus IgG*. Arthritis Rheum, 2004. **50**(6): p. 1861-72.
117. Rowland, S.L., et al., *Early, transient depletion of plasmacytoid dendritic cells ameliorates autoimmunity in a lupus model*. J Exp Med, 2014. **211**(10): p. 1977-91.
118. Shao, W.H. and P.L. Cohen, *Disturbances of apoptotic cell clearance in systemic lupus erythematosus*. Arthritis Res Ther, 2011. **13**(1): p. 202.

119. Eloranta, M.L., et al., *Regulation of the interferon-alpha production induced by RNA-containing immune complexes in plasmacytoid dendritic cells*. *Arthritis Rheum*, 2009. **60**(8): p. 2418-27.
120. Chang, N.H., et al., *Interferon-alpha induces altered transitional B cell signaling and function in Systemic Lupus Erythematosus*. *J Autoimmun*, 2015. **58**: p. 100-10.
121. Braun, D., I. Caramalho, and J. Demengeot, *IFN-alpha/beta enhances BCR-dependent B cell responses*. *Int Immunol*, 2002. **14**(4): p. 411-9.
122. Vasconcellos, R., et al., *Type I IFN sets the stringency of B cell repertoire selection in the bone marrow*. *Int Immunol*, 1999. **11**(2): p. 279-88.
123. Jaitin, D.A. and G. Schreiber, *Upregulation of a small subset of genes drives type I interferon-induced antiviral memory*. *J Interferon Cytokine Res*, 2007. **27**(8): p. 653-64.
124. Hahm, B., et al., *Viruses evade the immune system through type I interferon-mediated STAT2-dependent, but STAT1-independent, signaling*. *Immunity*, 2005. **22**(2): p. 247-57.
125. Yen, J.H., W. Kong, and D. Ganea, *IFN-beta inhibits dendritic cell migration through STAT-1-mediated transcriptional suppression of CCR7 and matrix metalloproteinase 9*. *J Immunol*, 2010. **184**(7): p. 3478-86.
126. Santini, S.M., et al., *Type I interferon as a powerful adjuvant for monocyte-derived dendritic cell development and activity in vitro and in Hu-PBL-SCID mice*. *J Exp Med*, 2000. **191**(10): p. 1777-88.

127. Wilson, E.B., et al., *Blockade of chronic type I interferon signaling to control persistent LCMV infection*. Science, 2013. **340**(6129): p. 202-7.
128. Shiow, L.R., et al., *CD69 acts downstream of interferon-alpha/beta to inhibit SIP1 and lymphocyte egress from lymphoid organs*. Nature, 2006. **440**(7083): p. 540-4.
129. Fallet, B., et al., *Interferon-driven deletion of antiviral B cells at the onset of chronic infection*. Sci Immunol, 2016. **1**(4).
130. Moseman, E.A., et al., *Type I interferon suppresses virus-specific B cell responses by modulating CD8+ T cell differentiation*. Sci Immunol, 2016. **1**(4).
131. Sammiceli, S., et al., *Inflammatory monocytes hinder antiviral B cell responses*. Sci Immunol, 2016. **1**(4).
132. Essers, M.A., et al., *IFNalpha activates dormant haematopoietic stem cells in vivo*. Nature, 2009. **458**(7240): p. 904-8.
133. Xu, H.C., et al., *Type I interferon protects antiviral CD8+ T cells from NK cell cytotoxicity*. Immunity, 2014. **40**(6): p. 949-60.
134. Huber, J.P. and J.D. Farrar, *Regulation of effector and memory T-cell functions by type I interferon*. Immunology, 2011. **132**(4): p. 466-74.
135. Crouse, J., U. Kalinke, and A. Oxenius, *Regulation of antiviral T cell responses by type I interferons*. Nat Rev Immunol, 2015. **15**(4): p. 231-42.
136. Becker, A.M., et al., *SLE peripheral blood B cell, T cell and myeloid cell transcriptomes display unique profiles and each subset contributes to the interferon signature*. PLoS One, 2013. **8**(6): p. e67003.

137. Dorner, T., et al., *Abnormalities of B cell subsets in patients with systemic lupus erythematosus*. J Immunol Methods, 2011. **363**(2): p. 187-97.
138. Strauss, R., et al., *Type I interferon as a biomarker in autoimmunity and viral infection: a leukocyte subset-specific analysis unveils hidden diagnostic options*. J Mol Med (Berl), 2017.
139. Landolt-Marticorena, C., et al., *Lack of association between the interferon-alpha signature and longitudinal changes in disease activity in systemic lupus erythematosus*. Ann Rheum Dis, 2009. **68**(9): p. 1440-6.
140. Gresser, I., *Biologic effects of interferons*. J Invest Dermatol, 1990. **95**(6 Suppl): p. 66S-71S.
141. Lienenklaus, S., et al., *Novel reporter mouse reveals constitutive and inflammatory expression of IFN-beta in vivo*. J Immunol, 2009. **183**(5): p. 3229-36.
142. Hata, N., et al., *Constitutive IFN-alpha/beta signal for efficient IFN-alpha/beta gene induction by virus*. Biochem Biophys Res Commun, 2001. **285**(2): p. 518-25.
143. Gough, D.J., et al., *Constitutive type I interferon modulates homeostatic balance through tonic signaling*. Immunity, 2012. **36**(2): p. 166-74.
144. Chen, H.M., et al., *Critical role for constitutive type I interferon signaling in the prevention of cellular transformation*. Cancer Sci, 2009. **100**(3): p. 449-56.
145. Taniguchi, T. and A. Takaoka, *A weak signal for strong responses: interferon-alpha/beta revisited*. Nat Rev Mol Cell Biol, 2001. **2**(5): p. 378-86.

146. Gresser, I. and F. Belardelli, *Endogenous type I interferons as a defense against tumors*. Cytokine Growth Factor Rev, 2002. **13**(2): p. 111-8.
147. Shechter, Y., et al., *Prolonging the half-life of human interferon-alpha 2 in circulation: Design, preparation, and analysis of (2-sulfo-9-fluorenylmethoxycarbonyl)7- interferon-alpha 2*. Proc Natl Acad Sci U S A, 2001. **98**(3): p. 1212-7.
148. Lee-Kirsch, M.A., *The Type I Interferonopathies*. Annu Rev Med, 2017. **68**: p. 297-315.
149. Honda, K., A. Takaoka, and T. Taniguchi, *Type I interferon [corrected] gene induction by the interferon regulatory factor family of transcription factors*. Immunity, 2006. **25**(3): p. 349-60.
150. Honda, K., et al., *IRF-7 is the master regulator of type-I interferon-dependent immune responses*. Nature, 2005. **434**(7034): p. 772-7.
151. Sato, M., et al., *Distinct and essential roles of transcription factors IRF-3 and IRF-7 in response to viruses for IFN-alpha/beta gene induction*. Immunity, 2000. **13**(4): p. 539-48.
152. Panne, D., T. Maniatis, and S.C. Harrison, *An atomic model of the interferon-beta enhanceosome*. Cell, 2007. **129**(6): p. 1111-23.
153. Gough, D.J., et al., *Functional crosstalk between type I and II interferon through the regulated expression of STAT1*. PLoS Biol, 2010. **8**(4): p. e1000361.
154. Basagoudanavar, S.H., et al., *Distinct roles for the NF-kappa B RelA subunit during antiviral innate immune responses*. J Virol, 2011. **85**(6): p. 2599-610.

155. Cheng, C.S., et al., *The specificity of innate immune responses is enforced by repression of interferon response elements by NF-kappaB p50*. *Sci Signal*, 2011. **4**(161): p. ra11.
156. Hooks, J.J., et al., *Multiple interferons in the circulation of patients with systemic lupus erythematosus and vasculitis*. *Arthritis Rheum*, 1982. **25**(4): p. 396-400.
157. Wong, D., et al., *Interferon and biologic signatures in dermatomyositis skin: specificity and heterogeneity across diseases*. *PLoS One*, 2012. **7**(1): p. e29161.
158. Crow, M.K., *Autoimmunity: Interferon alpha or beta: which is the culprit in autoimmune disease?* *Nat Rev Rheumatol*, 2016. **12**(8): p. 439-40.
159. Hua, J., et al., *Functional assay of type I interferon in systemic lupus erythematosus plasma and association with anti-RNA binding protein autoantibodies*. *Arthritis Rheum*, 2006. **54**(6): p. 1906-16.
160. Bengtsson, A.A., et al., *Activation of type I interferon system in systemic lupus erythematosus correlates with disease activity but not with antiretroviral antibodies*. *Lupus*, 2000. **9**(9): p. 664-71.
161. Lamken, P., et al., *Ligand-induced assembling of the type I interferon receptor on supported lipid bilayers*. *J Mol Biol*, 2004. **341**(1): p. 303-18.
162. Erlandsson, L., et al., *Interferon-beta is required for interferon-alpha production in mouse fibroblasts*. *Curr Biol*, 1998. **8**(4): p. 223-6.
163. Takaoka, A., et al., *Cross talk between interferon-gamma and -alpha/beta signaling components in caveolar membrane domains*. *Science*, 2000. **288**(5475): p. 2357-60.

164. Phipps-Yonas, H., et al., *Interferon-beta pretreatment of conventional and plasmacytoid human dendritic cells enhances their activation by influenza virus*. PLoS Pathog, 2008. **4**(10): p. e1000193.
165. Coelho, L.F., et al., *Interferon-alpha and -beta differentially regulate osteoclastogenesis: role of differential induction of chemokine CXCL11 expression*. Proc Natl Acad Sci U S A, 2005. **102**(33): p. 11917-22.
166. Garcin, G., et al., *Differential activity of type I interferon subtypes for dendritic cell differentiation*. PLoS One, 2013. **8**(3): p. e58465.
167. de Weerd, N.A., et al., *Structural basis of a unique interferon-beta signaling axis mediated via the receptor IFNAR1*. Nat Immunol, 2013. **14**(9): p. 901-7.
168. Gimeno, R., et al., *Stat1 and Stat2 but not Stat3 arbitrate contradictory growth signals elicited by alpha/beta interferon in T lymphocytes*. Mol Cell Biol, 2005. **25**(13): p. 5456-65.
169. Tanabe, Y., et al., *Cutting edge: role of STAT1, STAT3, and STAT5 in IFN-alpha beta responses in T lymphocytes*. J Immunol, 2005. **174**(2): p. 609-13.
170. Hurtado-Guerrero, I., et al., *Activation of the JAK-STAT Signaling Pathway after In Vitro Stimulation with IFNs in Multiple Sclerosis Patients According to the Therapeutic Response to IFNs*. PLoS One, 2017. **12**(1): p. e0170031.
171. Zheng, H., et al., *Ligand-stimulated downregulation of the alpha interferon receptor: role of protein kinase D2*. Mol Cell Biol, 2011. **31**(4): p. 710-20.
172. Marijanovic, Z., et al., *Comparable potency of IFNalpha2 and IFNbeta on immediate JAK/STAT activation but differential down-regulation of IFNAR2*. Biochem J, 2007. **407**(1): p. 141-51.

173. Shrivastav, M. and T.B. Niewold, *Nucleic Acid sensors and type I interferon production in systemic lupus erythematosus*. Front Immunol, 2013. **4**: p. 319.
174. International Consortium for Systemic Lupus Erythematosus, G., et al., *Genome-wide association scan in women with systemic lupus erythematosus identifies susceptibility variants in ITGAM, PXX, KIAA1542 and other loci*. Nat Genet, 2008. **40**(2): p. 204-10.
175. Kaufman, K.M., et al., *Fine mapping of Xq28: both MECP2 and IRAK1 contribute to risk for systemic lupus erythematosus in multiple ancestral groups*. Ann Rheum Dis, 2013. **72**(3): p. 437-44.
176. Junt, T. and W. Barchet, *Translating nucleic acid-sensing pathways into therapies*. Nat Rev Immunol, 2015. **15**(9): p. 529-44.
177. Hanten, J.A., et al., *Comparison of human B cell activation by TLR7 and TLR9 agonists*. BMC Immunol, 2008. **9**: p. 39.
178. Schlee, M. and G. Hartmann, *Discriminating self from non-self in nucleic acid sensing*. Nat Rev Immunol, 2016. **16**(9): p. 566-80.
179. Chen, Q., L. Sun, and Z.J. Chen, *Regulation and function of the cGAS-STING pathway of cytosolic DNA sensing*. Nat Immunol, 2016. **17**(10): p. 1142-9.
180. Kariuki, S.N., M.K. Crow, and T.B. Niewold, *The PTPN22 C1858T polymorphism is associated with skewing of cytokine profiles toward high interferon-alpha activity and low tumor necrosis factor alpha levels in patients with lupus*. Arthritis Rheum, 2008. **58**(9): p. 2818-23.

181. Kariuki, S.N., et al., *Trait-stratified genome-wide association study identifies novel and diverse genetic associations with serologic and cytokine phenotypes in systemic lupus erythematosus*. *Arthritis Res Ther*, 2010. **12**(4): p. R151.
182. Harley, I.T., et al., *The role of genetic variation near interferon-kappa in systemic lupus erythematosus*. *J Biomed Biotechnol*, 2010. **2010**.
183. Oliveira, L., et al., *Dysregulation of antiviral helicase pathways in systemic lupus erythematosus*. *Front Genet*, 2014. **5**: p. 418.
184. Theofilopoulos, A.N., et al., *Intracellular nucleic acid sensors and autoimmunity*. *J Interferon Cytokine Res*, 2011. **31**(12): p. 867-86.
185. Celhar, T., R. Magalhaes, and A.M. Fairhurst, *TLR7 and TLR9 in SLE: when sensing self goes wrong*. *Immunol Res*, 2012. **53**(1-3): p. 58-77.
186. Deane, J.A., et al., *Control of toll-like receptor 7 expression is essential to restrict autoimmunity and dendritic cell proliferation*. *Immunity*, 2007. **27**(5): p. 801-10.
187. Miettinen, M., et al., *IFNs activate toll-like receptor gene expression in viral infections*. *Genes Immun*, 2001. **2**(6): p. 349-55.
188. Zarembek, K.A. and P.J. Godowski, *Tissue expression of human Toll-like receptors and differential regulation of Toll-like receptor mRNAs in leukocytes in response to microbes, their products, and cytokines*. *J Immunol*, 2002. **168**(2): p. 554-61.
189. Bourke, E., et al., *The toll-like receptor repertoire of human B lymphocytes: inducible and selective expression of TLR9 and TLR10 in normal and transformed cells*. *Blood*, 2003. **102**(3): p. 956-63.

190. Komatsuda, A., et al., *Up-regulated expression of Toll-like receptors mRNAs in peripheral blood mononuclear cells from patients with systemic lupus erythematosus*. Clin Exp Immunol, 2008. **152**(3): p. 482-7.
191. Lyn-Cook, B.D., et al., *Increased expression of Toll-like receptors (TLRs) 7 and 9 and other cytokines in systemic lupus erythematosus (SLE) patients: ethnic differences and potential new targets for therapeutic drugs*. Mol Immunol, 2014. **61**(1): p. 38-43.
192. Ronnblom, L., M.L. Eloranta, and G.V. Alm, *The type I interferon system in systemic lupus erythematosus*. Arthritis Rheum, 2006. **54**(2): p. 408-20.
193. Chauhan, S.K., et al., *Distinct autoantibody profiles in systemic lupus erythematosus patients are selectively associated with TLR7 and TLR9 upregulation*. J Clin Immunol, 2013. **33**(5): p. 954-64.
194. Blanco, P., et al., *Induction of dendritic cell differentiation by IFN-alpha in systemic lupus erythematosus*. Science, 2001. **294**(5546): p. 1540-3.
195. Celhar, T. and A.M. Fairhurst, *Toll-like receptors in systemic lupus erythematosus: potential for personalized treatment*. Front Pharmacol, 2014. **5**: p. 265.
196. Hochreiter-Hufford, A. and K.S. Ravichandran, *Clearing the dead: apoptotic cell sensing, recognition, engulfment, and digestion*. Cold Spring Harb Perspect Biol, 2013. **5**(1): p. a008748.
197. Mahajan, A., M. Herrmann, and L.E. Munoz, *Clearance Deficiency and Cell Death Pathways: A Model for the Pathogenesis of SLE*. Front Immunol, 2016. **7**: p. 35.

198. Biermann, M.H., et al., *The role of dead cell clearance in the etiology and pathogenesis of systemic lupus erythematosus: dendritic cells as potential targets*. *Expert Rev Clin Immunol*, 2014. **10**(9): p. 1151-64.
199. Klarquist, J., et al., *Dendritic Cells in Systemic Lupus Erythematosus: From Pathogenic Players to Therapeutic Tools*. *Mediators Inflamm*, 2016. **2016**: p. 5045248.
200. Chan, V.S., et al., *Distinct roles of myeloid and plasmacytoid dendritic cells in systemic lupus erythematosus*. *Autoimmun Rev*, 2012. **11**(12): p. 890-7.
201. Colonna, M., G. Trinchieri, and Y.J. Liu, *Plasmacytoid dendritic cells in immunity*. *Nat Immunol*, 2004. **5**(12): p. 1219-26.
202. Cederblad, B., et al., *Patients with systemic lupus erythematosus have reduced numbers of circulating natural interferon-alpha-producing cells*. *J Autoimmun*, 1998. **11**(5): p. 465-70.
203. Weigent, D.A., et al., *Human B lymphocytes produce leukocyte interferon after interaction with foreign cells*. *Infect Immun*, 1981. **32**(2): p. 508-12.
204. Pogue, S.L., et al., *The receptor for type I IFNs is highly expressed on peripheral blood B cells and monocytes and mediates a distinct profile of differentiation and activation of these cells*. *J Interferon Cytokine Res*, 2004. **24**(2): p. 131-9.
205. Oganessian, G., et al., *IRF3-dependent type I interferon response in B cells regulates CpG-mediated antibody production*. *J Biol Chem*, 2008. **283**(2): p. 802-8.
206. Schafer, S.L., et al., *Regulation of type I interferon gene expression by interferon regulatory factor-3*. *J Biol Chem*, 1998. **273**(5): p. 2714-20.

207. Marie, I., J.E. Durbin, and D.E. Levy, *Differential viral induction of distinct interferon-alpha genes by positive feedback through interferon regulatory factor-7*. EMBO J, 1998. **17**(22): p. 6660-9.
208. Sato, M., et al., *Positive feedback regulation of type I IFN genes by the IFN-inducible transcription factor IRF-7*. FEBS Lett, 1998. **441**(1): p. 106-10.
209. Zhao, M., et al., *Stochastic expression of the interferon-beta gene*. PLoS Biol, 2012. **10**(1): p. e1001249.
210. Zawatzky, R., E. De Maeyer, and J. De Maeyer-Guignard, *Identification of individual interferon-producing cells by in situ hybridization*. Proc Natl Acad Sci U S A, 1985. **82**(4): p. 1136-40.
211. Rand, U., et al., *Multi-layered stochasticity and paracrine signal propagation shape the type-I interferon response*. Mol Syst Biol, 2012. **8**: p. 584.
212. Hu, J., et al., *Chromosome-specific and noisy IFNB1 transcription in individual virus-infected human primary dendritic cells*. Nucleic Acids Res, 2007. **35**(15): p. 5232-41.
213. Patil, S., et al., *Single-cell analysis shows that paracrine signaling by first responder cells shapes the interferon-beta response to viral infection*. Sci Signal, 2015. **8**(363): p. ra16.
214. Soni, C., et al., *B cell-intrinsic TLR7 signaling is essential for the development of spontaneous germinal centers*. J Immunol, 2014. **193**(9): p. 4400-14.
215. Zaritsky, L.A., J.R. Bedsaul, and K.C. Zoon, *Virus Multiplicity of Infection Affects Type I Interferon Subtype Induction Profiles and Interferon-Stimulated Genes*. J Virol, 2015. **89**(22): p. 11534-48.

216. Perry, D., et al., *Murine models of systemic lupus erythematosus*. J Biomed Biotechnol, 2011. **2011**: p. 271694.
217. Baccala, R., et al., *Anti-IFN-alpha/beta receptor antibody treatment ameliorates disease in lupus-predisposed mice*. J Immunol, 2012. **189**(12): p. 5976-84.
218. Katewa, A., et al., *Btk-specific inhibition blocks pathogenic plasma cell signatures and myeloid cell-associated damage in IFNalpha-driven lupus nephritis*. JCI Insight, 2017. **2**(7): p. e90111.
219. Genin, P., et al., *Differential regulation of human interferon A gene expression by interferon regulatory factors 3 and 7*. Mol Cell Biol, 2009. **29**(12): p. 3435-50.
220. Demoulines, T., et al., *Poly (I:C) induced immune response in lymphoid tissues involves three sequential waves of type I IFN expression*. Virology, 2009. **386**(2): p. 225-36.
221. Kaminski, D.A., et al., *Advances in human B cell phenotypic profiling*. Front Immunol, 2012. **3**: p. 302.
222. Honda, K., et al., *Regulation of the type I IFN induction: a current view*. Int Immunol, 2005. **17**(11): p. 1367-78.
223. Tak, P.P., *IFN-beta in rheumatoid arthritis*. Front Biosci, 2004. **9**: p. 3242-7.
224. Cantaert, T., et al., *Type I IFN and TNFalpha cross-regulation in immune-mediated inflammatory disease: basic concepts and clinical relevance*. Arthritis Res Ther, 2010. **12**(5): p. 219.

225. Ivashkiv, L.B., *Type I interferon modulation of cellular responses to cytokines and infectious pathogens: potential role in SLE pathogenesis*. *Autoimmunity*, 2003. **36**(8): p. 473-9.
226. Cherukuri, A., et al., *Immunologic human renal allograft injury associates with an altered IL-10/TNF-alpha expression ratio in regulatory B cells*. *J Am Soc Nephrol*, 2014. **25**(7): p. 1575-85.
227. Hall, J.C., et al., *Molecular Subsetting of Interferon Pathways in Sjogren's Syndrome*. *Arthritis Rheumatol*, 2015. **67**(9): p. 2437-46.
228. Quartuccio, L., et al., *Type I interferon signature may influence the effect of belimumab on immunoglobulin levels, including rheumatoid factor in Sjogren's syndrome*. *Clin Exp Rheumatol*, 2017.
229. Vlachogiannis, N.I., et al., *Increased frequency of the PTPN22W* variant in primary Sjogren's Syndrome: Association with low type I IFN scores*. *Clin Immunol*, 2016. **173**: p. 157-160.

APPENDIX A

APPROVAL FORM FROM THE
INSTITUTIONAL ANIMAL CARE AND USE COMMITTEE (IACUC)

MEMORANDUM

DATE: 20-Dec-2016
TO: Mountz, John D
FROM: 
Robert A. Kesterson, Ph.D., Chair
Institutional Animal Care and Use Committee (IACUC)
SUBJECT: NOTICE OF APPROVAL

The following application was approved by the University of Alabama at Birmingham Institutional Animal Care and Use Committee (IACUC) on 20-Dec-2016.

Protocol PI: Mountz, John D

Title: Follicular Exclusion of Self Antigens Prevents Development of Autoantibodies

Sponsor: National Institute of Allergy and Infectious Diseases/NIH/DHHS

Animal Project Number (APN): IACUC-10028

This institution has an Animal Welfare Assurance on file with the Office of Laboratory Animal Welfare (OLAW), is registered as a Research Facility with the USDA, and is accredited by the Association for Assessment and Accreditation of Laboratory Animal Care International (AAALAC).

Institutional Animal Care and Use Committee (IACUC)		Mailing Address:
CH19 Suite 403		CH19 Suite 403
933 19th Street South		1530 3rd Ave S
(205) 934-7692		Birmingham, AL 35294-0019
FAX (205) 934-1188		

APPENDIX B

APPROVAL FORM FROM THE
INSTITUTIONAL REVIEW BOARDS FOR HUMAN USE (IRBs)

Form 4: IRB Approval Form
Identification and Certification of Research
Projects Involving Human Subjects

UAB's Institutional Review Boards for Human Use (IRBs) have an approved Federalwide Assurance with the Office for Human Research Protections (OHRP). The Assurance number is FWA00005960 and it expires on January 24, 2017. The UAB IRBs are also in compliance with 21 CFR Parts 50 and 56.

Principal Investigator: HSU, HUI-CHEN
Co-Investigator(s):
Protocol Number: **X091215011**
Protocol Title: *Deletion of Lupus Autoreactive Cells Using an Anti-hDR5 Antibody*

The IRB reviewed and approved the above named project on 11-8-16. The review was conducted in accordance with UAB's Assurance of Compliance approved by the Department of Health and Human Services. This Project will be subject to Annual continuing review as provided in that Assurance.

This project received EXPEDITED review.

IRB Approval Date: 11-8-16

Date IRB Approval Issued: 11-8-16

IRB Approval No Longer Valid On: 11-8-17



Expedited Reviewer
Member - Institutional Review Board
for Human Use (IRB)

Investigators please note:

The IRB approved consent form used in the study must contain the IRB approval date and expiration date.

IRB approval is given for one year unless otherwise noted. For projects subject to annual review research activities may not continue past the one year anniversary of the IRB approval date.

Any modifications in the study methodology, protocol and/or consent form must be submitted for review and approval to the IRB prior to implementation.

Adverse Events and/or unanticipated risks to subjects or others at UAB or other participating institutions must be reported promptly to the IRB.

470 Administration Building
701 20th Street South
205.934.3789
Fax 205.934.1301
irb@uab.edu

The University of
Alabama at Birmingham
Mailing Address:
AB 470
1720 2ND AVE S
BIRMINGHAM AL 35294-0104